

Novel carbene complexes with pyrrole ligands

By

ANDREW JOHN OLIVIER

Submitted in partial fulfilment of the degree

MAGISTER SCIENTIAE
In Chemistry

In the Faculty of Natural- and Agricultural Sciences

UNIVERSITY OF PRETORIA
Pretoria

Supervisor: Prof S. Lotz

March 2001

Novel carbene complexes with pyrrole ligands

By

ANDREW JOHN OLIVIER

Submitted in partial fulfilment of the degree

MAGISTER SCIENTIAE
In Chemistry

In the Faculty of Natural- and Agricultural Sciences

UNIVERSITY OF PRETORIA
Pretoria

Supervisor: Prof S. Lotz

March 2001

ACKNOWLEDGEMENTS

I would like to express my sincere gratitude to

my Creator.

Prof Simon Lotz, my supervisor, for his patience and guidance.

Mr Eric Palmer, Dr Helmar Görts and Mr Ian Vorster, for providing me with data on my complexes.

the NRF and UP for financial support.

my colleagues (past and present), especially Dr. Hubert Nienaber, for their assistance and friendship.

and lastly, my parents, family and friends, for their moral support.

Andrew.

TABLE OF CONTENTS

Chapter 1: Introduction

1	<u>GENERAL</u>	1
1.1	DINUCLEAR COMPLEXES WITH BRIDGING LIGANDS.	1
1.2	TRANSFER OF ELECTRONS ACROSS ORGANIC BRIDGES – MOLECULAR WIRES.	3
2	<u>LIGANDS</u>	10
2.1	N-METHYLPYRROLE, N,N'-DIMETHYLBIPYRROLE AND N,N'-DIMETHYLPYRROLO[3,2-β]PYRROLE.	10
2.2	AROMATICITY.	11
2.3	CONDUCTING POLYMERS.	12
3	<u>CARBENE COMPLEXES</u>	14
3.1	PROPERTIES OF CARBENE COMPLEXES	14
3.2	SYNTHESIS OF CARBENE COMPLEXES	18
3.3	REACTIONS OF CARBENE COMPLEXES	20
3.4	CARBENE COMPLEXES AS POTENTIAL MOLECULAR WIRES.	24
4	<u>AIM</u>	26

Chapter 2: Carbene Complexes of N-methylpyrrole

1	<u>BACKGROUND</u>	27
2	<u>SYNTHESIS</u>	30
3	<u>CHARACTERIZATION OF COMPLEXES</u>	31
3.1	TUNGSTEN COMPLEXES	31
3.1.1	NMR SPECTROSCOPY	31
3.1.2	MASS SPECTROMETRY	37
3.1.3	INFRARED SPECTROSCOPY	38
3.1.4	ULTRAVIOLET SPECTROSCOPY	38
3.1.5	CRYSTAL STRUCTURE	39
3.2	CHROMIUM COMPLEXES	41
3.2.1	NMR SPECTROSCOPY	41
3.2.2	MASS SPECTROMETRY	46



3.2.3	INFRARED SPECTROSCOPY	47
3.2.4	ULTRAVIOLET SPECTROSCOPY	49
3.2.5	CRYSTAL STRUCTURE	50

Chapter 3: Carbene Complexes of N,N'-dimethylbipyrrole

1	BACKGROUND	53
2	SYNTHESIS	56
3	CHARACTERIZATION OF COMPLEXES	58
3.1	TUNGSTEN COMPLEXES	58
3.1.1	NMR SPECTROSCOPY	58
3.1.2	MASS SPECTROMETRY	63
3.1.3	INFRARED SPECTROSCOPY	64
3.1.4	ULTRAVIOLET SPECTROSCOPY	64
3.1.5	CRYSTAL STRUCTURE	65
3.2	CHROMIUM COMPLEXES	68
3.2.1	NMR SPECTROSCOPY	68
3.2.2	MASS SPECTROMETRY	74
3.2.3	INFRARED SPECTROSCOPY	75
3.2.4	ULTRAVIOLET SPECTROSCOPY	75

Chapter 4: Carbene Complexes of N,N'-dimethylpyrrolo[3,2-*b*]pyrrole

1	BACKGROUND	77
2	SYNTHESIS	83
3	CHARACTERIZATION OF COMPLEXES	86
3.1	TUNGSTEN COMPLEXES	86
3.1.1	NMR SPECTROSCOPY	86
3.1.2	MASS SPECTROMETRY	90
3.1.3	INFRARED SPECTROSCOPY	92
3.1.4	ULTRAVIOLET SPECTROSCOPY	93
3.1.5	CRYSTAL STRUCTURE	94

Chapter 5: Conclusion

Chapter 6: Experimental Information

<u>1</u>	<u>PRODUCTS</u>	99
<u>2</u>	<u>INFORMATION</u>	100
2.1	NMR	100
2.2	MS	100
2.3	IR	100
2.4	UV	100
2.5	REACTIONS	101
<u>3</u>	<u>PREPARATION OF THE N-METHYLPYRROLE CARBENE COMPLEXES</u>	102
3.1	TUNGSTEN COMPLEXES	102
3.2	CHROMIUM COMPLEXES	103
<u>4</u>	<u>PREPARATION OF N,N'-DIMETHYLBIPYRROLE AND THE MONOCARBENE AND BISCARBENE TUNGSTEN AND CHROMIUM COMPLEXES</u>	104
4.1	PREPARATION OF THE BIPYRROLE	104
4.2	TUNGSTEN COMPLEXES	105
4.3	CHROMIUM COMPLEXES	106
<u>5</u>	<u>PREPARATION OF N,N'-DIMETHYLPYRROLO[3,2-B]PYRROLE AND THE MONOCARBENE AND BISCARBENE TUNGSTEN COMPLEXES</u>	107
5.1	PREPARATION OF THE PYRROLO[3,2-B]PYRROLE	107
5.2	TUNGSTEN COMPLEXES	110
	<u>Appendix A</u>	111
	<u>Appendix B</u>	115
	<u>Appendix C</u>	122
	<u>Appendix D</u>	126

SUMMARY

This study describes the synthesis and characterization of Fischer mono- and bisethoxycarbene complexes of tungsten and chromium with deprotonated N-methylpyrrole (H-P-H), N,N'-dimethylbipyrrole (H-P-P-H) and N,N'-dimethylpyrrolo[3,2-*b*]pyrrole (H-PP-H) as spacer units. The pyrrole derivatives were metallated and also doubly metallated with butyl lithium, reacted with the metal hexacarbonyls of chromium and tungsten, and subsequently alkylated with triethyloxonium tetrafluoroborate, affording the resulting Fischer-type carbene complexes. The monocarbene complexes $[M(CO)_5C(OEt)\text{-spacer-H}]$ and biscarbene complexes $[M(CO)_5C(OEt)\text{-spacer-C(OEt)M(CO)}_5]$ were isolated, purified by column chromatography and recrystallized in reasonable yields.

The complexes were characterized by NMR spectroscopy, mass spectrometry, infrared spectroscopy and ultraviolet spectroscopy. Solution studies revealed that electronic charge was transferred to the cationic carbene carbon atom from the oxygen atom of the ethoxy substituent, from the metal *d*-orbitals (t_{2g}) and, especially important for this study, from the heteroaromatic pyrrole substituents. In some instances long distances charge transfer via conjugated π -orbitals, could be established.

Crystal structures were obtained of four of the complexes and not only confirmed the structures of these complexes, but also gave valuable information of structural features in the solid state. The rings were in most cases planar (also in a plane with the carbene sp^2 carbon), enabling π -conjugation and stabilization of the electronic constraints enforced by the carbene carbon. In another instance, the two rings of bipyrrole was twisted due to steric interactions of the methyl substituents on the pyrrole nitrogen atoms. Preferred configurations with regard to the pyrrole rings and carbene substituents were established and studied.

OPSOMMING

Hierdie studie beskryf die sintese en karakterisering van Fischer mono- en bisetoksiekarbeenkomplekse van wolfram en chroom met gedeprotoneerde N-metielpirrool (H-P-H), N,N-dimetielpirrool (H-P-P-H) en N,N'-dimetielpirrolo[3,2-*b*]pirrool (H-PP-H) as spasiëringseenhede. Die pirroolderivate is gemetalleer en ook dubbeld gemetalleer met butiellitium, gereageer met die metaalheksakarboniele van chroom en wolfram, en daarna het alkilering met tri-etieloksoniumtetrafluoroboraat die Fischer-tipe karbeenkomplekse gegee. Die monokarbeenkomplekse $[M(CO)_5C(OEt)\text{-brug-H}]$ en biskarbeenkomplekse $[M(CO)_5C(OEt)\text{-brug-C(OEt)M(CO)}_5]$ is geïsoleer, gesuiwer met kolom chromatografie en geherkristalliseer in redelike opbrengste.

Die komplekse is gekarakteriseer met KMR spektroskopie, massaspektrometrie, infrarooispektroskopie en ultravioletspektroskopie. Oplossingstudies het gewys dat elektroniese lading na die kationiese karbeenkoolstof atoom oorgedra word vanaf die suurstofatoom van die etoksiesubstituent, die metaal *d*-orbitale (t_{2g}) en, veral belangrik vir hierdie studie, vanaf die heteroaromatiese pirroolsubstituent. In sommige gevalle kon lang-afstand lading oordrag, via die gekonjugeerde π -orbitale, opgemerk word.

Kristalstruktuurbepalings is verkry van vier van die komplekse en het nie net die strukture van hierdie komplekse bevestig nie, maar het waardevolle inligting gegee oor die struktureienskappe in die vastetoestand. Die ringe is in die meeste gevalle planêr (ook in 'n vlak met die karbeen sp^2 koolstof), wat π -konjugasie, asook stabilisering van elektrondigtheid oor die brugligand toelaat. In 'n ander geval is die twee ringe van bipirrool gedraai weens steriese interaksies van die metielsubstituent op die pirrool stikstofatome. Konfigurasies van die pirroolringe en karbeensubstituent is vasgestel en bestudeer.


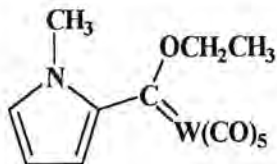
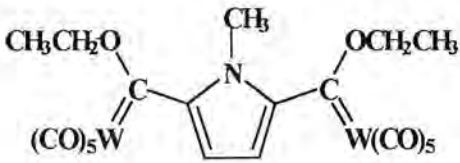
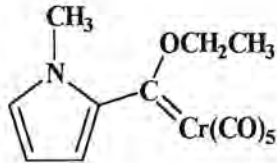
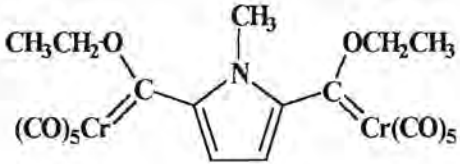
LIST OF ABBREVIATIONS

Bu	butyl
CDCl ₃	deuteriochloroform
CHCl ₃	chloroform
CSI	chlorosulfonyl isocyanate
CH ₂ Cl ₂	dichloromethane
d	doublet
dd	doublet of doublets
DMAD	dimethyl acetylenedicarboxylate
dt	doublet of triplets
Et	ethyl
HETCOR	heteronuclear correlation
IR	infrared
J	coupling constant
L-type ligand	neutral donor ligand
MS	mass spectrometry
M	transition metal

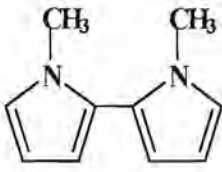
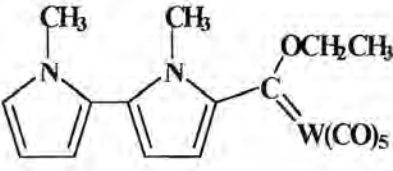
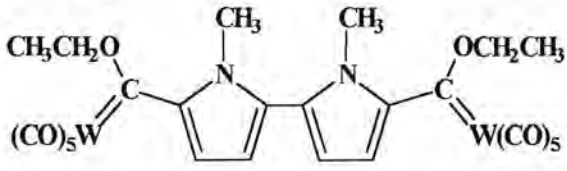
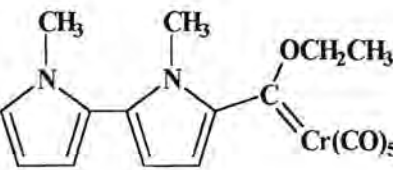
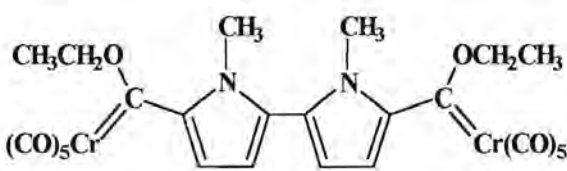
Me	methyl
NMR	nuclear magnetic resonance
P	N-Methylpyrrole
P-P	N,N'-Dimethylbipyrrole
PP	N,N'-Dimethylpyrrolo[3,2- <i>b</i>]pyrrole
q	quartet
s	singlet
THF, thf	tetrahydrofuran
t	triplet
UV	ultraviolet
Å	angstrom
δ	chemical shift
η ⁿ	substrate indicates the number of coordinated carbons

LIST OF COMPOUNDS

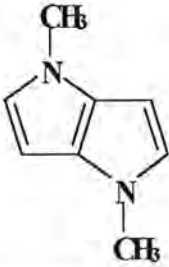
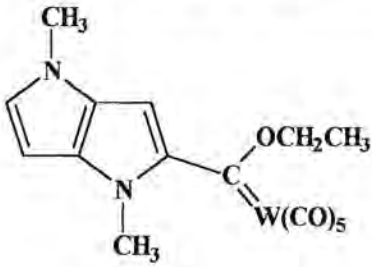
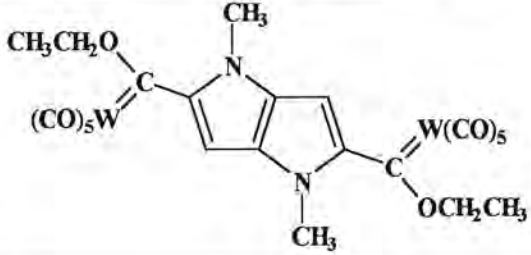
Pyrrole

Complex	Short Name	Number
	H-P-H	L1
	W(CO) ₅ C(OEt)-P-H	P1
	W(CO) ₅ C(OEt)-P-C(OEt)W(CO) ₅	P2
	Cr(CO) ₅ C(OEt)-P-H	P3
	Cr(CO) ₅ C(OEt)-P-C(OEt)Cr(CO) ₅	P4

Bipyrrole

Complex	Short Name	Number
	H-P-P-H	L2
	W(CO) ₅ C(OEt)-P-P-H	P5
	W(CO) ₅ C(OEt)-P-P-C(OEt)W(CO) ₅	P6
	Cr(CO) ₅ C(OEt)-P-P-H	P7
	Cr(CO) ₅ C(OEt)-P-P-C(OEt)Cr(CO) ₅	P8

Pyrrolopyrrole

Complex	Short Name	Number
 <p>Chemical structure of 1,4-dimethylpyrrolo[2,1-b]pyrrole, showing two fused five-membered rings with nitrogen atoms at the 1 and 4 positions, each substituted with a methyl group (CH₃).</p>	H-PP-H	L3
 <p>Chemical structure of 1,4-dimethyl-2-(W(CO)₅C(OEt))pyrrolo[2,1-b]pyrrole, showing the pyrrolopyrrole core with methyl groups at the 1 and 4 positions and a W(CO)₅C(OEt) group at the 2 position.</p>	W(CO) ₅ C(OEt)-PP-H	P9
 <p>Chemical structure of 1,4-dimethyl-2,5-bis(W(CO)₅C(OEt))pyrrolo[2,1-b]pyrrole, showing the pyrrolopyrrole core with methyl groups at the 1 and 4 positions and W(CO)₅C(OEt) groups at the 2 and 5 positions.</p>	W(CO) ₅ C(OEt)-PP- C(OEt)W(CO) ₅	P10

Chapter 1

Introduction

1 General

1.1 Dinuclear Complexes with Bridging Ligands.

Hydrocarbons can serve as σ,σ -, σ,π -, and π,π -bound bridging ligands between two metal fragments. “Early” and “Late” transition metals can be linked with a bridging hydrocarbon ligand¹.

Dinuclear complexes with bridging hydrocarbon chains are formed in most cases when organometallic nucleophiles are combined with electrophiles. For instance: reacting $[(\text{CO})_5\text{Re}(\eta^2\text{-C}_2\text{H}_4)]^+$ with $[\text{Re}(\text{CO})_5]^-$ gives a bimetallic complex with a C,C connecting ethylene bridge, $[(\text{OC})_5\text{ReCH}_2\text{CH}_2\text{Re}(\text{CO})_5]^-$ ². Organometallic nucleophiles, especially $[\text{Re}(\text{CO})_5]^-$, can be added to cationic complexes, incorporating as ligands: allyl, η^4 -diene, trimethylenemethane, dienyl, benzene, cycloheptatriene and tropylium. As a result, homo- and heterodimetallic complexes with σ,π -hydrocarbon bridges are formed. Complex **2** (figure 1) is thermodynamically favoured. When crystals of the σ,π -bonded dinuclear complex **1** were dissolved in polar solvents, they spontaneously underwent a metal-exchange process to afford **2**³.

¹ S. Lotz, P.H. van Rooyen, R. Meyer, *Advances in Organometallic Chemistry*, **1995**, Academic Press, 37, 219-320.

² K. Raab, U.Nagel, W.Beck; *Z Naturforsch. B*, **1983**, 38, 1466.

³ T.A. Waldbach, P.H. van Rooyen, S. Lotz; *Angew. Chem. Int. Ed. Engl.*, **1993**, 32, 710-712

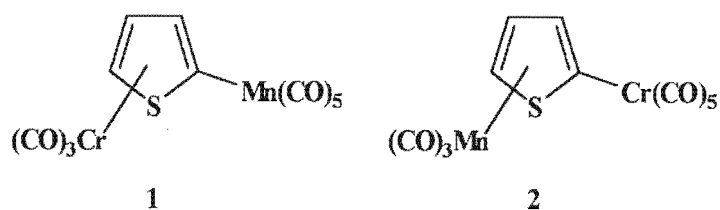


Figure 1: $(\eta^1\text{-tpMn}, \eta^5\text{-tpCr}) \rightarrow (\eta^1\text{-tpCr}, \eta^5\text{-tpMn})$ thiophene (tp) conversion

Pd(0) catalysts catalyse metal-carbon bond formation in a similar manner than they catalyse carbon-carbon bond formation. Metal iodides and trialkyltin moieties can smoothly couple in the presence of palladium, to afford σ -acetylides in appreciable yields⁴. Lo Sterzo and coworkers⁵ prepared the heterobimetallic complex in figure 2. Interplay of the two different metal groups may allow a fine-tuning of the properties of these materials.

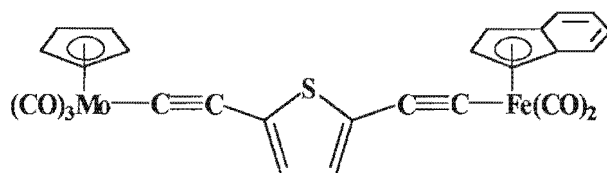


Figure 2: Heterobimetallic complex.

Crescenzi and Lo Sterzo⁶ investigated the coupling reaction of a variety of tin acetylides with the iron-halide complex $\text{CpFe}(\text{CO})_2\text{I}$, with the formation of an iron acetylide complex. There are other methods to prepare (σ -alkynyl)metal complexes, by the reaction of metal halides with anionic alkynylating reagents, but the advantage of their method relies on mild reaction conditions and on the use of easily accessible transition metal halides and alkynylstannanes. They extended the palladium catalysed alkynylation reaction to the preparation of metal acetylide complexes containing the 1,3-butadiyne ligand. (A convenient preparation for these types of complexes can give easy access to the building blocks of the metal-polyyne polymers). The starting material was recovered unchanged when reactions were run in the absence of the catalyst, and adding the palladium as PdCl_2 to the mixture also did not lead to the

⁴ E. Viola, C. Lo Sterzo, R. Crescenzi, G. Frachey, *J. Organomet. Chem.*, **1995**, 493, C9-C13.

⁵ E. Viola, C. Lo Sterzo, F. Trezzi, *Organometallics*, **1996**, 15, 4352-4354.

⁶ R. Crescenzi, C. Lo Sterzo, *Organometallics*, **1992**, 11, 4301-4305.

formation of any products. This is evidence that Pd⁰ is the species responsible for the promotion of the metal-carbon bond formation.

Pd/Cu catalysed C-C cross-coupling and selective desilylation reactions associated with 4-trimethylsilylethynyl as building block give simple access to several polyynes derived from 1,4-diethynylbenzene. These reactions allow the step-by-step synthesis of conjugated poly-yne with controlled length. They are potentially new precursors to establish extended π -conjugated rigid systems in organic polymers or bridges between metals⁷.

1.2 Transfer of electrons across organic bridges – Molecular wires.

Organometallic compounds can have a large diversity of oxidation states and ligand environments. The compounds have great possibilities for redox changes, a property that is largely associated with the metal centre. Facile redox ability can be seen to lead to large hyperpolarizability, with the metal centre being an extremely strong electron donor or acceptor. Organometallic compounds also have advantages in the range and mix of non-aromatic ligands that can be attached to the metals. These ligands can shift the occupied and unoccupied metal *d* orbitals that interact with the π -electron orbitals of the conjugated ligand system⁸.

Unsaturated hydrocarbons can act as electronic bridges between metal atoms.⁹ An important requirement for effective metal-metal communication is conjugation across the bridging ligands. The rigidity of the bridging ligands has a significant effect on the metal-metal interaction. Effective metal orbital-ligand orbital overlap is important. By varying the electron-donating ability of the bridging ligand, the amount of electronic communication may be modified.

⁷ O. Lavastre, L. Ollivier, P. H. Dixneuf, *Tetrahedron*, **1996**, *52*, 5495-5504.

⁸ N. J. Long; *Angew. Chem. Int. Ed. Engl.*, **1995**, *34*, 21-38.

⁹ W. Beck, B. Niemer, M. Wieser; *Angew. Chem. Int. Ed Engl.*, **1993**, *32*, 923-949.

The most obvious manifestation of electronic interaction between metal centres bridged by a common ligand is a separation of the two metal-centred redox potentials for metals that are apparently in chemically identical environments¹⁰. The *d*-electrons of the metal ions are in *d*(π) orbitals which can effectively overlap with the π -acceptor ligand and are delocalised across the conjugated bridge. If the one metal centre is oxidized the second becomes harder to oxidize. The comproportionation constant, K_c , expresses the stability of a mixed-valence complex relative to the isovalent states. When the interaction is strong, the odd electron is evenly delocalised between both metals. In complexes where the interaction is weaker, the valences are localized in the mixed-valence state, and there is the possibility of transferring an electron from the metal in the lower oxidation state to the one in the higher oxidation state (intervalence charge transfer, IVCT) within the molecule. Measuring IVCT processes allows easy assessment of the ability of particular bridging ligands to act as “molecular wires”.

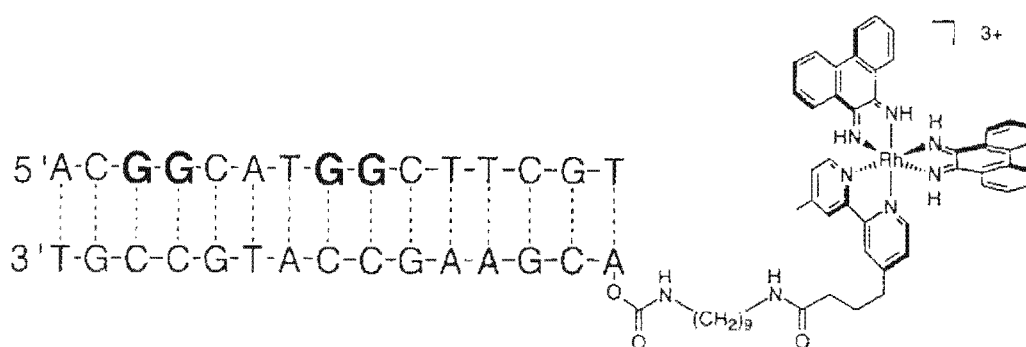


Figure 3: DNA duplex containing 5'-GG-3' doublet oxidation states, modified by covalent attachment of the functionalised rhodium intercalator.

The DNA double helix can serve as a molecular bridge for photo-induced electron transfer between metallointercalators. A phi complex of rhodium(III) binds DNA avidly by intercalation in the major groove. Barton *et al*¹¹ prepared oligomeric DNA duplexes with a rhodium intercalator covalently attached to one end, and separated spatially from 5'-GG-3' doublet sites of oxidation. They used the metallointercalator to introduce a photoexcited hole into the DNA- π -stack. Rhodium-induced photo-oxidation occurred specifically at the 5'-G and was observed up to 37Å away from the

¹⁰ M. D. Ward; *Chem Soc Rev*, **1995**, 121-134.

¹¹ D.B. Hall, R.E. Holmlin, J.K. Barton; *Nature*, **1996**, 382, 731-735.

site of rhodium intercalation. The yield of oxidative damage was found to depend sensitively on oxidation potential and π stacking, but not on distance. These results raised the question of the possibility that the DNA helix can act as a molecular wire.

Alkynylated Organometallic Structures

Several groups have looked at metal complexes with carbon sp (sp^2) bridges. Studies of metal-containing polyenes and polyynes are topical because of the expected novel properties of these materials. The sp bridge is the most basic and fundamental class of ligand of unsaturated organic ligand carbon chains. Fischer *et al*¹² studied the reactions of cationic carbyne complexes with carbonylmetalates. Adding $[\text{Co}(\text{CO})_4]^-$ to the cationic carbyne, $[\text{Cp}(\text{OC})_2\text{Mn}\equiv\text{CR}]^+$, afforded $[\text{Cp}(\text{OC})_2\text{Mn}=\text{C}(\text{R})-\text{Co}(\text{CO})_4]^-$ with a carbon link between the two metal atoms and could be classified as a possible electron conductor or molecular wire.

The group of Lapinte¹³ prepared $[\text{Fe}(\text{Cp}^*)(\text{dppe})] (\text{C}\equiv\text{C})-(\text{C}\equiv\text{C})[(\text{dppe})(\text{Cp}^*)\text{Fe}]$, and subjected the compound to cyclic voltammetry analysis (two reversible one-electron processes). The second iron centre has an electron-donor effect that reduces the first oxidation potential. The electron-donating bridge is large enough to balance the electron-withdrawing effect of the positive charge. The one-dimensional- C_4 -bridge acts as a molecular wire to convey the odd electron from the one metal centre to the other. Strong exchange interactions between the iron centres are propagated through the orbitals of the bridge. The metal-metal C_4 bridge in the half-sandwich series appears to be much more efficient for electronic coupling of the Fe^{II} and Fe^{III} centres than two C_2 bridges between two ferrocene units.

Lapinte^{13c} also prepared a much longer alkyne bridge, with eight carbon atoms. The cyclic voltammogram established that the C_8 -bridge acts as a molecular wire, connecting the electron-rich organo-iron centres (two reversible one-electron processes). These chains are stabilized by nonreactive terminal substituents.

¹² E.O. Fischer, J.K.R. Wanner, G. Müller, J. Riede; *Chem. Ber.*, **1985**, *118*, 3311.

¹³ (a) N. Le Narvor, L. Toupet, C. Lapinte; *J. Am. Chem. Soc.*, **1995**, *117*, 7129-7138; (b) N. Le Narvor, C. Lapinte; *J. Chem. Soc., Chem. Commun.*, **1993**, 357-359; (c) F. Coat, C. Lapinte; *Organometallics*, **1996**, *15*, 477-479.

Other groups¹⁴ have prepared similar complexes with Re instead of Fe. The terminal iron groups are more electron releasing, and diiron complexes are much easier to oxidize thermodynamically. The E°_1 and E°_2 values differ more in the diiron series, giving a larger value for K_c .

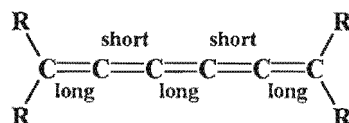
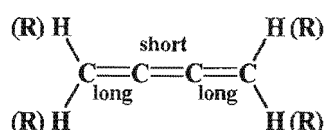
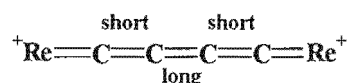
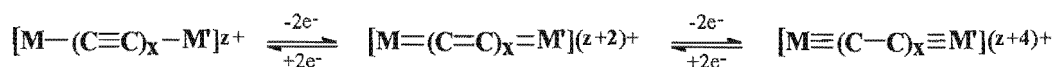


Figure 4: Representative redox states for even carbon chain complexes and the structure of the dication of (SS,RR)- $A^{2+}2PF_6^-$ and comparison with organic cumulenes.

A ReC_4Re assembly; $[(\eta^5-C_5Me_5)(NO)(PPh_3)Re(C\equiv C-C\equiv C)Re(Ph_3P)(ON)(\eta^5-C_5Me_5)](A)$, was isolated in three different oxidation states. The fragment $(\eta^5-C_5Me_5)Re(NO)(PPh_3)$ is sterically congested and strongly π -donating. Addition of $Ag^+PF_6^-$ yielded deep blue (SS, RR)- and (SR, RS)- $A^{2+}2PF_6^-$ salt. Reactions of (SS, RR)- $A^{2+}2PF_6^-$ with (SS,RR)-A yielded a green radical cation: (SS,RR)- $A^+PF_6^-$. Cyclic voltammograms of (SS, RR)-A were recorded and two chemically reversible one-electron oxidations were identified. Crystal structures established $Re=C$ conformations that allow for high degrees of overlap of the carbon p acceptor orbitals and the rhenium d -type HOMO. The IR spectrum of the cation radical complex gives only one ν_{NO} band, between the dication and A. The ground state of the radical cation was concluded to feature a ReC_4Re assembly with bond orders intermediate between A and $A^{2+}2PF_6^-$. Higher homologues will have increased numbers of resonance forms with reduced $C\equiv C$ bond orders and increased C-C bond orders. There is a distinct

¹⁴ M. Brady, W. Weng, Y. Zhou, I. W. Seyler, A. J. Amoroso, A. M. Arif, M. Böhme, G. Frenking, J. A. Gladysz, *J. Am. Chem. Soc.*, **1997**, *119*, 775.

possibility that immediately higher homologues may have paramagnetic, triplet biradical ground states, best described by the valence formulation: $^{++}\text{ReC}\equiv\text{C}(\text{C}\equiv\text{C})_x\text{C}\equiv\text{CRe}^{++}$.

Fulvalene Bridges

Dinuclear iron complexes display strong interactions between the metal centres because of extensive electronic delocalisation across a fulvalene bridge. Ligand exchange reactions between biferrocene and C_6Me_6 (HMB), provided $[\text{Fe}_2(\text{Fv})(\text{HMB})_2]^{2+}$ ($\text{Fv} = \mu_2, \eta^{10}\text{-C}_{10}\text{H}_8$) and analogues with other arenes.¹⁵ Fulvalene can also act as a molecular wire, connecting two metals. The bications all present four one-electron reduction waves. Comparing the potentials with those of the monomers outlined the electron withdrawing effect of the positive charge on the second iron centre. The differences could be attributed to strong interchange between the iron centres, propagated through the orbitals of the fulvalene ring. The stabilization of the $\text{Fe}^{\text{I}}\text{Fe}^{\text{II}}$ states was shown by the high values of the comproportionation constants.

Three isostructural oxidation states were isolated, consistent with the electrochemical and chemical reversibilities observed for the first two waves. There is little probability that a deep structural rearrangement interferes in the third ET (electron transfer). This is not the case for the fourth ET.

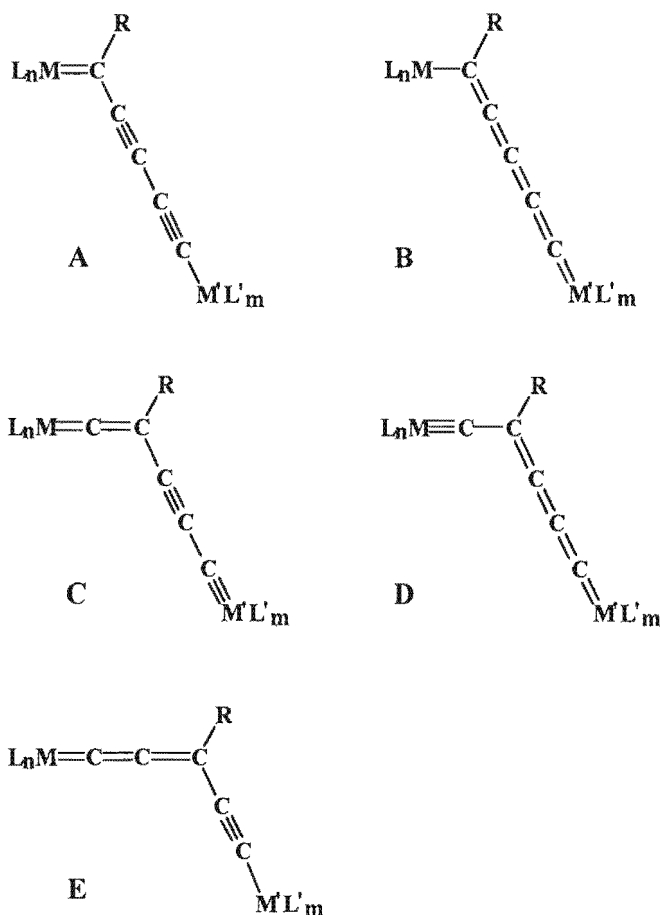
Other conjugated chains

Apart from naked C_x linkages, other types of π -conjugated carbon chains are also possible. Fischer and Hartbaum¹⁶ reported on the synthesis of some bi- and trinuclear complexes with a C_5R carbon bridge. For these complexes, several structural types are conceivable (Scheme 1, A–E). Gladysz *et al*¹⁷ prepared $[\text{Cp}^*(\text{NO})(\text{PPh}_3)\text{ReC}\equiv\text{C}-\text{C}\equiv\text{CC}(\text{OMe})=\text{Mn}(\text{CO})_2(\eta^5\text{-C}_5\text{Cl}_5)]$, the only example of a complex of the valence types A/B. The introduction of a metal centre without coligands is also possible to give trinuclear complexes (figure 5).

¹⁵ M-H Desbois, D. Astruc; *Organometallics*, **1989**, *8*, 1841-1847.

¹⁶ C. Hartbaum and H. Fischer, *Chem. Ber./Recueil*, **1997**, *130*, 1063.

¹⁷ W. Weng, T. Bartik, J.A. Gladysz; *Angew. Chem. Int. Ed. Engl.* **1994**, *106*, 2269-2272; *Angew. Chem. Int. Ed. Engl.* **1994**, *33*, 2199-2202.



Scheme 1: Binuclear carbon atoms with an odd number of carbon atoms linking the metal centres.

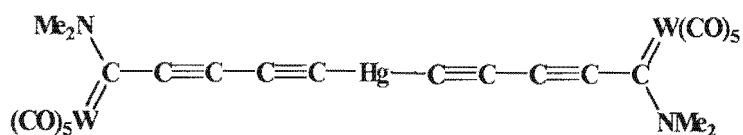


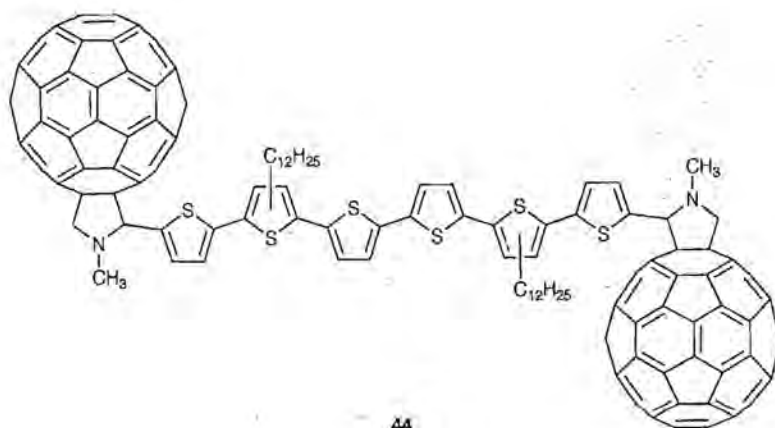
Figure 5: Trinuclear Complex.

Smith and coworkers¹⁸ synthesized directly fused oligoporphyrins sharing a common extended π electron system based on pyrrole-fused building blocks.

Fullerene dimers connected *via* molecular active bridges are interesting as they can find applications in areas such as artificial photosynthesis and novel molecular

¹⁸ L. Jaquinod, O. Siri, R.G. Khoury, K.M. Smith; *Chem. Commun.*, 1998, 1261.

electronic devices. In the following complex two fullerene spheres are connected through a molecular electroactive bridge¹⁹.



44

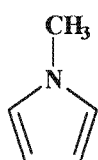
Figure 6: Structure of conjugated oligomer end-capped with two C₆₀ moieties.

¹⁹ J. L. Segura, N. Martin, *Chem. Soc. Rev.*, **2000**, *29*, 13-25.

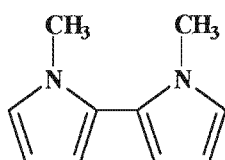
2 Ligands

2.1 N-Methylpyrrole, N,N'-Dimethylbipyrrole and N,N'-Dimethylpyrrolo[3,2-*b*]pyrrole.

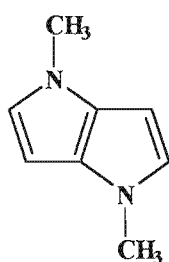
In this study heteroaromatic spacer units are important components of the unique ligands. Pyrrole derivatives were chosen and as metallation reactions of the ring protons are crucial for the forming of carbene ligands, N-methyl derivatives were used. The three types of pyrrole spacers selected were N-methylpyrrole, N,N'-dimethylbipyrrole and N,N'-dimethylpyrrolo[3,2-*b*]pyrrole. The ring protons adjacent to the nitrogen atom are activated for deprotonation by butyl lithium.



**N-Methylpyrrole
(L1)**



**N,N'-Dimethyl
bipyrrole
(L2)**



**N,N'-Dimethyl
pyrrolo[3,2-*b*]pyrrol
(L3)**

Figure 7: Spacer units of pyrrole.

2.2 Aromaticity²⁰.

N-Methylpyrrole is an aromatic molecule. No generally agreed precise definition of aromaticity exists. Aromaticity has originally been treated as a consequence of the π -electron structure. The π -electrons provide the frontier orbitals (HOMO and LUMO) of high polarizability, which consequently control the aromatic properties of the molecules. Accordingly the concept of hardness (half the HOMO/LUMO gap) is well associated with the aromatic character of cyclic π -electron systems.

Features and properties of aromatic compounds:

1. (Planar) cyclic delocalised π -electron systems.
2. More stable than their olefinic analogues by an energy called the resonance energy.
3. With bond lengths intermediate between those of typical single and double bonds.
4. With a π -electron ring current induced by an external magnetic field leading to increased diamagnetic susceptibility and typical diatropic [low field] chemical shifts of exocyclic protons in the ^1H NMR spectra.
5. Generally undergo substitution reactions more easily than addition.
6. Show higher energy ultraviolet/visible spectral bands and a more symmetrical structure for their IR spectra.

The formulation of any quantitative definition(s) of aromaticity needs to cover the different standpoints: firstly that of the molecule in its electronic ground state and secondly that of reactivity. Most quantitative measures of aromaticity are necessarily based on an assumption of some reference state.

²⁰ T.M. Krygowski, M.K. Cyrański, Z. Czarnocki, G. Häfeliinger, A.R. Katritzky; *Tetrahedron*, 2000, 56, 1783-1796.

Energetic criteria: Resonance energy was the first quantitative measure of aromaticity. The difficulties inherent in estimating any stabilization energy are (i) the selection of a proper and sufficiently well-defined reference state, (ii) limited precision and accuracy of the energy determination and (iii) the perturbation of derived energies by extraneous effects. Theoretical calculations are another source of energetic information for molecules and are based on graph-topological models.

Geometric criteria: Bond lengths are used as a criterion of aromaticity.

Magnetic criteria: ^1H NMR spectroscopy is very useful for studying aromatic character. Exocyclic protons exhibit characteristic low-field (diatropic) chemical shifts due to the induction of a diamagnetic ring current in a cyclic π -system.

From the point of view of chemical reactivity: Aromatic compounds tend to retain the π -electron system in their reactions. Electrophilic substitution reactions are more typical of aromatic compounds than addition reactions, but there are several exceptions to this rule.

2.3 Conducting polymers.

Polypyrrole films are formed through electrochemical oxidation and polymerisation of the monomers²¹. It is thought to form exclusively via α - α' linkages and represents a conducting organic polymer. Conductivities ranging between 10 and 100 S/cm are typically obtained. These materials uniquely combine the attractive mechanical properties of polymers and the electronic properties of metals or semiconductors. Polypyrrole become conducting when properly doped²². Doping agents produce bond breakings and formations. Polypyrroles are materials with a low degree of crystallinity. Polypyrroles are a mixture of pyrrolic chains with large weight dispersion and a mass density usually of the order of 1g/cm^3 . Structural data obtained

²¹ R. J. Waltman, J. Bargon, A.F. Diaz; *J. Phys. Chem.*, **1983**, 87, 1459-1463.

²² (a) R. Colle, A. Curioni; *J. Am. Chem. Soc.*, **1998**, 120, 4832-4839. (b) G.B. Street, J.L. Bredas; *J. Chem. Phys.*, **1984**, 5643-5648.

from polypyrrole samples suggest a structure of α,α' -linked rings in the transplanar conformation, with an estimated inter-ring distance of approximately $1.43 \pm 0.09\text{\AA}$.

The molecular structures of 2,2'-bipyrrole and 2,2':5',2''-terpyrrole were determined. The data indicates the rings are coplanar, adjacent rings are connected at the α -position and alternate, such that the nitrogen atoms point in opposite directions, and the bond length between the rings is very short, an indication that this bond has significant double bond character. Colle and Curioni^{21a} also noted that on increasing the size of the unit cell, one observes a clear reduction of the single/double bond alternation that indicates a larger delocalisation of the π -orbitals (there is a trend towards a larger quinoid character, towards a less pronounced alternation of double and single bonds in the carbon backbone). Another result was the almost perfect planarity of the optimised structure of the pyrrolic chains. The counterion in the oxidation process is crucial for the localization of charge and structural defects.

An electrode that is polymer modified can provide very dense reaction sites^{23a}, and can mediate electron transfer to a solution species. Oxidation-reduction of a conducting polymer electrode allows ionic species to go into/out of the polymer to maintain its electroneutrality. The binding capacity of polypyrrole disappears when it is reduced.

The properties of the conducting pyrrole polymers may be altered by β -substituents; appropriate substituents should induce a “push-pull” effect on the π -electrons. β -substitution is difficult with pyrrole. (β -substituted thiophenes are much more readily obtained.)^{23b}

²³ (a) T. Komura, T. Kobayashi, T. Yamaguti, K. Takahasi; *Bull. Chem. Soc. Jpn.* **1997**, *70*, 1061-1067; (b) R. J. Waltman, J. Bargon, A.F. Diaz; *J. Phys. Chem.*, **1983**, *87*, 1459-1463.

3 Carbene Complexes

3.1 Properties of Carbene Complexes.

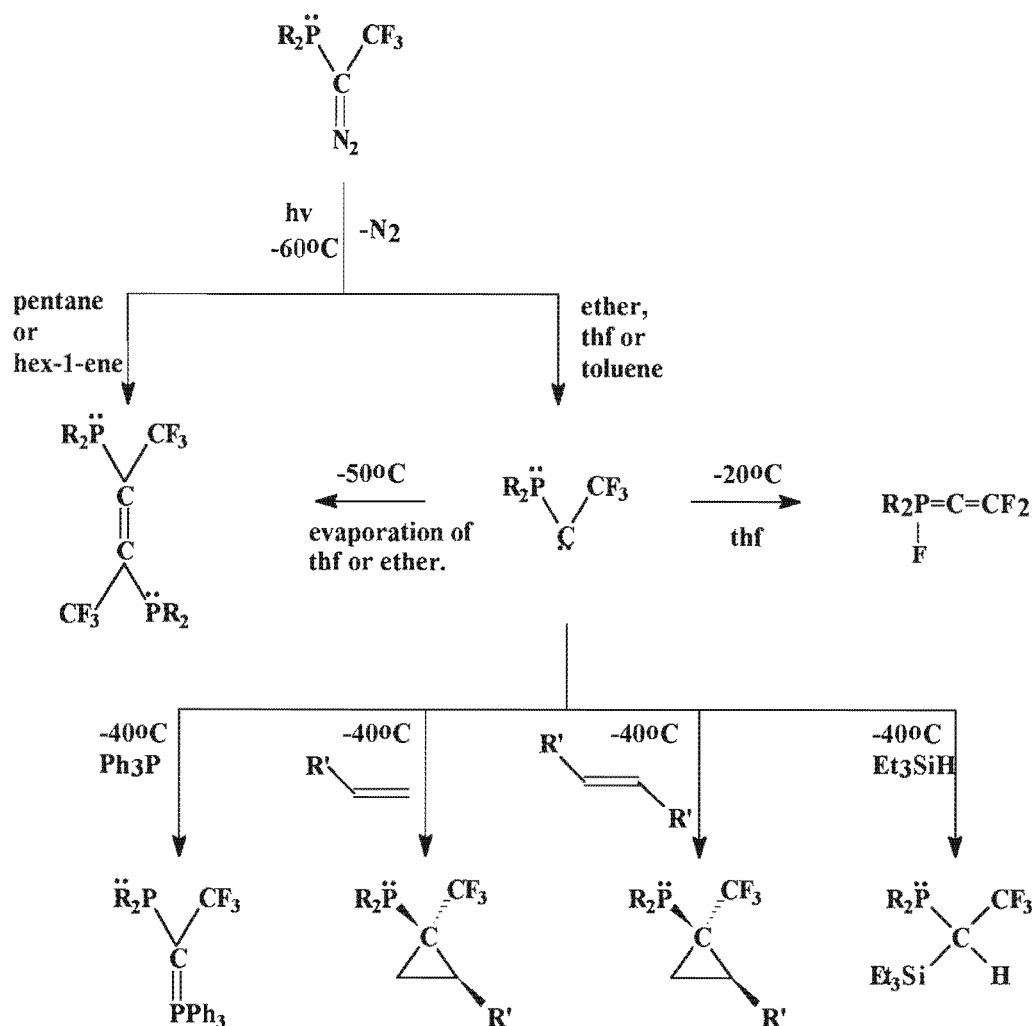
In 1964 E.O. Fischer and co-workers²⁴ synthesized the complexes referred to as metal carbenes. A carbene is an organic fragment consisting of a neutral discoordinate carbon with two substituents and two electrons not involved in bonding. It features a lone pair (singlet state) and an accessible vacant orbital, or two singly occupied nonbonding orbitals (triplet state).

Push-pull stabilization is very effective for preparing carbenes featuring high thermodynamic stability, without destroying their typical carbene reactivity. Bertrand *et al*²⁵ synthesized a singlet carbene that was stable in solution up to -30°C for weeks and whose chemistry exactly parallels that of its transient congeners. Photolysis of [bis(dicyclohexylamino)phosphanyl]-(trifluoromethyl)diazomethane in donor solvents cleanly generated the desired free carbene. The phosphanyl group features both resonance and inductive push effects, and provides greater steric bulk than the methoxy group. The CF_3 group has a pull-inductive effect.

Evaporation of the solvent resulted in dimerization, generating the alkene. Upon warming the thf solution to -20°C , a clean rearrangement occurred, affording the cumulene. Treating the thf solution with the carbene at -40°C with triphenylphosphine, a strong Lewis base, yielded the phosphorus ylide, confirming the interaction of thf and ether with the carbene, and therefore the Lewis acid character of the carbene. Even subtle effects, observed with transient carbenes could be reproduced with the carbene.

²⁴ E.O. Fischer, A. Maasböl; *Angew. Chem.* **1964**, *76*, 645.

²⁵ C. Buron, H. Gornitzka, V. Romanenko, G. Bertrand; *Science*, **2000**, *288*, 834-836.



Scheme 2: Preparation and reactions of the singlet carbene.

Carbenes can be stabilized by coordination to a metal fragment²⁶. The carbene carbon is connected to the metal via the electron pair in a metal-carbon double bond. The metal is usually a low-valent Group VI to VIII transition metal (Cr, Fe, Mn), but other transition metal carbene complexes, especially those of group X have also been synthesized and studied (Ni(II), Pt(II), etc).

To obtain a strong metal-carbon σ -bond, the use of a strongly directed orbital of the metal is much more necessary than is required for bonding ligands of the type of carbon monoxide²⁷. The formation of stable metal-to-carbon σ -bonds may be considered to require significant p character in order to achieve the desired directional

²⁶ H. Rudler, A. Parlier, M. Rudler, J. Vaissermann; *J. Organomet. Chem.*; **1998**, 567, 101-117.

²⁷ T.S. Piper, and G. Wilkinson; *J. Inorg. Nucl. Chem.*, **1956**, 3, 104-124.

property for good overlap with the carbon orbitals. The energy of the p orbitals decreases, relative to the d and s orbitals, in going from the first to the third series of transition elements. The participation of the p orbitals in the bonding of groups other than the π -cyclopentadienyl ring should become increasingly easy and the strength of the metal-to-carbon σ -bond should increase with increasing atomic weight of the metal.

In Fischer carbene complexes one substituent of the carbene acts as a π -donor, allowing for electronic stabilization of the electron deficient carbene carbon. The other substituent may be a saturated or an unsaturated group. Ligands with π -acceptor properties (carbon monoxide, phosphine or cyclopentadienyl ligands) stabilize the low-valent metal centre.

Some excellent review articles of carbene complexes have appeared in literature²⁸ and newer studies focuses on the application of carbene complexes in synthesis, or new novel methods of synthesis. A selection of some interesting results in carbene synthesis, which appear in literature over the past few years, will be given. They are acetylide modifications, carbene transfer reactions, vinylidene intermediates, carbene modifications and multimetal carbene complexes

Carbene complexes have recently been prepared from the reaction of $\text{PhC}\equiv\text{CH}$ in 2-chloroethanol with the solvent-cationic complex $\text{trans}[\text{Pt}(\text{Me})(\text{PPh}_3)_2(\text{solv})][\text{BF}_4]$. In the reactions of halo alcohols, in the presence of 1 equivalent of HBF_4 , with the acetylides afforded alkylalkoxycarbene complexes $\text{trans}[\text{Pt}(\text{CH}_3)(\text{C}\equiv\text{CR})(\text{PPh}_3)_2]$ ($\text{R} = \text{Ph, p-tolyl}$)²⁹.

Diaminocarbene complexes are quite stable species, and carbene transfer reactions between transition metal complexes have been reported³⁰. Diaminocarbene ligands were transferred from tungsten metal to a palladium centre. This method was also used to synthesize $\text{Pt}(\text{II})$, $\text{Rh}(\text{I})$ and $\text{Au}(\text{I})$ carbene complexes.

²⁸ (a) K.H. Dötz, H. Fischer, P. Hofmann, F.R. Kreissl, U. Schubert, K. Weiss; *Transition Metal Carbene Complexes*, **1983**, Verlag Chemie, Weinheim.; (b) G. Bertrand (Editor); *J. Organomet. Chem. Special Issue: Transition Metal Complexes of Carbenes and Related Species in 2000*; **2001**, 3-754.

²⁹ R. A. Micheli, M. Mozzon, B. Vialetto, and R. Bertani; *Organometallics*, **1998**, *17*, 1220-1226.

³⁰ S-T. Liu, T-Y. Hsieh, G-H. Lee, and S-M. Peng; *Organometallics*, **1998**, *17*, 993-995.

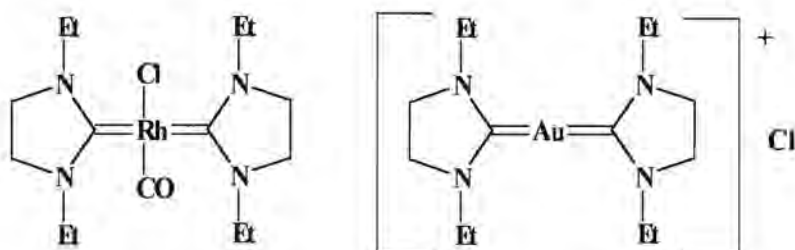


Figure 8: Gold and Rhodium carbene complexes.

Reacting³¹ $\text{RuL}_{\text{OEt}}(\text{PPh}_3)_2\text{Cl}$ with $\text{Me}_3\text{SiC}\equiv\text{CH}$ in the presence of NH_4PF_4 afforded the methoxycarbene complex $[\text{L}_{\text{OEt}}(\text{PPh}_3)_2\text{Ru}=\text{C}(\text{OMe})\text{Me}]\text{PF}_6$, formed presumably via nucleophilic attack of MeOH on the vinylidene intermediate. The L_{OEt} fragment was found to be considerably more basic than the CpRu congener, capable of stabilizing a variety of π -acid ligands, like vinylidenes, olefins and cyclic carbenes. Ruthenium and rhodium complexes of L_{OR} were found to be catalysts for the oxidation of hydrocarbons and alcohols and the hydrogenation of olefins. The $\text{Ru}-\text{O}$ (*trans* to carbene C) distance is long, apparently due to the strong *trans* influence of the carbene ligand. Treating $\text{RuL}_{\text{OEt}}(\text{PPh}_3)_2\text{Cl}$ with 2-phenyl-3-butyn-2-ol afforded the allenylidene complex. From cyclic voltammetry data it was clear that the π -acidity of carbene, vinylidene and allenylidene ligands are comparable to that of the carbonyl ligand.

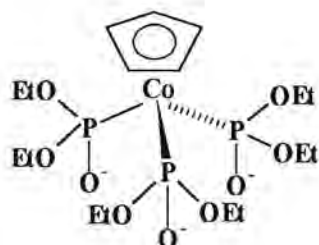


Figure 9: L_{OEt}

Macomber *et al*³² used α,β -unsaturated carbene complexes as electrophiles, and by reaction with α -deprotonated carbene complexes, were able to prepare numerous di-

³¹ W-H Leung, E.Y.Y. Chan, W-T. Wong; *Organometallics*, **1998**, *17*, 1245-1247.

³² (a) D.W. Macomber, M.-H Hung, A.G. Verma, R.D. Rogers; *Organometallics*, **1988**, *7*, 2072-2074; (b) D.W. Macomber, M.-H Hung, P. Madhukar, M. Liang, R.D. Rogers; *ibid.* **1991**, *10*, 737-746; (c)

and even some tricarbene complexes. An example of a trinuclear carbene complex of tungsten is shown in figure 10.

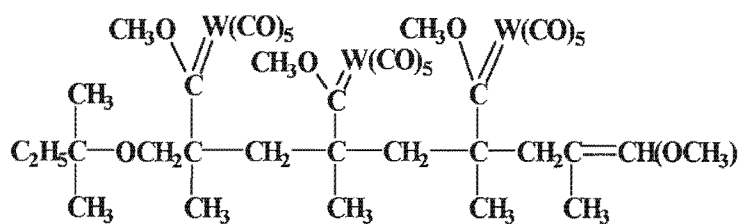


Figure 10: Trinuclear carbene complex of tungsten.

Rose-Munch *et al*³³ synthesized five new η^5 -cyclohexadienyl complexes by adding anionic Fischer carbene complexes of W and Cr to the (η^6 -benzene)tricarbonylmanganese cation. Hydrogen atoms α to the carbene carbon atom in Fischer carbene complexes are acidic and can be easily removed on treatment with bases, such as BuLi, to form carbene anions or 'enolates', of the type $\text{Li}[\text{ML}_n\{\text{C}(\text{OR})\text{CH}_2\}]$. These anions have been found to add to cationic Re, Cr and Mo complexes and also cationic Fe cyclohexadienyl complexes.

3.2 Synthesis of Carbene Complexes.

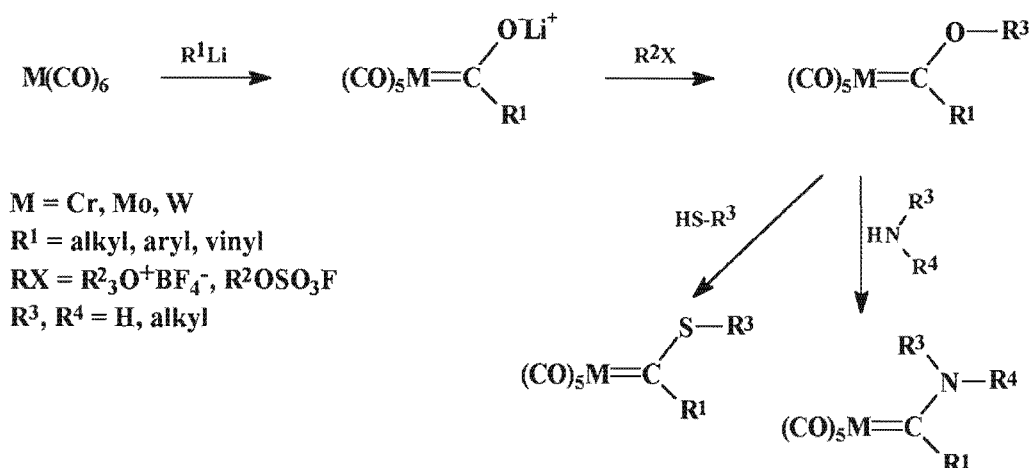
The most general route is the addition of an organolithium nucleophile to a metal carbonyl to give an acyl metallate, which undergoes O-alkylation by strong alkylating reagents, like trialkyloxonium salts, alkyl fluorosulfonates or alkyl trifluoromethanesulfonates, to form alkoxy carbene complexes. Treating alkoxy carbene complexes with amine or thiol nucleophiles affords amino and sulfur containing carbene complexes.

The classical Fischer route²⁴ to metal carbene complexes is given in Scheme 3.

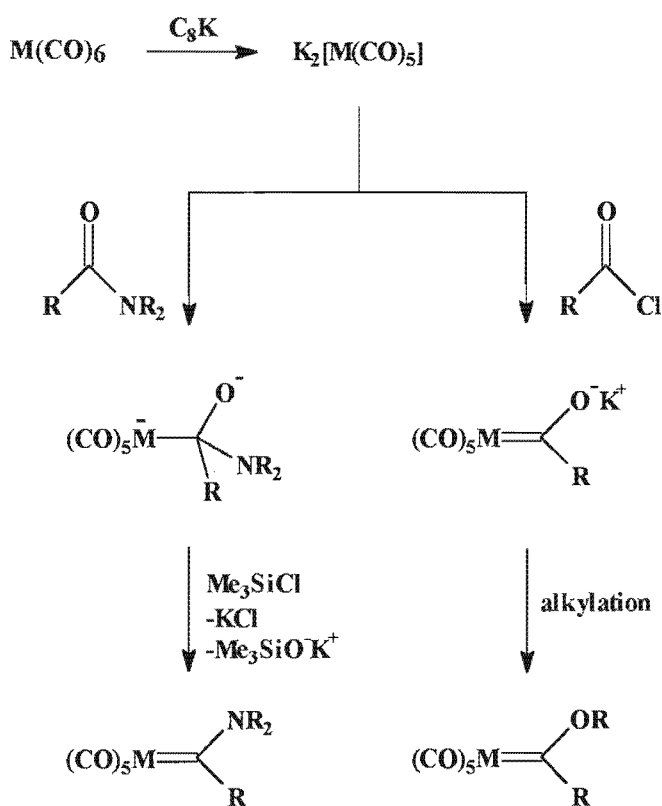
D. W. Macomber, M.-H. Hung; *J. Organomet. Chem.* **1989**, *366*, 147-154; (d) D. W. Macomber, P. Madhukar, R. D. Rogers; *Organometallics*, **1991**, *10*, 2121-2126.

³³ F. Rose-Munch, C. Le Corre-Susanne, F. Balssa, E. Rose, J. Vaisserman, E. Licandro, A. Papagni, S. Maiorana, W.-d Meng, G. R. Stephenson; *J. Organomet. Chem.* **1997**, *545-546*, 9.

Hegedus and Semmelhack³⁴ developed an alternative approach (Scheme 4) by combining an organoelectrophile and a metal nucleophile.



Scheme 3: Fischer route to metal carbene complexes.



Scheme 4: Hegedus-Semmelhack approach to alkoxy- and aminocarbene complexes.

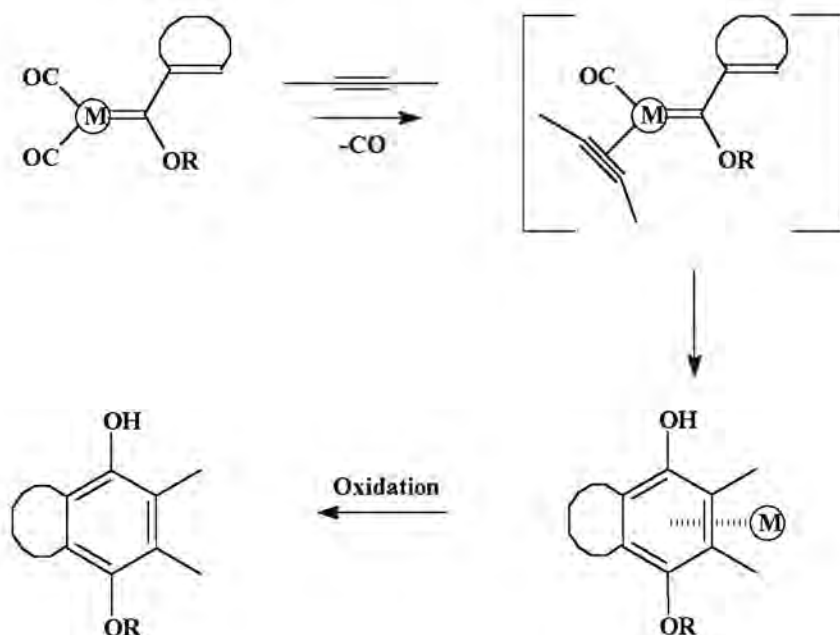
³⁴ (a) M.A. Schwindt, T. Lejon, L.S.Hegedus; *Organometallics*, **1990**, *9*, 2814-2819; (b) M.F. Semmelhack, G.R. Lee; *Organometallics*, **1987**, *6*, 1839.

Alkylation generates the alkoxy-carbene complexes, while TMSCl-assisted deoxygenation of the tetrahedral intermediate affords aminocarbene complex. C_8K was found to be an efficient reducing agent to convert $Cr(CO)_6$ to $K_2Cr(CO)_5$. The reaction procedure and purification of products were much more convenient than those for the sodium naphthalene procedure.

3.3 Reactions of Carbene Complexes.

Many important reactions of Fischer carbene complexes have been recorded of which nucleophilic attack on the carbene carbon, carbyne synthesis and modification of carbene substituents are but a few. A widely applied reaction is the so-called Dötz³⁵ reaction.

The benzannulation ([3+2+1] carbonylative cycloaddition with alkynes) of alkoxy-carbene complexes with unsaturated substituents (vinyl or aryl), to give cyclohexadienones or phenols, is one of the most unique types of carbene reactions.

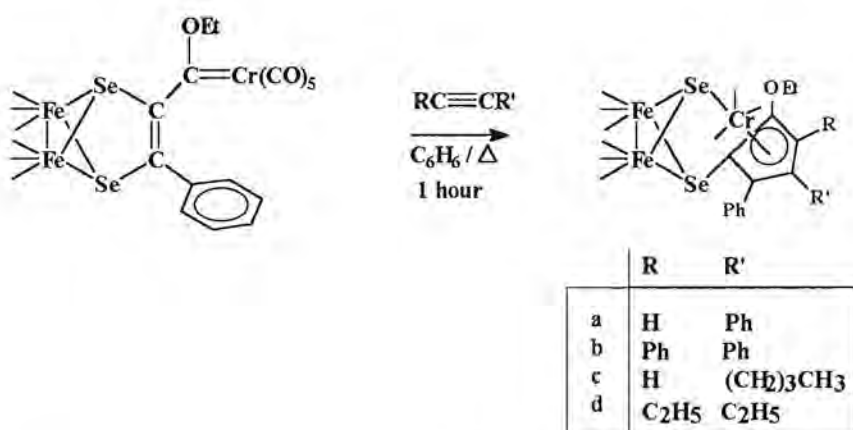


Scheme 5: Benzannulation of carbene complexes.

³⁵ K.H. Dötz, P. Tomuschat; *Chem. Soc. Rev.*, 1999, 28, 187-198.

Chromium is the metal template of choice, as it allows excellent chemo- and regioselectivity under mild conditions. By contrast the tungsten homologues result in the formation of formal [3+2] cycloaddition products without carbonyl incorporation. The benzannulation is compatible with a broad substitution pattern in the alkyne and the unsaturated carbene side chain. Benzannulation is an attractive methodology for the synthesis of natural products with hydroquinoid, quinoid or fused phenolic structures.

Mathur and Ghosh³⁶ reacted cluster supported carbene complexes with alkynes. Alkoxy carbene complexes of chromium with unsaturated substituents normally afforded the benzannulation products, while tungsten analogues and amino carbene complexes of chromium with similar substituents afforded indane derivatives (insertion of a CO group from the metal carbonyl does not take place during annulation).



Scheme 6: Benzannulation reaction with cluster-supported carbene complexes.

Other reactions of importance for organic synthesis are:

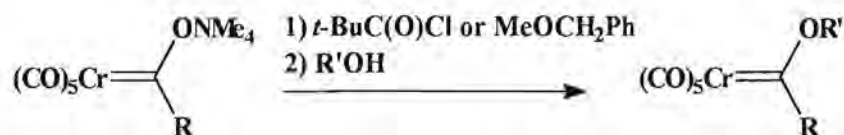
[2+2] cycloadditions, [3+2] cycloadditions, [4+2] cycloadditions, *ene* reactions and sigmatropic rearrangements, coupling of anions of the carbene ligand with C-X σ -bonds, coupling of anions of the carbene ligand with C-X π -bonds, Michael additions

³⁶ P. Mathur, S. Ghosh; *Organometallics*, 1998, 17, 3926-3930.

to α,β -unsaturated carbene complexes, and nucleophilic substitutions at and cleavage of the carbene ligand³⁷.

Recent work of interest based on syntheses with carbene complexes is discussed in the remainder of this section:

Iwasawa³⁸ synthesized fully substituted furan, pyrrole, butenolide and 2-butene-4-lactam esters. Anionic propargyl derivatives of group 6 metals are generated by the addition reaction of alkynyllithiums to Fischer carbene complexes. These species react with various electrophiles like aldehydes, sulfonylimines, carbon dioxide and tosyl isocyanate to give trisubstituted furans, pyrroles, butenolide and 2-butene-4-lactam esters, respectively. The reaction with an aldehyde is thought to proceed via a [3+2] cycloaddition path with concomitant migration of the metal group to give a vinylmetallic intermediate, which was oxidized with iodine. Tungsten complexes were usually employed, due to their stability, but in some cases a molybdenum complex was employed because the corresponding propargyl complex display higher reactivity towards electrophiles.



Scheme 7: Friedel crafts acylation of chromium carbene complexes.

Photolysis of chromium carbene complexes generates species with ketene-like reactivity. Bueno *et al*³⁹ examined the use of chromium-stabilized ketenes as electrophiles for the Friedel-Crafts acylation reaction.

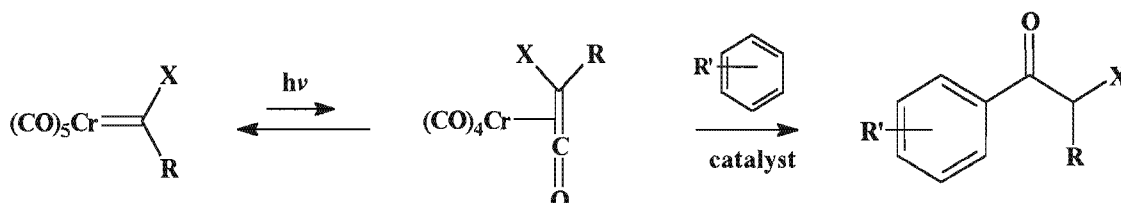
The aromatic system could be attached either to the heteroatom (generated *in situ* from tetramethylammonium *ate* complexes by the exchange reaction of aromatic ring-containing alcohols with acyloxy carbene complexes), or the R group (alkylation of a preformed carbene or by utilizing chromium pentacarbonyl dianion and the requisite

³⁷W.D. Wulff, *Comprehensive Organic Synthesis*, Trost, Fleming, 5, 1065-1114.

³⁸N. Iwasawa, T. Ochiai, and K. Maeyama; *J. Org. Chem.*, **1998**, *63*, 3164-3165.

³⁹A. B. Bueno, W. H. Moser, and L. S. Hegedus; *J. Org. Chem.*; **1998**, *63*, 1462-1466.

acid chloride), obviating the need to utilize the aromatic substrate in large excess. They found that the photochemically activated chromium carbene complexes were active electrophiles for the intramolecular Friedel-Crafts acylation in the presence of catalytic or equivalent amounts of ZnCl_2 , provided at least one activating group is present in the aromatic system.



Scheme 8: Generation of carbene complex in which the aromatic system is tethered by the heteroatom.

The precursors (β -dialkylaminoalkenyl)carbenechromium complexes can lead to a great variety of products, including cyclopentadienes, complexed fulvenes, methylenecyclopentenones, (aminoalkenyl)cyclopentenones, acylcyclopentenones, cyclopenta[*b*]-pyranes and even spiro[4.4]nonatrienes⁴⁰. The complex shown in figure 11 reacts with three molecules of arylalkyne in THF to give spiro[4.4]nonatrienes. When treated with mesitylethyne under the same conditions, complete conversion was detected after seven days and η^5 -tricarbonyl(dihydroazepinyl)chromium was obtained.

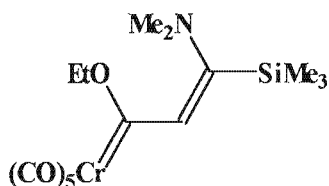


Figure 11: Carbene complex with α -ene substituents.

Formally, the overall conversion is a [5+2] cycloaddition. Bulky terminal alkynes lead to (isobutyrylmethylene)pyrrolidines, that arise from a primarily formed η^5 -tricarbonylchromium-complexed formal [5+2] cycloadduct.

⁴⁰ H. Schirmer, T. Labahn, B. Flynn, Y-T. Wu, A. de Meijere; *Synlett.*; **1999**, 12, 2004-2006.

Finally, Mori *et al*⁴¹ synthesized medium sized lactones (8-membered, 9-membered and 10-membered) from alkynes, having the hydroxy group in a tether using chromium carbene complexes. The yields were improved when alkynes had substituents in the chain. The hydroxy or silyloxy group in a tether attacks the ketene moiety to produce lactones.

3.4 Carbene Complexes as potential molecular wires.

Several complexes with unsaturated cyclic π -conjugated carbon bridges linking two metal-carbene fragments are known, including phenyl-, biphenyl-, binaphthyl-, anthracenyl-, or 1.6-methanol-[10]annulen-2,7-diyl-bridged complexes and derivatives with an ammonium pentadiene bridge.

Fischer *et al*⁴² synthesized biscarbene complexes with an alkynediyl fragment linking two $(\text{CO})_5\text{M}=\text{C}(\text{R})$ units. They prepared the aminocarbene complexes. The alkoxy carbene complexes are very labile. By insertion of electron-rich alkynes into the metal-carbene bond, which is a typical reaction of electrophilic carbene complexes, the complexes shown in figure 12 could be prepared.

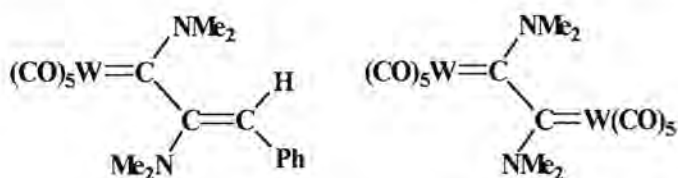


Figure 12: Products that formed from the insertion of an alkyne into the $\text{W}=\text{C}$ bond of $(\text{CO})_5\text{W}=\text{CHPh}$.

⁴¹ M. Mori, T. Norizuki, T. Ishibashi; *Heterocycles*, **1998**, *47*, 651-655.

⁴² C. Hartbaum, E. Mauz, G. Roth, K. Weissenbach, H. Fischer; *Organometallics*, **1999**, *18*, 2619-2627.

In the biscarbene complex the carbene planes are almost orthogonal, which excludes the presence of a bridging delocalised π -system. The NMR data of the following complex, however, also prepared by them, indicates considerable π -delocalization in the bridge.

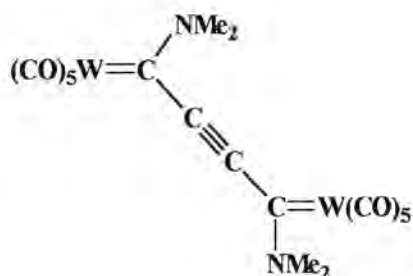


Figure 13: Biscarbene complex with π delocalisation.

Pd-catalyzed coupling of complexes $[(\text{CO})_5\text{W}=\text{C}(\text{NMe}_2)(\text{C}\equiv\text{C})_x\text{I}]$ ($x = 2, 3$) with the C-stannylated alkynylcarbene complexes afforded the binuclear $\text{C}_{10}(\text{NMe}_2)_2$ - and $\text{C}_{14}(\text{NMe}_2)_2$ -bridged complexes $[(\text{CO})_5\text{W}=\text{C}(\text{NMe}_2)(\text{C}\equiv\text{C})_x(\text{Me}_2\text{N})\text{C}=\text{W}(\text{CO})_5]$ ($x = 4, 6$). Spectroscopic data indicated that the $\text{C}\equiv\text{C}$ units are essentially localized, while, in the above molecule (figure 13), the data indicate it is best described as a hybrid of a dipolar allenyl-type compound and an alkynylcarbene complex.

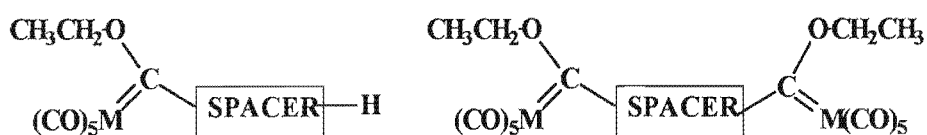
4 Aim

The objective of this study was to investigate aspects of the synthesis, characterization and structural features of carbene complexes with heteroaromatic substituents. In the biscarbene complexes there are extended conjugation, with the conjugation extending over the rings to the metal-carbene carbon double bond. Such complexes have been prepared, with a number of organic bridges.

Pyrrole, bipyrrrole and pyrrolo[3,2-*b*]pyrrole were used as carbene substituents and bridging moieties in chromium and tungsten mono- and biscarbene complexes. The Fischer method was used to synthesize the new carbene complexes.

The influence of the carbocationic carbene centre on the pyrrole rings was investigated to see if charge delocalisation could be established in solution (NMR) and in the solid state (X-ray diffraction). Also, the relative stability of the carbene complexes with different heteroatom substituents is of interest in our laboratories and the pyrrole derivatives will be compared with analogues thiophene carbene complexes.

Additional aspects of interest are the synthesis of the bipyrrrole and condensed pyrrolopyrrole substrates, as well as the conditions required for double metallation reactions of the substrate.



M = W, Cr

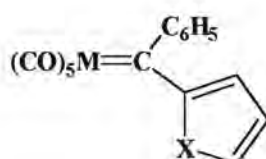
Spacer: pyrrole, bipyrrrole, pyrrolopyrrole

Chapter 2

Carbene Complexes of Pyrrole

1 Background.

In 1976 Fischer *et al*¹ prepared a series of products by reacting pentacarbonyl-(arylmethoxycarbene) complexes of chromium(0) and tungsten(0) with aryllithium compounds at low temperatures to give addition products. On purification using silica gel/ pentane chromatography, they isolated and characterized, among others, the following type of bisarenyl carbene complexes. These included examples of pyrrole and thiophene.



M = Cr, W
X = NMe, S

The electronic effects of the heteroatom in the ring are important to consider. Gleiter² and his group described the electronic effects of the heteroatom in five-membered heterocycles. They found that pyrrole differs from furan, thiophene and selenophene

¹ E.O. Fischer, W. Held, F.R. Kreissl, A. Frank, G. Huttner; *Chem. Ber.*, **1977**, *110*, 656.

² R. Gleiter, M. Kobayashi, J. Spanget-Larsen, S. Gronowitz, A. Konar, M. Farnier; *J. Org. Chem.*, **1977**, *42*, 2230.

with regard to the first and second ionisation potentials. The electrons are removed from the highest and second highest molecular orbitals, the $a_2(\pi)$ and the $b_1(\pi)$, respectively.

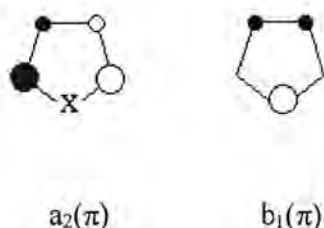


Figure 1: Molecular orbitals of heteroatomic five-membered rings.

The energy of the $a_2(\pi)$ level should be much less affected than the $b_1(\pi)$ level by a change in the heteroatom (there is a node on the heteroatom), according to simple perturbation theory. Pyrrole is a striking exception in the series furan, pyrrole, thiophene and selenophene. The shift of the $a_2(\pi)$ level is much larger than the shift of the $b_1(\pi)$ level, and there is an inconsistent shift toward lower binding energies, even though nitrogen is the second most electronegative element, when compared with oxygen, sulfur and selenium.

N is a much stronger σ electron acceptor than a π electron donor. The N-H group has a large inductive effect on the carbon frame. The replacement of sulfur by selenium is a minor perturbation, but it is not a minor perturbation if either one is replaced with NH. Simple perturbation theory no longer applies. An all-valence electron model, including electron interaction terms, is appropriate.

Replacing O by S or NH leads to an increase in the potential and kinetic energy term, but a decrease in the repulsion. Part of the attracting core and part of the repulsing electron density is moved away from the HOMO orbital (localized in the butadiene fragment). The N-H bond polarity is high, and it increases the electron density on the ring, which increases the e^-e^- repulsion. Substituting the hydrogen for a methyl leads to further destabilization. In the thiophene case the stabilizing and destabilizing effects cancel, but not in the case of pyrrole.

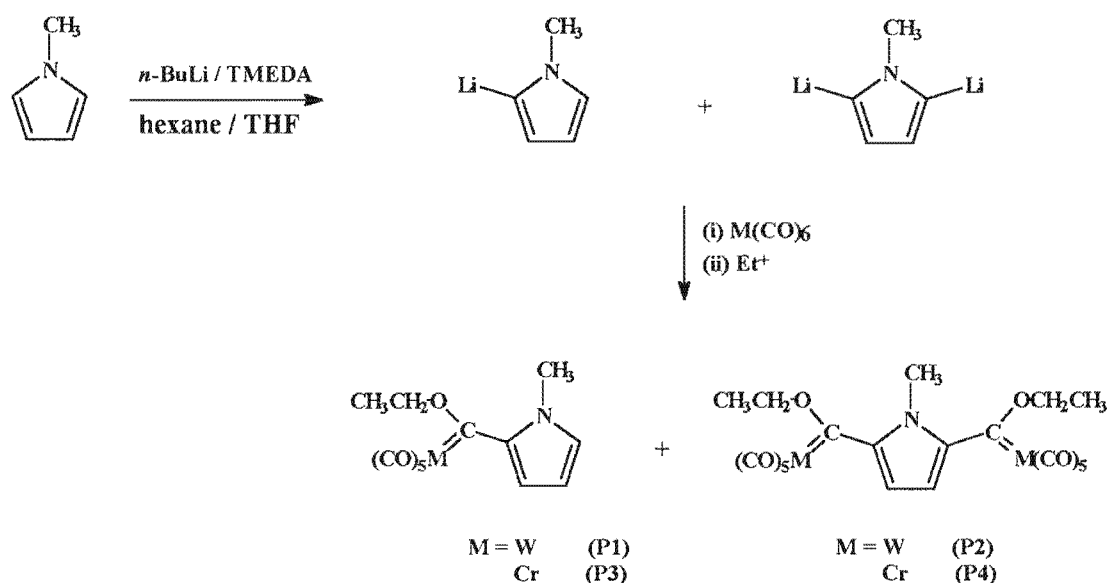
With the second highest occupied orbital – $b_1(\pi)$ – the electronegativity of the heteroatom is expected to stabilize the level, since the orbital has a high amplitude on the heteroatom. The effective electronegativity of the NH group is much less than that of the nitrogen atom, since the nitrogen can withdraw electrons from the hydrogen atom. Therefore the level is not stabilized on going from S to NH.

2 Synthesis.

The biscarbene complex was prepared by lithiating the ligand in the 2 and 5 positions, according to the method of Karas *et al.*³ To a solution of TMEDA in hexane was added *n*-butyl lithium, in a 1:1 molar ratio. The mixture was stirred, N-methylpyrrole was added, and the mixture was refluxed. The mole ratio of the pyrrole to butyl lithium was approximately one to two.

The mixture was cooled and then W(CO)₆ or Cr(CO)₆ was added whereby the solution became very dark. The hexane was removed under vacuum and the metal acylate was alkylated with the oxonium salt, Et₃OBF₄.

Separation of the products on silica gel afforded the monocarbene complex in the tungsten case and the biscarbene product in the chromium case. The monocarbene chromium product was prepared later from reacting only one equivalent of butyl lithium with N-methylpyrrole.



Scheme 1: Fischer method of carbene synthesis.

³ J. Karas, G. Huttner, K. Heinze, P. Rutsch, L. Zsolnai; *Eur. J. Inorg. Chem.*, **1999**, 405.

3 Characterization of Complexes.

3.1 Tungsten Complexes

Mono- and biscarbene complexes with pyrrole substituents were obtained and characterized by NMR, IR and UV spectroscopy and MS spectrometry. The spectroscopic data is given below and discussed.

3.1.1 NMR spectroscopy

The ^1H NMR data is given in table 1 and the ^{13}C NMR data is given in table 2.

PROTON NMR SPECTROSCOPY

Monocarbene complex

The chemical shift of the quartet in the proton spectrum at 4.92ppm indicates that the product that formed is an electrophilic carbene complex. The signal of the OCH_2CH_3 protons is shifted downfield compared to the other methylene protons adjacent to an oxygen atom because of the stabilization of the carbene carbon by the oxygen. These protons couple with the OCH_2CH_3 protons, splitting their signal into a triplet.

Three proton signals for the protons on the ring are seen in the aromatic region (between 6 and 8ppm). The signal at 6.26ppm is taken to be the signal of one proton, C4-H. (Integration values confirms this). It is split into a doublet of doublets. The C4 proton signal would be split by C3-H and C5-H.

Compared to the data for the N-methylpyrrole substrate, the signals of the protons bound to C3, C4 and C5 are respectively shifted downfield by: 1.53ppm, 0.14ppm and 0.30ppm. The carbene carbon drains electron density from the pyrrole ring, and so deshields the ring protons. The C3 proton is affected most by the carbene carbon, since

C3 is closer to the carbene carbon than the other two ring protons. It is interesting that the C4 proton is less affected by the carbene than the C-5 proton, even though it lies closer. An explanation for this could be found when one considers the π -resonance effect:

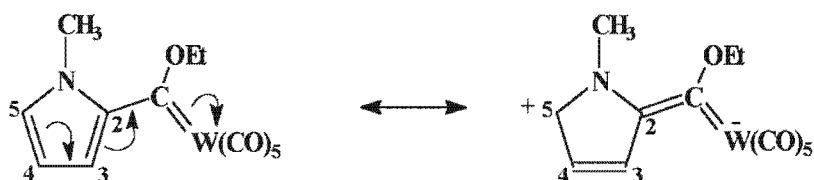


Figure 2: Delocalization of electrons in the monocarbene complex.

Positive charges are affected on the C5 and C3 protons, which are deshielded, but not on C4-H.

For the ring protons, the signals are not clearly resolved and for the ethyl protons there seem to be two signals. A possible explanation for this duplication is that the product consists of two isomers. The close proximity of the N-methyl, as well as charge transfer from pyrrole ring to the carbene carbon could result in restricted rotation around the C(pyrrole)-C(carbene) bond, resulting in two isomers shown in figure 3.

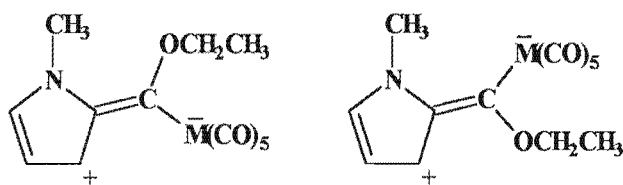


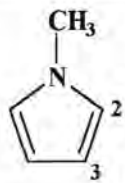
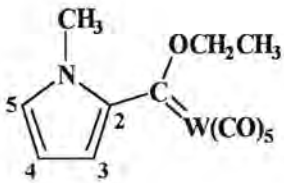
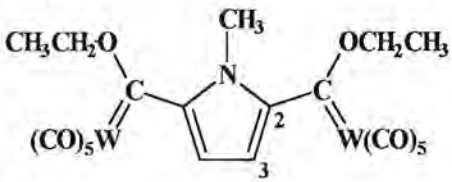
Figure 3: Restricted rotational isomers.

Biscarbene complex.

The characteristic carbene quartet is seen at 4.96ppm. The spectrum is as expected. A singlet is seen for the ring protons that are in the same chemical environment. Compared

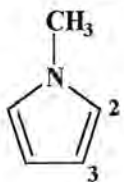
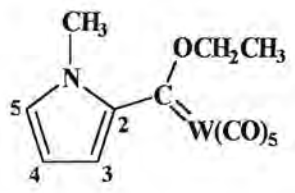
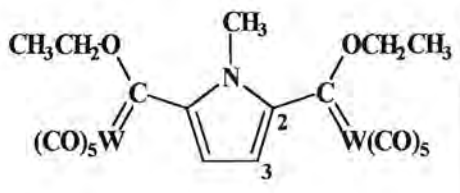
to N-methylpyrrole, the methyl resonance of the monocarbene complex is shifted downfield and in the case of the biscarbene complex it is shifted upfield.

Table 1: ^1H NMR resonances of the mono- and biscarbene complexes of tungsten.

Compound	Proton	δ (ppm)	J (Hz)
	N-CH ₃	3.66 (<i>s</i>)	-
	C2-H	6.60 (<i>t</i>)	$J_{2,3} = 2.07$
	C3-H	6.13 (<i>t</i>)	$J_{3,2} = 2.07$
	N-CH ₃	3.78 (<i>s</i>)	-
	OCH ₂ CH ₃	4.92 (<i>q</i>)	6.99
	OCH ₂ CH ₃	1.62 (<i>t</i>)	7.07
	C3-H	7.66 (<i>d</i>)	$J_{3,5} = 1.81$ $J_{3,4} = 4.39$
	C4-H	6.26 (<i>dd</i>)	$J_{4,3} = 4.40$ $J_{4,5} = 2.33$
	C5-H	6.90 (<i>dt</i>)	$J_{5,4} = 2.32$ $J_{5,3} = 1.81$
		N-CH ₃	3.58 (<i>s</i>)
OCH ₂ CH ₃		4.96 (<i>q</i>)	7.07
OCH ₂ CH ₃		1.67 (<i>t</i>)	7.24
C3-H		7.17 (<i>s</i>)	-

Solvent: CDCl₃

Table 2: ^{13}C NMR resonances of the mono- and biscarbene complexes of tungsten.

COMPOUND	CARBON	δ (ppm)	
	N-CH ₃	38.13	
	C2	124.34	
	C3	111.16	
	N-CH ₃	40.7	
	OCH ₂ CH ₃	78.1	
	OCH ₂ CH ₃	15.3	
	Carbene-C	278.7	
	C2	146.1	
	C3	136.2	
	C4	111.2	
	C5	135.0	
CO	198.4 (<i>cis</i>)	$J_{\text{cis}} =$ 63.6Hz	202.5 (<i>trans</i>)
	N-CH ₃	38.5	
	OCH ₂ CH ₃	79.1	
	OCH ₂ CH ₃	15.0	
	Carbene-C	296.1	
	C2	151.7	
	C3	125.8	
	CO	197.2 (<i>cis</i>)	203.0 (<i>trans</i>)

Solvent: CDCl₃

CARBON NMR SPECTROSCOPY

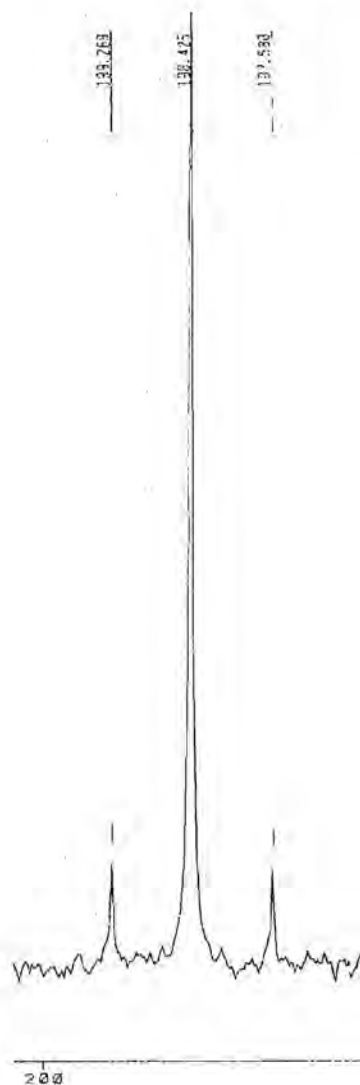


Figure 4: Portion of the ¹³C NMR spectrum of W(CO)₅C(OEt)-P-H (carbonyl resonances).

Carbon-13 NMR data for N-methyl pyrrole was found in an article by Cushley and coworkers⁴. Substitution of the N-proton for a methyl results in a downfield shift of the C2 carbons by 3.5ppm and the C-3 carbons by 0.4ppm. Strong deshielding is often observed for a carbon that is directly methylated (~ 10ppm).

⁴ R.J. Cushley, R.J. Sykes, C.-K. Shaw, H.H. Wasserman, *Can. J. Chem.*, 53, 1975, 148

Monocarbene complex.

The signal of the ring carbons are shifted downfield, due to deshielding by the electron-withdrawing group bound to C-2.

The *cis* carbonyl signal is split into a triplet. It is assumed to be a coupling between tungsten and a rare NMR active isotope of tungsten, ^{183}W . The coupling magnitude is 63.6Hz.

The carbene signal of the tungsten complex $\text{W}(\text{CO})_5\text{C}(\text{Ph})\text{-P-H}^1$ is at 278.7ppm, close to the value for $\text{W}(\text{CO})_5\text{C}(\text{OEt})\text{-P-H}$.

Biscarbene complex.

The carbene carbon signal is seen at 296.1ppm. The signal lies a lot more downfield than the carbene signal of the monocarbene complex. Two carbene carbons withdraw electron density from the ring. The ring is not able to provide electron density as efficiently as for only one carbocationic carbene carbon.

The *cis* carbonyl signal is not split into a triplet, as was observed with the monocarbene complex.

3.1.2 Mass Spectrometry

The mass spectral data for the monocarbene complex is given in table 3. The molecular mass of the complex is 461.083amu. An M^+ peak is observed for the complex at $m/z = 461$, but a stronger peak is observed at $m/z = 459$. Tungsten has four isotopes that are present in significant quantities in nature, as can be seen in table 4. Some of the complexes may be with the lighter isotopes of tungsten, and the peak at $m/z = 459$ can also be seen as a M^+ peak.

Table 3: Fragment ions of the monocarbene tungsten product.

m/z (I, %)	Fragment Ion	M/z (I, %)	Fragment Ion
459 (1)	M^+	301 (13.9)	M^+ -4CO-Et-Me
429 (1)	M^+ -CO	273 (11.1)	M^+ -5CO-Et-Me
329 (6.5)	M^+ -3CO-Et-Me	245 (9.8)	M^+ -6CO-Et-Me

Table 4: Tungsten isotopes: abundance, atomic mass and nuclear spin⁵.

Isotope	Abundance (%)	Atomic Mass	Nuclear Spin (I)
¹⁸⁰ W	0.12	179.946701	0+
¹⁸² W	26.3	181.948202	0+
¹⁸³ W	14.28	182.950220	½-
¹⁸⁴ W	30.7	183.950928	0+
¹⁸⁶ W	28.6	185.954357	0

The spectrum is difficult to interpret. There is no peak at $m/z = 323$, which would correspond to the loss of all five carbonyl ligands, and no peak at $m/z = 294$, which

⁵ J. Emsley, In "The Elements", 2nd Ed., 1991, Clarendon Press, Oxford, 202-203.

would correspond to the loss of all five carbonyl ligands and the ethyl group. The peak at $m/z = 429$ (a difference of 30 if taken from $m/z = 459$) could be due to the loss of a carbonyl ligand. The fact that this peak appears at $m/z = 429$, may be due to an isotope effect. A change from $m/z = 429$ to 329 could indicate a loss of two carbonyl ligands, an ethyl and a methyl fragment.

3.1.3 Infrared Spectroscopy

The most informative infrared spectrum of a substance is obtained when it is dissolved in an inert solvent⁶. It is important for good resolution of bands that the interaction between the solute and the solvent is small, and this is especially true for spectra in the carbonyl region. Hexane was used as solvent, as the interaction between solvent and solute is suitably weak. Other solvents, like alcohols, methylene chloride or chloroform interact to a greater extent, and using CH_2Cl_2 leads to peak broadening and overlapping bands.

Peaks observed for the monocarbene complex are at 2062 ($A_1^{(1)}$), 1950 (B_1), 1942 ($A_1^{(2)}$) and 1934 (E). In the product, the metal is bound to five carbonyls, in a square pyramidal C_{4v} arrangement. The A_1 and E modes are infrared active. Small distortions can render the B_2 mode infrared active. The E-vibration is twice degenerate, and is the strongest peak on the spectrum.

3.1.4 Ultraviolet Spectroscopy

The UV data is given together with the chromium data at the end of the chromium section.

⁶ P.S. Braterman, *Metal Carbonyl Spectra*, Academic Press, 1975, 65-72.

3.1.5 Crystal Structure

Suitable crystals were obtained from a 1:1 hexane: dichloromethane solution of the monocarbene complex, and a X-ray structure determination was done. A ball and stick representation of the structure is given in figure 5. The full list with standard deviations is given in Appendix A. The orientation of the pyrrole ring is such that the N-Me group is on the same side as the ethoxy substituents of the carbene ligand.

The C(carbene)-C2, C(carbene)-OEt and W-C(carbene) bond lengths are very similar in the three complexes $W(CO)_5C(OEt)-P-H$, $W(CO)_5C(OEt)-P-P-C(OEt)W(CO)_5$ and $W(CO)_5C(OEt)-PP-C(OEt)W(CO)_5$ (table 5).

The bond lengths of the pyrrole ring of $W(CO)_5C(OEt)-P-H$ were compared with the bond lengths of one of the rings of $W(CO)_5C(OEt)-P-P-C(OEt)W(CO)_5$ (table 6). The ring bond that differ the most in length is N-CH₃ (longer in the complex $W(CO)_5C(OEt)-P-H$).

Table 5: Selected bond lengths (Å) of $W(CO)_5C(OEt)-P-H$, $W(CO)_5C(OEt)-P-P-C(OEt)W(CO)_5$ and $W(CO)_5C(OEt)-PP-C(OEt)W(CO)_5$

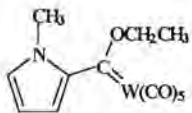
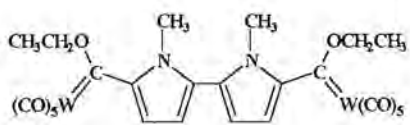
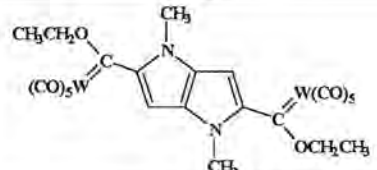
Compound	W-C (carbene)	W-C (<i>trans</i> -CO)	C2-C (carbene)
	2.24 (1)	2.00 (1)	1.45 (2)
	2.230 (4)	2.023 (5)	1.462 (6)
	2.238 (4)	2.034 (5)	1.453 (6)

Table 6: Selected bond lengths (Å) of $W(CO)_5C(OEt)-P-H$ and $W(CO)_5C(OEt)-P-P-C(OEt)W(CO)_5$

Bond		
N-C2	1.40 (1)	1.400 (6)
C2-C3	1.42 (2)	1.396 (6)
C3-C4	1.40 (2)	1.404 (6)
C4-C5	1.39 (2)	1.398 (6)
N-C5	1.33 (2)	1.384 (5)
N-CH₃	1.54 (2)	1.462 (6)

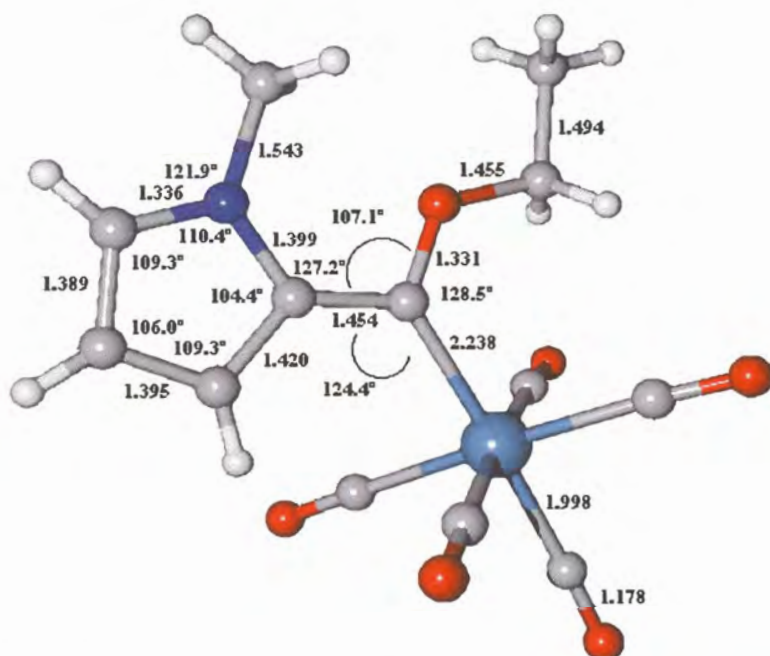


Figure 5: Ball and stick representation of the monocarbene tungsten complex.

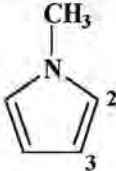
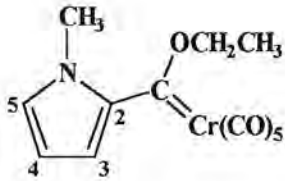
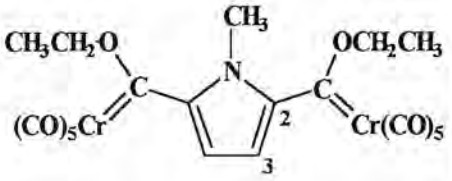
3.2 Chromium Complexes

Mono- and biscarbene complexes were obtained and characterized by NMR, UV and IR spectroscopy and MS spectrometry. The data is given below and discussed.

3.2.1 NMR Spectroscopy

^1H and ^{13}C NMR data are given for the complexes in tables 7 and 8, respectively.

Table 7: ^1H NMR resonances of the mono- and biscarbene chromium complexes.

Complex	Proton	δ (ppm)	J (Hz)
	N-CH ₃	3.66 (<i>s</i>)	-
	C2-H	6.60 (<i>t</i>)	$J_{2,3} = 2.07$
	C3-H	6.13 (<i>t</i>)	$J_{3,2} = 2.07$
	N-CH ₃	3.74 (<i>s</i>)	-
	C3-H	7.71 (<i>dd</i>)	$J_{3,4} = 4.39$ $J_{3,5} = 1.81$
	C4-H	6.26 (<i>dd</i>)	$J_{4,3} = 4.48$
	C5-H	6.79 (<i>s</i>)	$J_{5,3} = 1.81$
	OCH ₂ CH ₃	5.08 (<i>q</i>)	7.05
	OCH ₂ CH ₃	1.64 (<i>t</i>)	7.05
	N-CH ₃	3.43 (<i>s</i>)	-
	C3-H	7.14 (<i>s</i>)	-
	OCH ₂ CH ₃	5.05 (<i>q</i>)	7.12
	OCH ₂ CH ₃	1.66 (<i>t</i>)	7.12

Solvent: CDCl₃

PROTON NMR SPECTROSCOPY

Monocarbene Complex.

The monocarbene complex formed, as evidenced by the chemical shift of the methylene quartet, seen at 5.08ppm. This resonance is downfield from the 4.92ppm reported for the analogues tungsten complex.

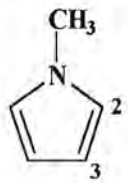
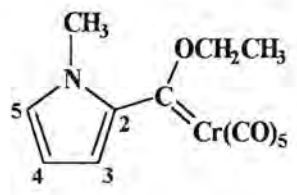
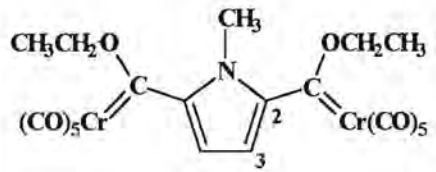
Integration values support the peak assignments, although the coupling constants are irregular for the ring protons. The proton on C5 gives a signal that is seemingly split into a triplet, but with coupling values of 2.29 and 1.90Hz. It was expected to give a signal that was split into a doublet by the C4 proton (strong coupling) and again into a doublet (of doublets) by coupling with C3-H. This is not observed. Michael De Rosa⁷ and his group prepared some 2-aminopyrroles and found that in acidic medium (acetic acid reaction mixture) there was no coupling between the protons at C3/C4 and C5 of the pyrrole ring. They attributed this phenomenon to the fast proton exchange at C5 that decoupled the C5 proton from the protons at C3 and C4 of the ring.

Biscarbene Complex.

The quartet at 5.05ppm, of the methylene protons, is slightly upfield compared to the analogous monocarbene complex as a result of the carbene carbons competing for the electron density of the pyrrole ring. The spectrum is simple, as expected since the protons of the molecule all fall in one of four groups of chemically equivalent protons. The two ring protons are in the same chemical environment. A singlet is seen at 7.14ppm. In N-methyl pyrrole, these protons give a peak resonance at 6.13ppm, so the Fischer carbene carbon atom significantly deshields these two ring protons, shifting the signal downfield by ~ 1ppm. The methyl resonance of the monocarbene complex is shifted downfield, and that of the biscarbene complex is shifted upfield, compared to the methyl resonance of N-methylpyrrole.

⁷ M. De Rosa, R. P. Issac, G. Houghton, *Tetrahedron Lett.*, **1995**, 36, 9261.

Table 8: ^{13}C NMR resonances of the mono- and biscarbene chromium complexes.

Compound	Carbon	δ (ppm)	
	N-CH ₃	38.13	
	C2	124.34	
	C3	111.16	
	N-CH ₃	40.7	
	OCH ₂ CH ₃	75.5	
	OCH ₂ CH ₃	15.5	
	Carbene-C	324.2	
	C2	144.4	
	C3	134.5	
	C4	110.9	
	C5	134.0	
	CO	217.9 (<i>cis</i>)	223.1 (<i>trans</i>)
	N-CH ₃	38.0	
	OCH ₂ CH ₃	76.6	
	OCH ₂ CH ₃	15.3	
	Carbene-C	327.4, 324.3	
	C2	148.0	
	C3	123.4	
	CO	216.4 (<i>cis</i>)	223.6 (<i>trans</i>)

CARBON NMR SPECTROSCOPY

Monocarbene complex.

The spectrum closely resembles the carbon-13 spectrum of the tungsten monocarbene product, but no coupling of the *cis* carbonyl signal is observed.

A 2D HETCOR experiment was also executed, to make sure that the peak assignments were correct. A part of the spectrum is given below (Figure 6):

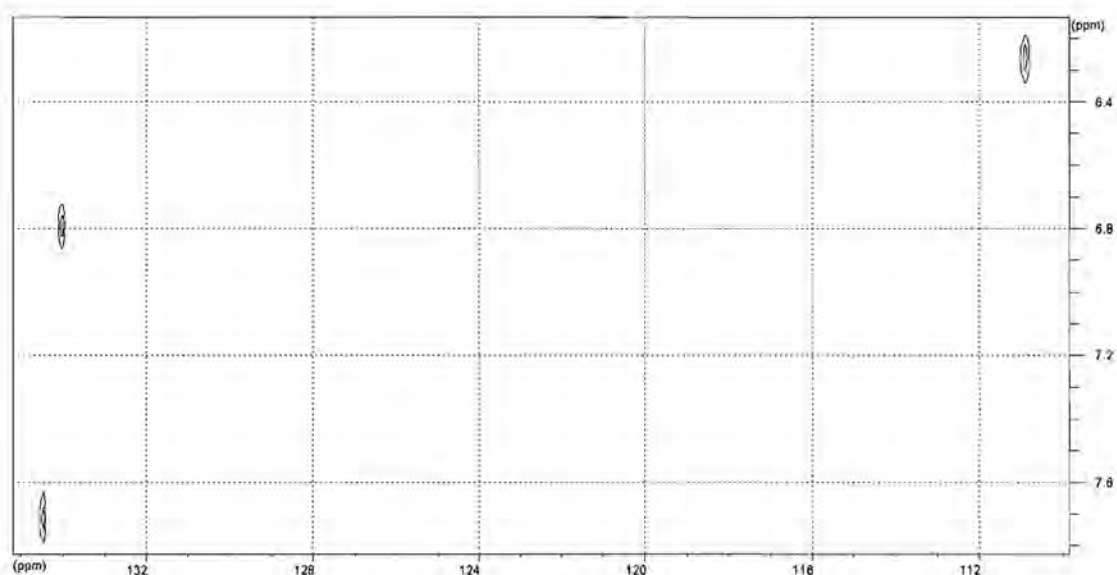


Figure 6: Portion of the 2D HETCOR spectrum of the monocarbene chromium complex.

On the ^{13}C NMR spectrum the peaks at 134.5 ppm and 134.0 ppm were difficult to assign, because they lie so close together. From the HETCOR can be seen that they are ring carbons and that they are respectively C3 and C5. C4 is not so much deshielded as C3 and C5 and lies at 110.9 ppm.

Biscarbene Complex.

The carbene signal of the chromium carbene complex $(\text{Cr}(\text{CO})_5\text{C}(\text{C}_6\text{H}_5)\text{-P-H})^1$ lies at 315.0ppm. The complex $\text{Cr}(\text{CO})_5\text{C}(\text{OEt})\text{-P-C}(\text{OEt})\text{Cr}(\text{CO})_5$ displays two carbene signals which lie at 327.4 and 324.3ppm. Why two signals are observed in the carbene region (Figure 7) cannot be explained.

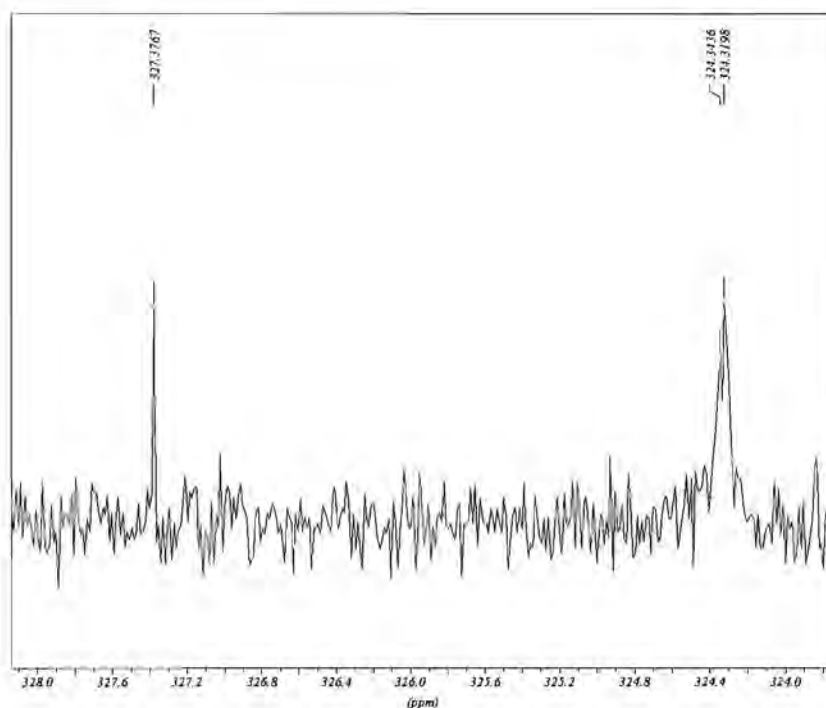


Figure 7: Portion of the carbon-13 spectrum of the chromium biscarbene complex.

3.2.2 Mass Spectrometry

Fragmentation data for the mono- and biscarbene products are given in table 9.

Table 9: Fragmentation data of the mono and biscarbene complexes of chromium.

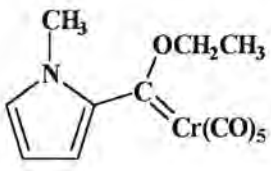
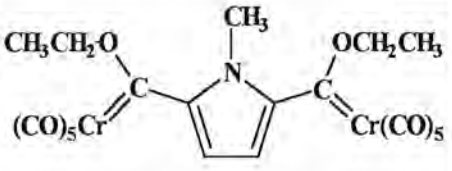
Complex	Fragment Ions (I, %)
	329 (4.5) M ⁺ ; 301 (10.7) M ⁺ -CO; 273 (11.6) M ⁺ -2CO; 245 (6.6) M ⁺ -3CO; 217(16.1) M ⁺ -4CO; 189(100) M ⁺ -5CO; 160(12.6) M ⁺ -5CO-Et; 132(78.9) M ⁺ -6CO-Et.
	578 (6) M ⁺ ; 550 (12) M ⁺ -CO; 494 (5) M ⁺ -3CO; 465 (7) M ⁺ -3CO-Et; 297 (26) M ⁺ -9CO-Et.

Table 10: Chromium isotopes: abundance, atomic mass and nuclear spin⁸.

Isotope	Abundance (%)	Atomic Mass	Nuclear Spin (I)
⁵⁰ Cr	4.35	49.946046	0+
⁵² Cr	83.79	51.940509	0+
⁵³ Cr	9.50	52.940651	3/2+
⁵⁴ Cr	2.36	53.938882	0+

⁸ J. Emsley, In "The Elements", 2nd Ed., 1991, Clarendon Press, Oxford, 52-53.

Monocarbene complex

At $m/z = 329.2$ the molecular ion peak was observed on the spectrum. The fragmentation pattern deduced is as follows: five carbonyl ligands are fragmented, followed by the ethyl group and then the last carbonyl of the carbene ligand. A chromium ion peak is seen at $m/z = 52$ (70.79%).

Biscarbene complex

The molecular ion M^+ peak is observed at $m/z = 578$. The carbonyls are fragmented first, but before all the carbonyls are lost, one of the ethyl groups breaks off. The rest of the carbonyl ligands are lost, followed by the other ethyl group. Lastly the N-methyl group is fragmented.

3.2.3 Infrared Spectroscopy

A portion of the infrared spectrum of the biscarbene complex is shown in figure 8. The infrared data for the mono- and biscarbene complexes are given in table 11.

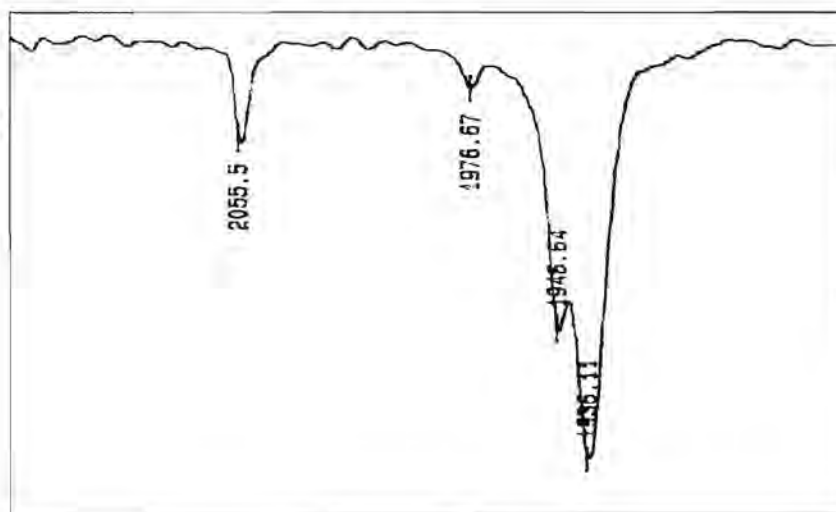
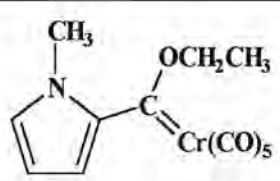
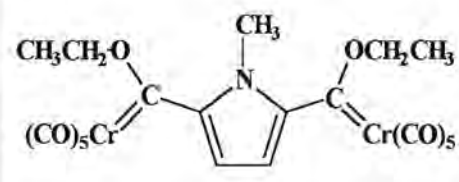


Figure 8: Infrared spectrum of the biscarbene chromium product in the carbonyl region.

Table 11: Infrared data^a of the mono- and biscarbene chromium products.

COMPLEX	$A_1^{(1)}$	B_1	$A_1^{(2)}$	E
	2056	1977	1946	1936
	2055	1976	1946	1936

^acarbonyl region

The infrared spectrum obtained for the carbene products clearly show the pattern one would expect for a metal that is bound to five carbonyls and a ligand L. The E band is twice degenerate and is the strongest band on the spectrum. The vibration depicted by $A_1^{(1)}$ couples with the $A_1^{(2)}$ vibration, and its intensity increases.

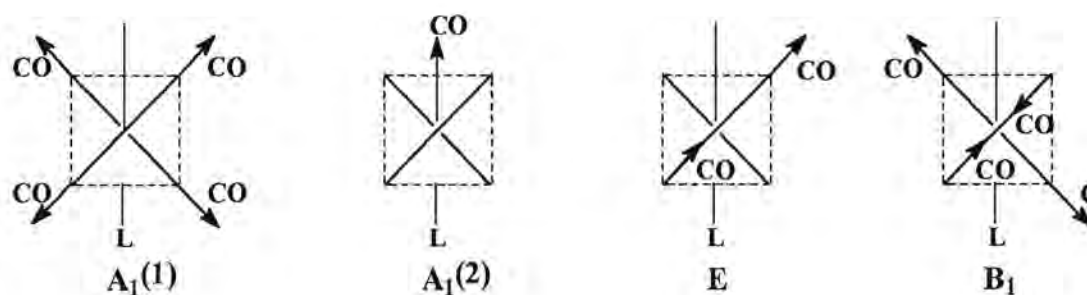


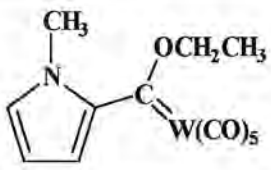
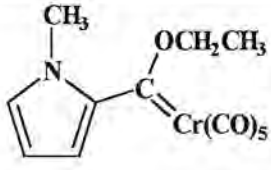
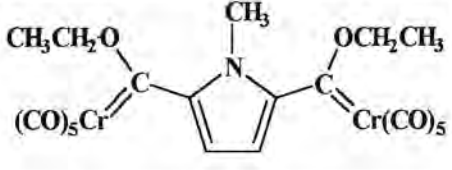
Figure 9: Stretching vibration modes of octahedral $ML(CO)_5$ complexes.

3.2.4 Ultraviolet Spectroscopy

The UV-spectra of the complexes were recorded in CH₂Cl₂. The data for the mono- and biscarbene chromium complexes and the monocarbene tungsten complex is given in table 10.

An increase in the length of a conjugated system results in a bathochromic shift (shift towards longer wavelength). This implies that an increase in conjugation decreases the energy required for electronic excitation. Comparing the monocarbene complexes of tungsten and chromium with one another, one sees that the corresponding peaks are similar. On comparison of these values with the biscarbene chromium complex, however, one sees peaks at $\lambda_{\max} = 340$ and 472 vs. $\lambda_{\max} = 313$ and 430 in the monocarbene case (chromium) and $\lambda_{\max} = 322$ and 433 in the case of the tungsten monocarbene complex. With unsaturated molecules $\pi \rightarrow \pi^*$ transitions of rather high energy become possible.

Table 12: Ultraviolet data for the monocarbene tungsten complex and the mono and biscarbene chromium complexes.

Compound	Peaks (λ)	Intensity	Transition
	241.0	2.371	Ligand based
	322.0	0.449	$\pi \rightarrow \pi^*$
	433.0	0.488	d-d
	250.0	3.250	Ligand based
	313.0	1.079	$\pi \rightarrow \pi^*$
	430.0	1.069	d-d
	241.0	2.314	Ligand based
	340.0	0.417	$\pi \rightarrow \pi^*$
	472.0	0.635	d-d

3.2.5 Crystal Structure.

Suitable crystals were obtained of the red biscarbene chromium product from a 1:1 dichloromethane: hexane mixture, and the crystal structure was determined.

A ball and stick representation of the structure of $\text{Cr}(\text{CO})_5\text{C}(\text{OEt})\text{-P-C}(\text{OEt})\text{Cr}(\text{CO})_5$ is given in figure 11. Bond distances and bond angles are included, but the full list, with standard deviations, is given in Appendix B. From the picture, a solid-state structural feature of importance is the position of the $\text{Cr}(\text{CO})_5$ fragments with respect to the pyrrole rings.

The bonds of the pyrrole ring are the same length, due to the electron drawing carbene carbons, which withdraw electron density from the ring. The Cr-C-C-N dihedral angles are -152.4° and $+151.4^\circ$.

The shortest Cr-C(carbene) distances are found when the $\text{Cr}(\text{CO})_5$ fragment is competing only with a thio or oxy function⁹. Replacement of these substituents by an amino group, a much better π -donor, reduces back bonding from the metal, thereby lengthening the Cr-C(carbene) distance. As the carbene carbon is increasingly stabilized by π bonding with the organic substituents, the carbene ligand becomes a weaker π -acceptor towards the metal. The result is more π bonding to the carbonyl ligands, especially the *trans*-CO ligand. If the back bonding is strongly decreased, significant shortening of the *trans*-CO distance is observed.

The Cr-C(carbene) distance is 2.07\AA in $\text{Cr}(\text{CO})_5\text{C}(\text{OEt})\text{-P-C}(\text{OEt})\text{Cr}(\text{CO})_5$. In the complexes $(\text{CO})_5\text{CrC}(\text{OMe})\text{Ph}$, $(\text{CO})_5\text{CrC}(\text{OEt})\text{Me}$ and $(\text{CO})_5\text{CrC}(\text{OEt})\text{C}\equiv\text{CPh}$ it is, respectively $2.04(3)$, $2.053(1)$ and $2.00(2)\text{\AA}$ ¹⁰. The metal-to-carbene carbon back bonding is the least in $\text{Cr}(\text{CO})_5\text{C}(\text{OEt})\text{-P-C}(\text{OEt})\text{Cr}(\text{CO})_5$. The three groups attached to the

⁹ U. Schubert; In *Transition Metal Carbene Complexes*, 1983; Verlag Chemie; Weinheim; 75-83.

¹⁰ $(\text{CO})_5\text{CrC}(\text{OMe})\text{Ph}$: O.S. Mills, A.D. Redhouse; *J. Chem. Soc. (A)*, 1968, 642-647.

$(\text{CO})_5\text{CrC}(\text{OEt})\text{Me}$: C. Krüger, R. Goddard, Y.-H. Tsay; from ref 7.

$(\text{CO})_5\text{CrC}(\text{OEt})\text{C}\equiv\text{CPh}$: G. Huttner, H. Lorenz; *Chem. Ber.*, 1975, 108, 1864-1870.

sp^2 hybridized carbene carbon atom compete with each other for π bonding to the formally empty p -orbital on the carbene carbon. There is increased π bonding from the pyrrole spacer ligand, compared to that of methyl and $C\equiv CPh$ substituents.

In $Cr(CO)_5C(OSiMe_3)CH(PMe_3)$ the Cr-C(carbene) bond length is $2.137(7)\text{\AA}$, and the Cr-C(CO,*trans*) distance is $1.859(8)\text{\AA}$ ¹¹. In $Cr(CO)_5C(OEt)-P-C(OEt)Cr(CO)_5$, these distances are, respectively, 2.067 and 1.883\AA . The Cr-C(carbene) distance is shorter, and the Cr-C(CO, *trans*) distance is longer in $Cr(CO)_5C(OEt)-P-C(OEt)Cr(CO)_5$. There is thus more back bonding to the carbene carbon, and less to the *trans* carbonyl carbon.

π -charges are given in figure 10¹².

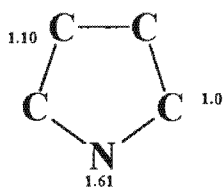


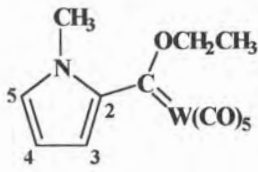
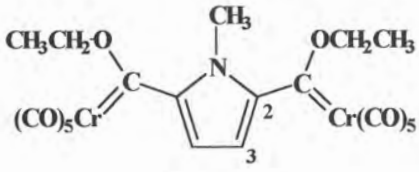
Figure 10: π -charges.

Selected bond lengths of the monocarbene tungsten complex and the biscarbene chromium complex are given in table 13. The bond lengths are very similar.

¹¹ S. Voran, H. Blau, W. Malisch, U. Schubert; *J. Organomet. Chem.*, **1982**, 232, C33-C40.

¹² J.M. André, D.P. Vercauteren, G.B. Street, J.L. Brédas; *J. Chem. Phys.*; **1984**, 80, 5643-5648.

Table 13: Selected bond lengths (Å) of $W(CO)_5C(OEt)-P-H$ and $Cr(CO)_5C(OEt)-P-C(OEt)Cr(CO)_5$.

Bond		Bond	
N-C2	1.40 (1)	N-C2	1.394 (3)
C2-C3	1.42 (2)	C2-C3	1.395 (4)
C3-C4	1.40 (2)	C3-C3'	1.391 (3)
C4-C5	1.39 (2)	C3'-C2'	1.395 (4)
N-C5	1.34 (2)	N-C2'	1.394 (3)
N-CH₃	1.54 (2)	N-CH₃	1.485 (3)

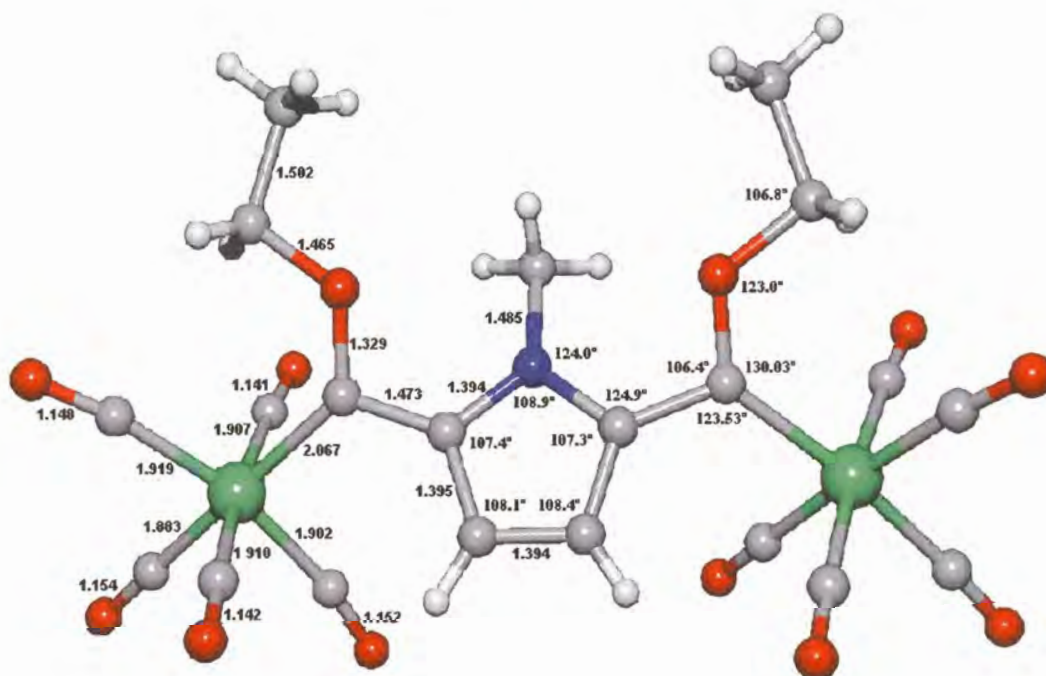


Figure 11: Ball and stick representation of the chromium biscarbene complex.

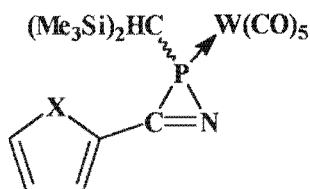
Chapter 3

Carbene Complexes of Bipyrrole

1 Background

Hexahalogenated 1,1'-dimethyl-2,2'-bipyrroles have been found in the eggs of Pacific and Atlantic Ocean seabirds and in bald eagle liver samples¹, dramatically revealing that natural organohalogen compounds are more pervasive in the environment than previously believed.

In the following complex² the almost coplanar arrangement of the two ring systems allows an effective π -electron interaction between the N-methylpyrrole group (π -donor) and the PCN-ring (π -acceptor).



X = NMe, O, S, HC=CH.

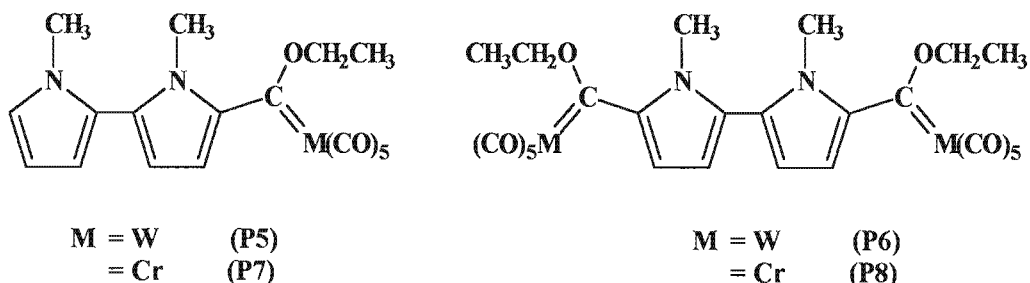
Figure 1. 2*H*-azaphosphirene tungsten complexes.

The carbon-carbon bonds in the pyrrole ring and the inter-ring bond (which is significantly shorter than the corresponding distance in the molecule with X = HC=CH) are equalized. The C=N bond is longer due to transfer of electron density to the tungsten.

¹ G. W. Gribble, D. H. Blank, J. P. Jasinski; *Chem. Commun.*, **1999**, 2195-2196.

² R. Streubel, S. Priemer, F. Ruthe, P. G. Jones, D. Gudat; *Eur. J. Inorg. Chem.*, **1998**, 575-578.

The syntheses of the following tungsten and chromium carbene complexes were undertaken:



It is important that the two rings be coplanar, for effective communication to occur. The long-range interactions between the metal centres would be disturbed if the conjugation were to be disrupted. The capability to do so by some form of external manipulation would mean that the complex could be used as a molecular switch. Such a possibility exists with the bipyrrrole ligand, but not with the pyrrole and rigid pyrrolo[3,2-*b*]pyrrole ligands.

Extended heterocyclic systems have been investigated by a number of researchers. Jones *et al*³ prepared compounds with alternating π -electron-deficient and π -electron-excessive heteroarenes. They synthesized and characterized simple 2-(pyrrole-2-yl)pyridines and oligomeric alternating pyrrole:pyridine systems. Diketones were converted in high yield into the corresponding pyrroles and 1-alkyl or 1-aryl-pyrroles.

The X-ray structural analysis of the following complexes, prepared by Behrens *et al*⁴, reveals almost coplanar *cyclo-C*₅ and *cyclo-C*₇ units in the sesquifulvalene ligands. In the solid state the electronic coupling is greatly facilitated between the donor and the acceptor. These complexes have unusually large hyperpolarizability.

³ R. A. Jones, M. Karatza, T.V. Voro, P.U. Civeir, A. Franck, O. Ozturk; J.P. Seaman, A.P. Whitmore, D.J. Williamson, *Tetrahedron*, **1996**, *52*, 8707.

⁴ U. Behrens, H. Brussaard, U. Hagenau, J. Heck, E. Hendrickx, J. Körnich, J.G.M. van der Linden, A. Persoons, A. L. Spek, N. Veldman, B. Voss, H. Wong; *Chem. Eur. J.*, **1996**, *2*, 98.

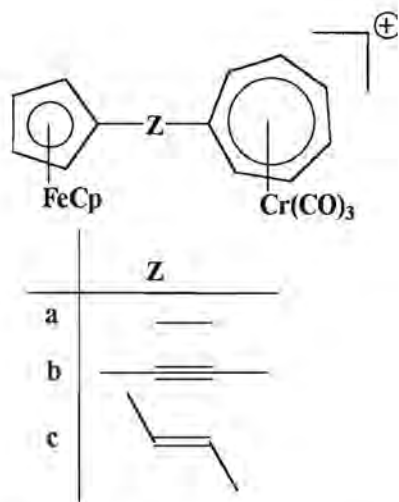
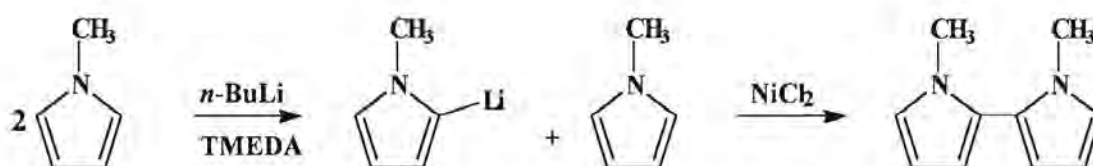


Figure 2. Bimetallic sesquifulvalene complexes.

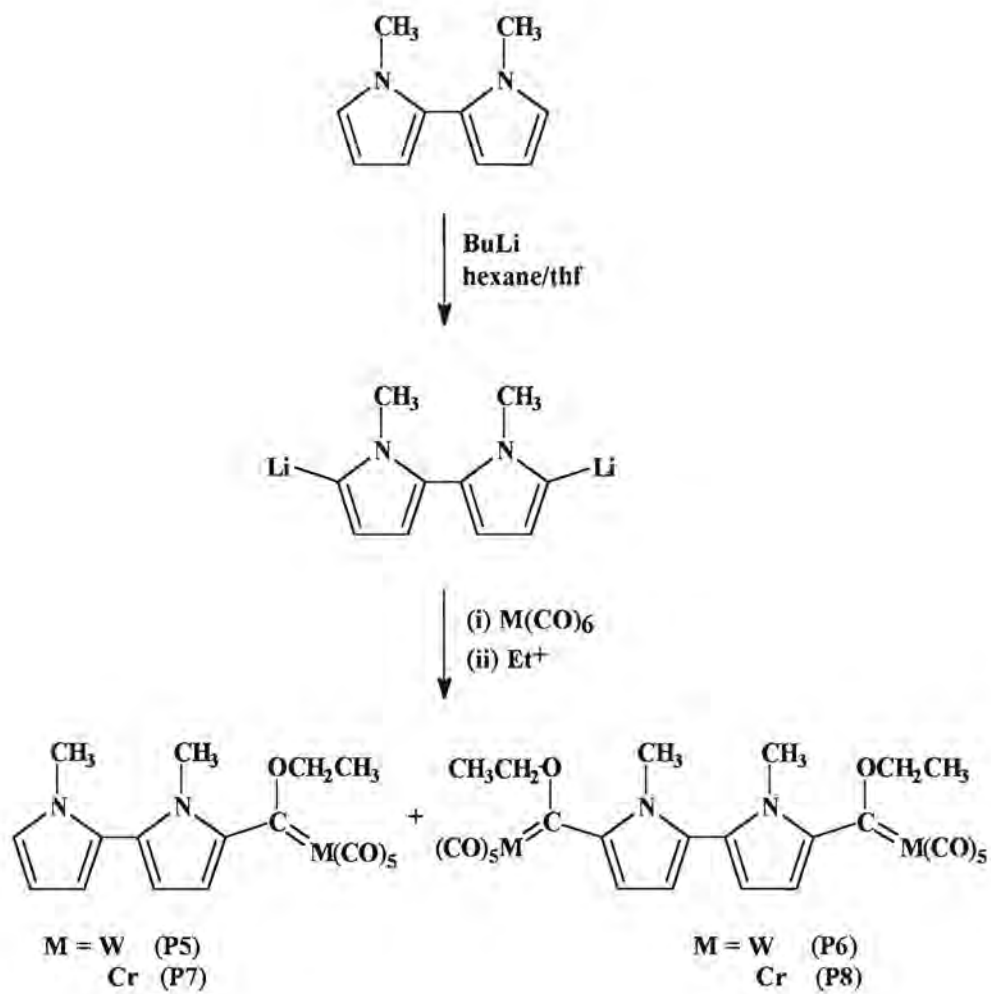
2 Synthesis

The 1,1'-dimethyl-2,2'-bispyrrole was synthesized according to the method of Kauffman and Lexy⁵. N-methylpyrrole was lithiated, after which a second equivalent of N-methylpyrrole was added. NiCl₂ was used as catalyst in the coupling reaction. Yields were low.



N,N'-dimethylbipyrrole was added to TMEDA and then, after cooling, metallated with *n*-BuLi. The initial colour of the solution was yellow, but when the reaction mixture was heated the solution became milky and whiter. The temperature was increased to near the boiling point of hexane, and left for 15 minutes at that temperature, after which the mixture was cooled down and the appropriate M(CO)₆ was added. The solution became very dark. An oxonium salt was used to alkylate the intermediate product. The solvent was removed and the products were separated. The mono- and the biscarbene products were obtained.

⁵ T. Kauffman, H. Lexy, *Chem. Ber.*, **1981**, *114*, 3674-3683.



Scheme 1: Preparation of the carbene complexes.

3 Characterization of complexes

3.1 Tungsten Complexes

Mono- and biscarbene complexes with bipyrrrole substituents were obtained and characterized by NMR, IR and UV spectroscopy and MS spectrometry. The spectroscopic data is given below and discussed.

3.1.1 NMR Spectroscopy

The ^1H NMR data is given in table 1 and the ^{13}C NMR data is given in table 2.

PROTON NMR SPECTROSCOPY

Monocarbene complex.

In the mono- and the biscarbene complexes, the N-CH₃ signals are slightly shifted downfield compared to the bipyrrrole substrate. The signal of the N'-CH₃ proton is shifted downfield as well, which would suggest that there is some conjugation across the C5-C6 double bond, as some electron density are withdrawn from the pyrrole ring of which N' is a member. The N alkyl group donates electron density to the ring (inductive effect).

The signals of C9-, C8- and C7-H are slightly shifted downfield (~0.1ppm) on the spectra of the monocarbene complex, compared to their signals for the substrate. The protons of C4 and C3 are shifted downfield by, respectively, 0.2 and 1.5ppm. C3-H is the most affected. In the monocarbene complex the carbene moiety withdraws electron density mainly from the ring to which it is bonded.

Figure 3 shows the electron delocalisation in the monocarbene complex. From the NMR data one would assume that the fourth structure (short range delocalisation) best shows the situation in the complex.

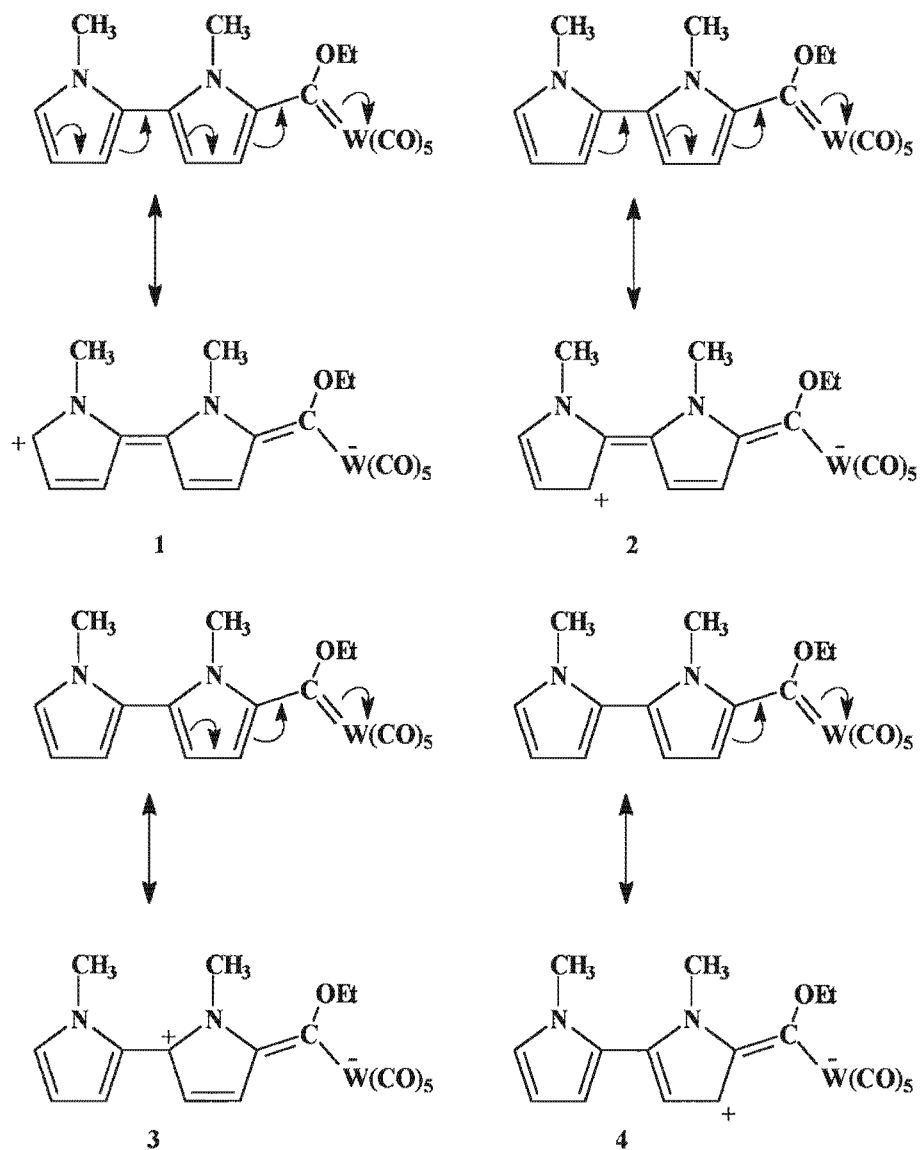


Figure 3. Electron delocalisation in the monocarbene complex.

Comparing the C3-H signal of the complex $W(CO)_5C(OEt)$ -P-H with the C3-H signal of $W(CO)_5C(OEt)$ -P-P-H, one notices that the protons are deshielded equally (1.52 and 1.53ppm, respectively). C4-H is slightly more deshielded in the bispyrrole case, than in the pyrrole case.

Biscarbene complex.

The N-CH₃ signal is shifted downfield, as was seen with the monocarbene complex. The signals of the ring protons are shifted by the electron-withdrawing carbene

moiety, especially that of the C3 proton, that is shifted by 1.5ppm downfield. The signal of the C4-H is shifted downfield by 0.3ppm.

Although the C3-H's in the biscarbene complex are slightly less deshielded than the corresponding resonance in the monocarbene complex, the C4-H resonance is more deshielded compared to the resonances of the C8-H's in the monocarbene complex and those of C3-H and C4-H in the bipyrrrole. This indicates the stronger electron withdrawing effect of two carbene carbons, compared to one carbene carbon.

CARBON NMR SPECTROSCOPY

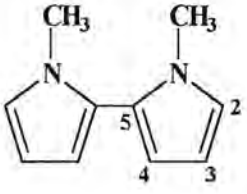
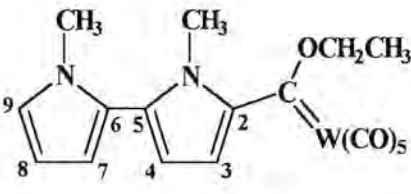
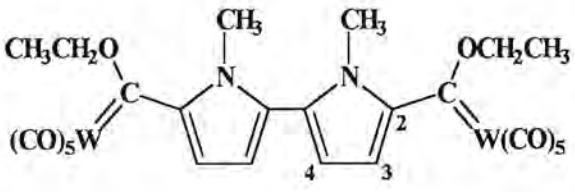
Monocarbene complex.

The signals of the ring carbons all lie close to each other. By looking at the height of the peaks and also comparing with the chromium case, for which a 2D HETCOR experiment was done, the peaks could be assigned. The C2 peak could not be distinguished from the background. The ^{13}C data seems to indicate that the fourth structure in figure 3 best shows the electron delocalisation in the complex, but the first structure is also an important contributing structure, indicating that there is electron delocalisation through the two rings.

Biscarbene complex.

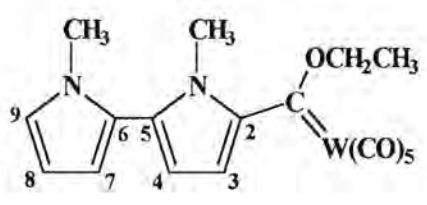
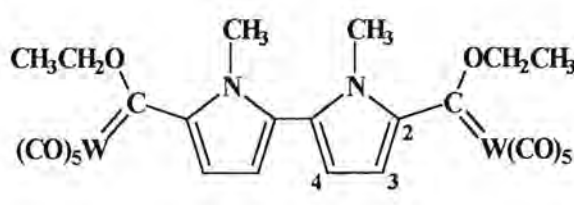
In the complexes $\text{W}(\text{CO})_5\text{C}(\text{OEt})\text{-P-H}$ and $\text{W}(\text{CO})_5\text{C}(\text{OEt})\text{-P-C}(\text{OEt})\text{W}(\text{CO})_5$, there is a large difference in the carbene-C values, with the carbene-C being much more deshielded in the biscarbene complex. In the complexes $\text{W}(\text{CO})_5\text{C}(\text{OEt})\text{-P-P-H}$ and $\text{W}(\text{CO})_5\text{C}(\text{OEt})\text{-P-P-C}(\text{OEt})\text{W}(\text{CO})_5$, however, the difference in the carbene-C values is smaller.

Table 1: ^1H NMR resonances of the mono- and biscarbene complexes of tungsten.

Compound	PROTON	δ (ppm)	J (Hz)
	N-CH ₃	3.49 (<i>s</i>)	-
	C2-H	6.70 (<i>dd</i>)	$J_{2,3} = 2.7$ $J_{2,4} = 1.81$
	C3-H	6.18 (<i>dd</i>)	$J_{3,2} = 2.7$ $J_{3,4} = 3.49$
	C4-H	6.14 (<i>dd</i>)	$J_{4,3} = 3.49$ $J_{4,2} = 1.81$
	N-CH ₃	3.65 (<i>s</i>)	-
	N'-CH ₃	3.57 (<i>s</i>)	-
	OCH ₂ CH ₂	4.92 (<i>q</i>)	7.12
	OCH ₂ CH ₃	1.62 (<i>t</i>)	7.12
	C3-H	7.71 (<i>d</i>)	$J_{3,4} = 4.39$
	C4-H	6.33 (<i>d</i>)	$J_{4,3} = 4.65$
	C7-H	6.23 (<i>dd</i>)	$J_{7,8} = 3.62$ $J_{7,9} = 1.81$
	C8-H	6.26 (<i>dd</i>)	$J_{8,9} = 2.72$ $J_{8,7} = 3.76$
	C9-H	6.79 (<i>dd</i>)	$J_{9,8} = 2.72$ $J_{9,7} = 1.81$
	N-CH ₃	3.62 (<i>s</i>)	-
	OCH ₂ CH ₃	4.98 (<i>q</i>)	7.12
	OCH ₂ CH ₃	1.65 (<i>t</i>)	7.12
	C3-H	7.69 (<i>d</i>)	$J_{3,4} = 4.39$
C4-H	6.39 (<i>d</i>)	$J_{4,3} = 4.39$	

Solvent: CDCl₃.

Table 2: ^{13}C NMR resonances of the mono- and biscarbene complexes of tungsten.

Compound	Carbon	δ (ppm)	
	N-CH ₃ , N'-CH ₃	37.8	
	OCH ₂ CH ₃	75.4	
	OCH ₂ CH ₃	15.5	
	Carbene-C	288.2	
	C2	137.1	
	C3	135.5	
	C4	114.9	
	C5	134.3	
	C6	114.0	
	C7	112.9	
	C8	108.5	
	C9	125.1	
	CO	198.2 (<i>cis</i>)	202.3 (<i>trans</i>)
	N-CH ₃	37.8	
	OCH ₂ CH ₃	78.6	
	OCH ₂ CH ₃	15.3	
	Carbene-C	282.4	
	C2	148.7	
	C3	134.2	
	C4	114.9	
	C5	134.6	
CO	198.2 (<i>cis</i>)	202.3 (<i>trans</i>)	

3.1.2 Mass Spectrometry

The mass spectrometry data for the monocarbene tungsten complex is given in table 3.

Table 3: Mass spectrometry data of the monocarbene tungsten complex.

<i>m/z</i> (I, %)	Fragment Ion	<i>m/z</i> (I, %)	Fragment Ion
540 (3.7)	M ⁺	427 (8.3)	M ⁺ -3CO-Et
512 (4.7)	M ⁺ -CO	399 (13.9)	M ⁺ -4CO-Et
484 (4.6)	M ⁺ -2CO	371 (8.0)	M ⁺ -5CO-Et
455 (5.4)	M ⁺ -2CO-Et	343 (9.3)	M ⁺ -6CO-Et

Monocarbene complex.

A molecular ion peak was observed. The fragmentation pattern displays initial loss of two carbonyls ligands, followed by the ethyl group, and then the rest of the carbonyl ligands fragmented. The mass spectrum confirms that the product that was obtained is the monocarbene tungsten complex, and that the fragmentation pattern is typical for these compounds (see chapter 2)

Biscarbene complex.

No molecular ion peak was observed ($M_r = 920.126$) for the biscarbene complex.

3.1.3 Infrared Spectroscopy

Four peaks are seen in the carbonyl region of the infrared spectrum of the monocarbene complex, as expected for a complex with a metal that is bound to five carbonyl ligands and another ligand. The bands observed are at 2062 ($A_1^{(2)}$), 1971 (B_1), 1944 ($A_1^{(2)}$) and 1934 (E) cm^{-1} . The values are very similar for mono- and biscarbene complexes, and is only sensitive to the nature of the metal and the type of unique ligand, in this case a carbene ligand.

3.1.4 Ultraviolet Spectroscopy

The UV data is given together with the chromium data at the end of the chromium section.

3.1.5 Crystal Structure.

A ball and stick representation of the structure of $\text{W}(\text{CO})_5\text{C}(\text{OEt})\text{-P-P-C}(\text{OEt})\text{W}(\text{CO})_5$ is given in figure 5. Bond distances and bond angles are included, but the full list with standard deviations is given in Appendix C. From the picture the solid-state structural features of importance are: (i) the position of the $\text{W}(\text{CO})_5$ fragments with respect to the pyrrole rings and (ii) the planarity of the biscarbene spacer ligand.

It is interesting to note that the two rings are positioned with the nitrogens on the same side. The ethoxy substituents of the carbene carbon are on the same side as the nitrogens atoms. This phenomenon has been observed with the other carbene products, $\text{W}(\text{CO})_5\text{C}(\text{OEt})\text{-P-H}$, $\text{Cr}(\text{CO})_5\text{C}(\text{OEt})\text{-P-C}(\text{OEt})\text{Cr}(\text{CO})_5$ and $\text{W}(\text{CO})_5\text{C}(\text{OEt})\text{-PP-C}(\text{OEt})\text{W}(\text{CO})_5$. Steric effects, resulting from the methyl substituents on the N-atoms, are taken to account for the slight "twisting" of the complex. Perhaps a biscarbene tungsten complex with a bispyrrole ligand would be planar.

From the crystal structure it can be seen that the two pyrrole rings are not coplanar, with a dihedral angle of 61.5° (N-C-C-N). The C5-C5' bond length is 1.45\AA , shorter than a single bond (1.54\AA) and longer than a double bond (1.34\AA). The bond therefore does have some double bond character. It can be said that the conjugation does extend across the C5-C5' bond.

The W-C-C-N angle is 171.4° . The W-C bond length is 2.23\AA . The W-C(*trans*-CO) bond length is shorter than the W-C(*cis*-CO) bond lengths. As the carbene carbon is stabilized by π -bonding with the organic substituents, the carbene ligand as a whole becomes a weaker π -acceptor towards the metal. This results in increased back bonding to the carbonyl ligands, particularly the *trans*-CO ligand.

By averaging the X-ray experimental data available for the crystalline dipyrrole and terpyrrole, the geometrical parameters were obtained⁶:

⁶ J.M. André, D.P. Vercauteren, G.B. Street, J.L. Brédas; *J. Chem. Phys.*; **1984**, *80*, 5643-5648.

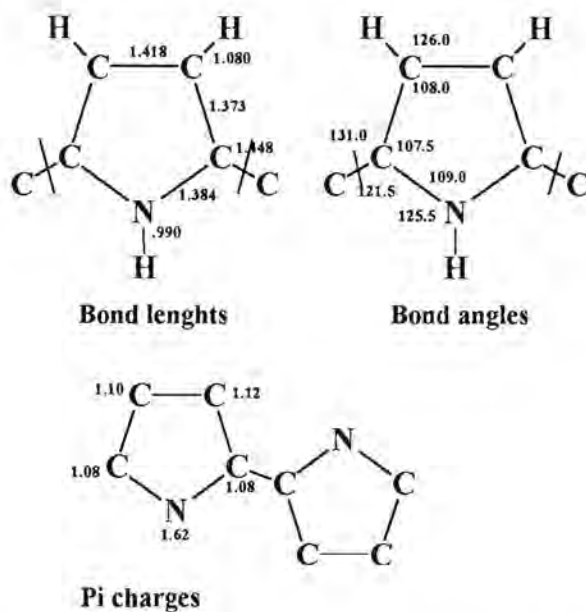
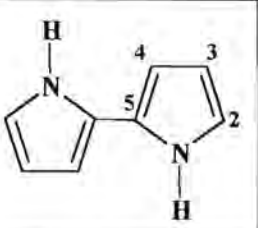
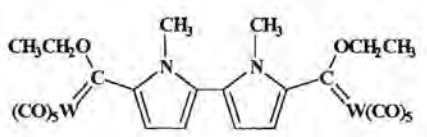
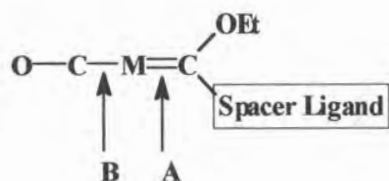


Figure 4. Averaged bond angles and lengths taken from the X-ray molecular structures of 2,2'-bipyrrrole and 2,2':5',2''-terpyrrrole and π charges, as obtained from Mulliken population analysis.

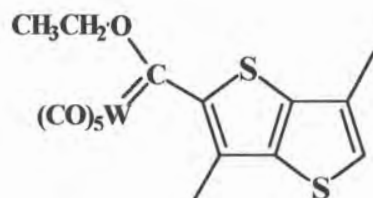
Table 4: Bond lengths of 2,2'-bispyrrrole and $W(CO)_5C(OEt)-P-P-C(OEt)W(CO)_5$.

Bond			Deviation
N-C2	1.384	1.400 (6)	+0.02
C2-C3	1.373	1.396 (6)	+0.02
C3-C4	1.418	1.404 (6)	-0.01
C4-C5	1.373	1.398 (6)	+0.03
N-C5	1.384	1.384 (5)	Same
C5-C5'	1.448	1.447 (8)	Same

The electron delocalisation has an effect on the bond lengths. C3-C4 is even shorter.



In the complex below⁷, the distance **A** is 2.219Å, and the distance **B** is 2.037Å.



In $W(CO)_5C(OEt)-P-P-C(OEt)W(CO)_5$, the distance **A** is 2.230Å, and the distance **B** is 2.023 Å. There is more back-bonding to the carbonyl ligands in the thieno[3,2-*b*]-thiophene complex. The carbene ligand of $W(CO)_5C(OEt)-P-P-C(OEt)W(CO)_5$ is a stronger π -acceptor towards the metal.

The carbene-C2 distance is the same for both complexes. The hetero-ring does not play a big role.

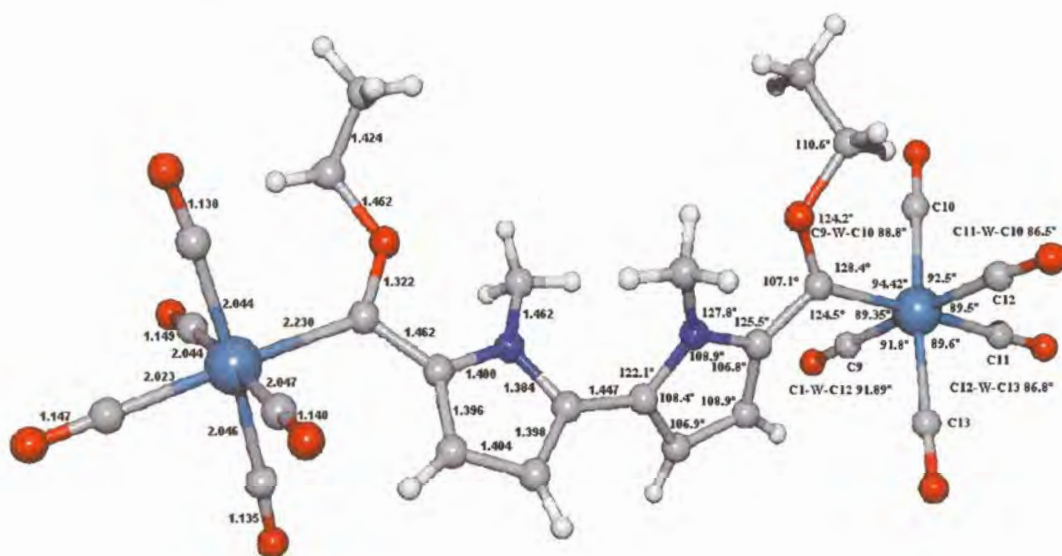


Figure 5. Ball and stick representation of the bis-carbene tungsten complex.

⁷ M. Landman, H. Görls, S. Lotz; *Eur. J. Inorg. Chem.*, **2001**, 233-238.

3.2 Chromium Complexes.

Mono- and biscarbene complexes were obtained and characterized by NMR, IR and UV spectroscopy and MS spectrometry.

3.2.1 NMR Spectroscopy

The ^1H NMR data is given in table 4 and the ^{13}C NMR data is given in table 5.

PROTON NMR SPECTROSCOPY

Monocarbene complex.

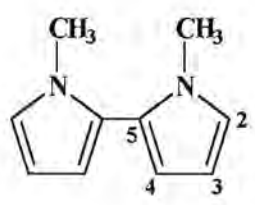
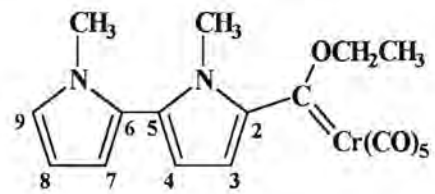
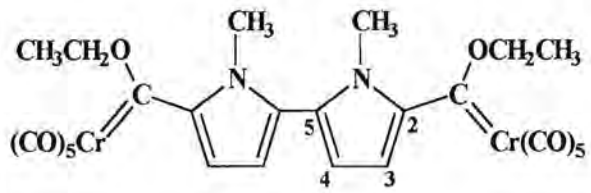
The peak assignment is difficult, as the ring protons are all in slightly different chemical environments. A 2D HETCOR experiment was also done to help resolve the spectrum.

The signals of the ring protons of C3 and C4 are shifted by the same amount than the matching protons of the tungsten carbene complex. The protons of C7, C8 and C9 are slightly more deshielded than the matching protons of the tungsten carbene complex $\text{W}(\text{CO})_5\text{C}(\text{OEt})\text{-P-P-H}$. The OCH_2CH_3 and OCH_2CH_3 signals are the same in the $\text{Cr}(\text{CO})_5\text{C}(\text{OEt})\text{-P-H}$ and $\text{Cr}(\text{CO})_5\text{C}(\text{OEt})\text{-P-P-H}$ complexes.

Looking at C3-H and C4-H in die complexes $\text{Cr}(\text{CO})_5\text{C}(\text{OEt})\text{-P-H}$ and $\text{Cr}(\text{CO})_5\text{C}(\text{OEt})\text{-P-P-H}$, one sees that the situation is the same as with the two tungsten complexes. The C3-H signal in both complexes is equally shifted (by $\sim 1.6\text{ppm}$). C4-H is slightly more deshielded in $\text{Cr}(\text{CO})_5\text{C}(\text{OEt})\text{-P-P-H}$ than in $\text{Cr}(\text{CO})_5\text{C}(\text{OEt})\text{-P-H}$. The same was observed for $\text{Cr}(\text{CO})_5\text{C}(\text{OEt})\text{-P-P-H}$ and $\text{Cr}(\text{CO})_5\text{C}(\text{OEt})\text{-P-H}$.

The protons, C7, C8 and C9 are unaffected by complexation. No electron density is withdrawn from the second ring.

Table 5: ^1H NMR resonances for the mono- and biscarbene chromium complexes.

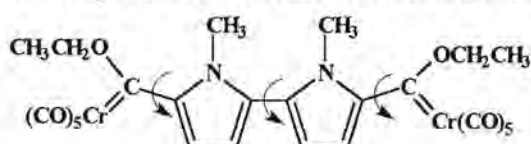
Compound	PROTON	δ (ppm)	J (Hz)
	N-CH ₃	3.49 (<i>s</i>)	-
	C2-H	6.70 (<i>dd</i>)	$J_{2,3} = 2.7$ $J_{2,4} = 1.70$
	C3-H	6.18 (<i>dd</i>)	$J_{3,2} = 2.7$ $J_{3,4} = 3.49$
	C4-H	6.14 (<i>dd</i>)	$J_{4,3} = 3.49$ $J_{4,2} = 1.70$
	N-CH ₃ , N'-CH ₃	3.49 (<i>s</i>)	-
	OCH ₂ CH ₃	5.08 (<i>q</i>)	J = 7.06
	OCH ₂ CH ₃	1.64 (<i>t</i>)	J = 6.99
	C3-H	7.75 (<i>d</i>)	$J_{3,4} = 4.66$
	C4-H	6.33 (<i>d</i>)	$J_{4,3} = 4.65$
	C7-H	6.14 (<i>dd</i>)	$J_{7,8} = 3.62$ $J_{7,9} = 1.81$
	C8-H	6.17 (<i>dd</i>)	$J_{8,7} = 3.62$ $J_{8,9} = 2.72$
	C9-H	6.70 (<i>dd</i>)	$J_{9,8} = 2.72$ $J_{9,7} = 1.81$
	N-CH ₃	3.60 (<i>s</i>) 3.57 (<i>s</i>) 3.56 (<i>s</i>)	- - -
	OCH ₂ CH ₃	5.14 (<i>q</i>)	J = 7.12
	OCH ₂ CH ₃	1.67 (<i>t</i>)	J = 7.12
	C3-H	7.73 (<i>d</i>)	$J_{3,4} = 4.38$
	C4-H	6.38 (<i>d</i>), 6.33 (<i>d</i>)	$J_{4,3} = 4.38$

Solvent: CDCl₃

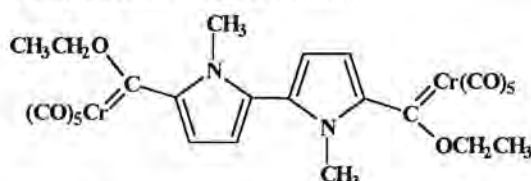
Biscarbene complex.

Three N-Me signals were observed. It is suggested that the compound has a number of different rotational isomers in solution. The rotations, that the complex can undergo is illustrated in scheme 1.

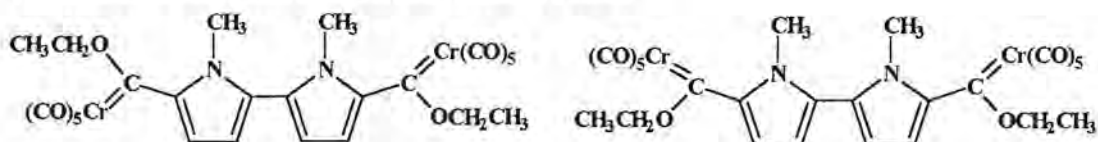
The complex can rotate around the bonds as indicated below:



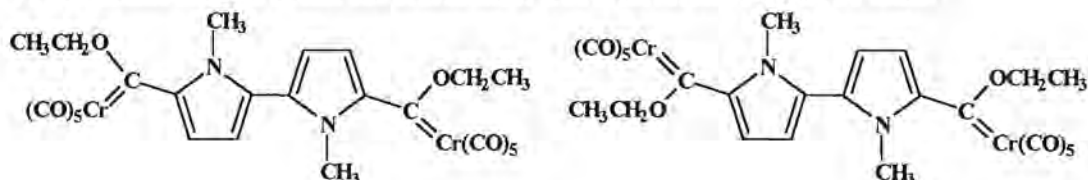
Twisted around the C5-C5' bond:



Twisted around one or both of the carbene carbon - C2 bonds:



Twisted around the C5-C5' bond and around one or both of the carbene carbon - C2 bonds:



Scheme 2: Possible rotamers that the chromium biscarbene compound can adopt in solution.

It is not possible to assign resonances to a particular isomer. However, the fact that the methylene resonances of the ethoxy substituent is duplicated, and that three resonances are observed for the N-methyl group, indicate two dominant isomers. These comprise of a symmetrically substituted biscarbene and an unsymmetrically substituted complex.

A second possibility would be three different structures of which two will give the same methylene (ethoxy group) resonances. In this case the solid state structure, the

structure representing a rotation around C5-C5 and twisted around both the carbene C2 bonds, could be the structures of the rotamers in solution.

CARBON NMR SPECTROSCOPY

The ^{13}C NMR data for the mono- and biscarbene chromium complexes is given in table 6.

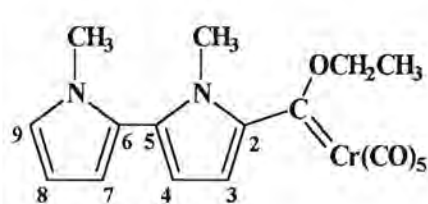
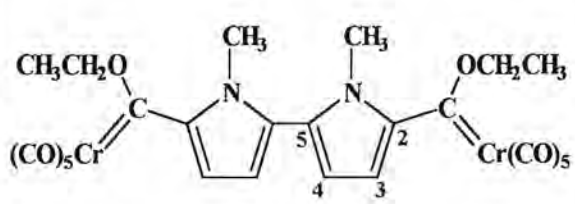
Monocarbene complex.

The carbene carbon signal is higher upfield than in the tungsten complex ($\text{W}(\text{CO})_5\text{C}(\text{OEt})\text{-P-P-H}$). The carbon atoms on the second ring are also less affected than in the tungsten case.

Biscarbene complex.

The chemical shift of the ring carbons C3 and C4 of the biscarbene tungsten complex and the biscarbene chromium complex are the same. The same is true for the carbons of the ethyl group of the ethoxy substituent. The signal of the carbonyl ligands and carbene carbons of the tungsten carbene complex is shifted upfield in the tungsten case, compared to the chromium complex. This relatively greater deshielding of the carbene by the chromium, compared to tungsten, is because of the greater electron accepting ability of the carbene carbon from the metal *d*-orbitals of chromium relative to tungsten. The π -donating *d*-orbitals of tungsten are further in energy from the π -acceptor orbitals of the carbene ligand, and less electron donation occurs.

Table 6: ^{13}C NMR resonances for the mono- and biscarbene chromium complexes.

Compound	Carbon	δ (ppm)
	N-CH ₃ , N'-CH ₃	37.8
	OCH ₂ CH ₃	77.4
	OCH ₂ CH ₃	15.5
	Carbene-C	330.3
	C2	133.6
	C3	124.9
	C4	112.9
	C5	122.6
	C6	110.5
	C7	108.5
	C8	107.3
	C9	113.8
CO	218.0 (<i>cis</i>) 223.2 (<i>trans</i>)	
	N-CH ₃	37.8
	OCH ₂ CH ₃	78.6
	OCH ₂ CH ₃	15.3
	Carbene-C	327.4
	C2	156.9
	C3	134.2
	C4	114.8
	C5	144.6
CO	218.0 (<i>cis</i>) 224.9 (<i>trans</i>)	

Solvent: CDCl₃

HETCOR.

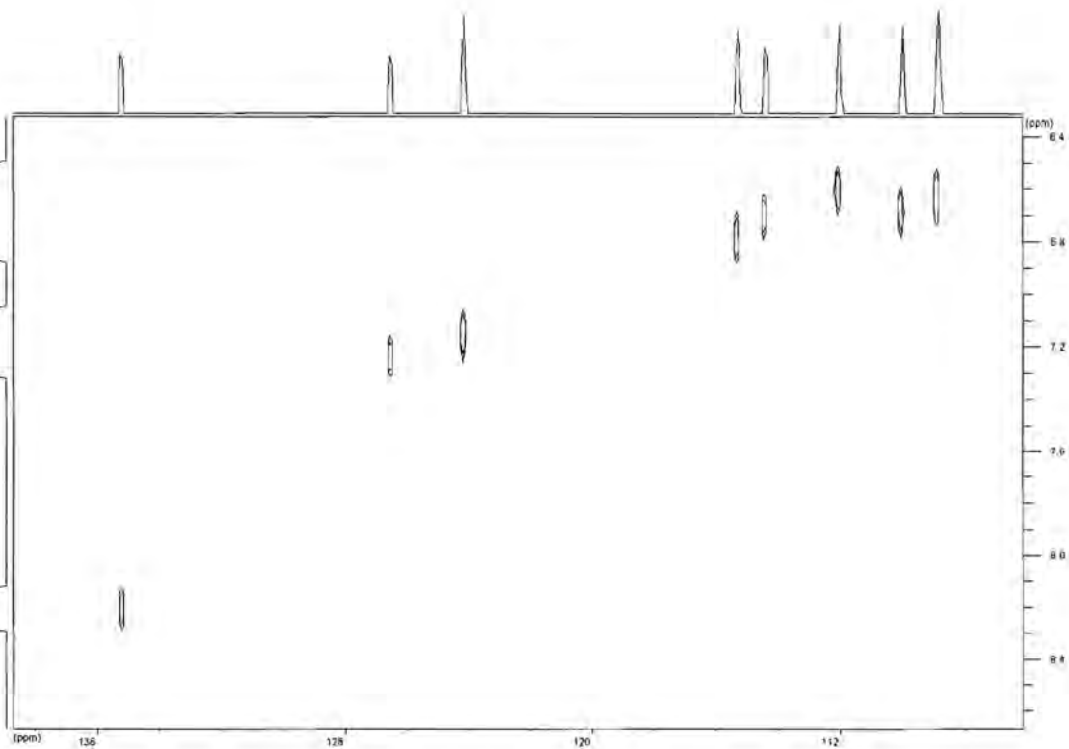


Figure 6. Part of the HETCOR of the monocarbene chromium complex.

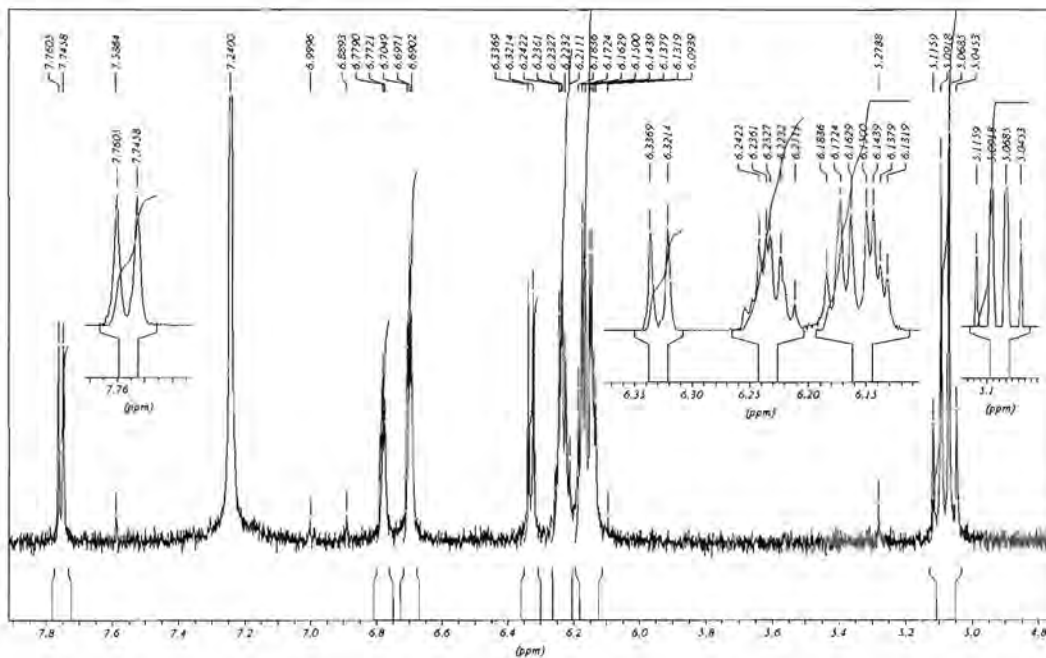


Figure 7. Proton NMR spectrum of P7 in the region 4.7-8.0ppm.

3.2.2 Mass Spectrometry

The monocarbene complex's fragment ions are given in table 7.

Table 7: Fragment ions of the monocarbene chromium complex.

<i>m/z</i> (I, %)	Fragment Ion	<i>m/z</i> (I, %)	Fragment Ion
408.0 (7)	M ⁺	268.1 (100)	M ⁺ -5CO
380.1 (25)	M ⁺ -CO	224.1 (46)	
352.1 (11)	M ⁺ -2CO	211.0 (85)	M ⁺ -6CO-Et
324.2 (13)	M ⁺ -3CO	51.9 (53)	Cr ⁺
296.1 (62)	M ⁺ -4CO		

Monocarbene complex.

The molecular mass of the monocarbene complex is 408.3amu and a molecular ion peak is found at this value. Five carbonyl groups are lost in a stepwise fashion. The second strongest peak on the spectrum is at $m/z = 210$.

The peak at m/z -values 224 is a little confusing. The mass loss from 268 to 211 represents the fragmentation of the carbene carbon and ethoxy substituent. It is a general phenomenon that after the carbonyl ligands, the carbene will fragment. In the process the bipyrrrole becomes attached to the metal.

Biscarbene complex.

The mass spectrum of P8 was determined twice, and a molecular ion peak was observed on neither of the spectrums.

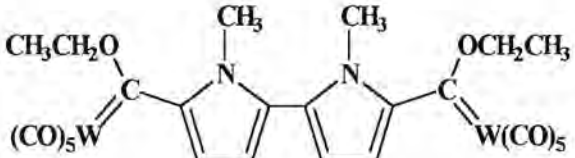
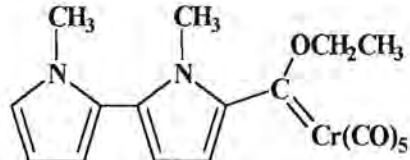
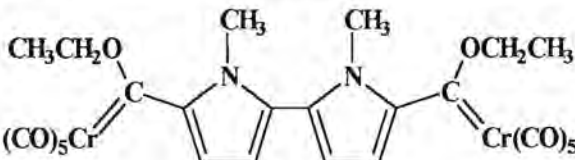
3.2.3 Infrared Spectroscopy

The bands observed for both P7 and P8 are at 2054 ($A_1^{(1)}$), 1943 ($A_1^{(2)}$) and 1934 (E) cm^{-1} . No B_1 peak was observed. These peaks are the same for the mono- and biscarbene chromium complexes P3 and P4, and support the similar NMR data of the two complexes.

3.2.4 Ultraviolet Spectroscopy

The UV data of the biscarbene tungsten complex and the mono- and biscarbene chromium complexes are given in table 8.

Table 8: Ultraviolet data for the biscarbene tungsten complex and the mono- and biscarbene chromium complexes.

Compound	Peaks (λ)	Intensity	Transition
	247	3.936	Ligand based
	283	3.721	Ligand based
	352	1.270	$\pi \rightarrow \pi^*$
	463	2.546	d-d
	218	1.453	Ligand based
	347	3.318	$\pi \rightarrow \pi^*$
	430	3.574	d-d
	247	2.421	Ligand based
	355	-	$\pi \rightarrow \pi^*$
	457	0.271	d-d

The ultraviolet absorption spectrum of 2,2'-bipyrrrole reveals peaks at 276 and 284nm⁸.

A comparison of the tungsten complexes $W(CO)_5C(OEt)-P-H$ (433nm) and $W(CO)_5C(OEt)-P-P-C(OEt)W(CO)_5$ (463nm), reveals a bathochromic shift. The d-d signal is shifted by 30nm.

The d-d signal of the chromium complex $Cr(CO)_5C(OEt)-P-C(OEt)Cr(CO)_5$ is at 457nm, and the d-d signal of $Cr(CO)_5C(OEt)-P-P-C(OEt)Cr(CO)_5$ is at 472nm. The bathochromic shift is indicative of an increased conjugation in the biscarbene complex $Cr(CO)_5C(OEt)-P-C(OEt)Cr(CO)_5$.

⁸ H. Rapoport, N. K.G. Holden; *J. Am. Chem. Soc.*, **1962**, 82, 635.

Chapter 4

Carbene Complexes of N,N'-Dimethylpyrrolo [3,2-*b*]pyrrole

1 Background.

N,N'-Dimethylpyrrolo[3,2-*b*]pyrrole has an extremely electron rich character (10 π -electrons). Satake and coworkers^{1a} reported the reaction of 3,3'-di-*tert*-butyl-[3,2-*b*]pyrrole with chlorosulfonyl isocyanate (ClSO₂NCO, CSI). The chlorosulfonyl group is strongly electron withdrawing and its reactivity was tested by the electron excessiveness of pyrrolo[3,2-*b*]pyrrole.

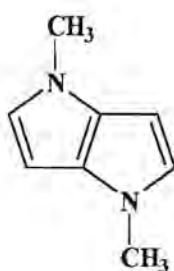


Figure 1: N,N'-Dimethylpyrrolo[3,2-*b*]pyrrole.

The reactivity of dimethyl 3,3'-di-*tert*-butylpyrrolo[3,2-*b*]pyrrole-1,4-dicarboxylate was compared with that of N-methoxycarbonyl derivatives of indole and pyrrole

¹ (a) K. Satake, K. Yano, M. Fujiwara, M. Kimura; *Heterocycles*, **1996**, *43*, 2361-2364. (b) K. Satake, D. Nakoge, M. Kimura; *Heterocycles*, **1998**, *48*, 433-436.

towards CSI. The complex reacted similar to pyrrole and indole and 3,6-di-*tert*-butylpyrrolo[3,2-*b*]pyrrolo-2,5-dicarbonitrile was formed by electrophilic addition. The reaction of 3,6-di-*tert*-butyl-pyrrolo[3,2-*b*]pyrrole-1,4-dicarboxylate with CSI gave the 1,2-carboxylic anhydride, however, which was not found with the indole and pyrrole (3-*tert*-butyl- and 3-methylindole derivatives) analogues. It is believed that the extreme electron excessiveness of the pyrrolo[3,2-*b*]pyrrole rings increases the nucleophilicity of the carbonyl oxygen atom of the N-methoxycarbonyl group.

Satake and colleagues^{1b} also reacted 3,3'-di-*tert*-butylpyrrolo[3,2-*b*]pyrrole (which is more stable than L3) with DMAD. DMAD adducts were obtained, even at 0°C. An electrophilic reaction occurred at the α position of the nitrogen. 2-vinyl- and 2,5-divinylpyrrolo[3,2-*b*]pyrrole derivatives were obtained. Under similar conditions pyrrole and indole did not give any adducts. The reaction suggests the extremely electron rich character of 3,3'-di-*tert*-butylpyrrolo[3,2-*b*]pyrrole.

Like pyrrole and N-methylpyrrole, the electropolymerization of pyrrolo[3,2-*b*]pyrrole gave electroactive polymeric films on the electrode surfaces. The molecule was used as a spacer ligand. The potential to transfer the high electron density on the rings, is interesting. Conducting polymers can exist in different oxidation states with different electrical and optical properties, depending on the applied voltage, if used as electrodic films. Oyama and coworkers² discussed the electropolymerization of pyrrolo[3,2-*b*]pyrrole. Pyrrolo[3,2-*b*]pyrrole oxidized more readily than pyrrole. The E_p^a values of poly-(pyrrolo[3,2-*b*]pyrrole) and bispyrrole are almost the same, and they explained that this may be due to increased delocalisation of the π electron systems in these molecules, as compared to pyrrole. The E_p^a value of 3,6-di-*tert*-butyl-pyrrolo[3,2-*b*]pyrrole-1,4-dicarboxylate was found to be very large, because the $-\text{COOCH}_3$ groups are electron withdrawing. The film degraded via electrochemical oxidation and chemical oxidation by oxygen in the air. The film is conducting only in the oxidized form. In an article published the next year, Oyama *et al*^{2b} presented their findings on the electropolymerization of N,N'-dimethylpyrrolo[3,2-*b*]pyrrole (H-PP-H). They studied the influence of the methyl groups on the electropolymerization and the electrochemical and physical behaviour

² a) N.Oyama, T. Ohsaka, K. Chiba, H. Miyamoto; *Synth. Met.*, **1987**, *20*, 245-258; b) N. Oyama, T. Ohsaka, H. Miyamoto, K. Chiba; *J. Chem. Soc., Perkin Trans. II*, **1988**, 833.

of the polymeric film prepared. The oxidation was not influenced by the methyl substituent. They found evidence that the film undergoes degradation *via* electrochemical oxidation, as seen for polypyrrole and polypyrrolo[3,2-*b*]pyrrole.

Beggatio and coworkers³ studied copolymers, obtained by electrochemical methods from dithienothiophene, dithienopyrrole and thionaphteneindole. It was discovered in a previous study on the copolymers of poly(dithienopyrrole-thionaphteneindole) that the presence of thionaphteneindole (> 30%) in the copolymer backbone resulted in the material being neither conducting, nor electrochromic. The authors found that the films of the thionaphteneindole- dithienothiophene copolymer could not be reduced or oxidized by changing the applied voltage. The thionaphteneindole moiety had an interrupting effect on the conjugation, and consequently the flow of charges along the chains. By contrast poly(thionaphteneindole) is a good ionic conductor. The film also changed filmability, depending on the ratios. The electrochromic properties of poly-(dithienopyrrole-dithienothiophene) were not found to be greatly affected by the ratio of the monomer units in the chain. The electrochromic features of the homopolymers are very similar.

The fused five-membered heteroaromatics **1** are slightly more stable than their isomers **2**, for X = NH and S⁴ (figure 2).

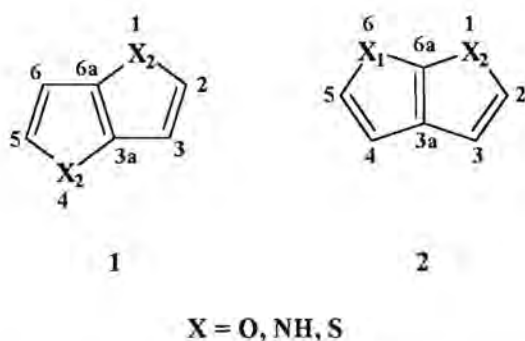


Figure 2: Condensed ligands. Cross conjugation (**1**) and linear conjugation (**2**).

Fused five-membered heteroaromatics contain [6e/6p], [6e/5p] and [6e/4p] (p: position). The X-C=C-X system is [6e/4p]. The (C=C)-(C=C)-X system is [6e/5p],

³ G. Beggatio, G. Casalbore-Miceli, A. Geri, A. Berlin, G. Pagani; *Synth. Met.*, **1996**, *82*, 11-15.

⁴ S. Inagaki, M. Urushibata; *Bull. Chem. Soc. Jpn.*, **1990**, *63*, 3117-3121.

cross in **1**, linear in **2**. The (C=C)-(C=C)-(C=C) system is [6e/6p], linear in **1** and cross in **2**. The observed thermodynamic stabilities suggest a little preference of [6e/6p] over [6e/5p] and [6e/4p], since only [6e/6p] prefers **1**.

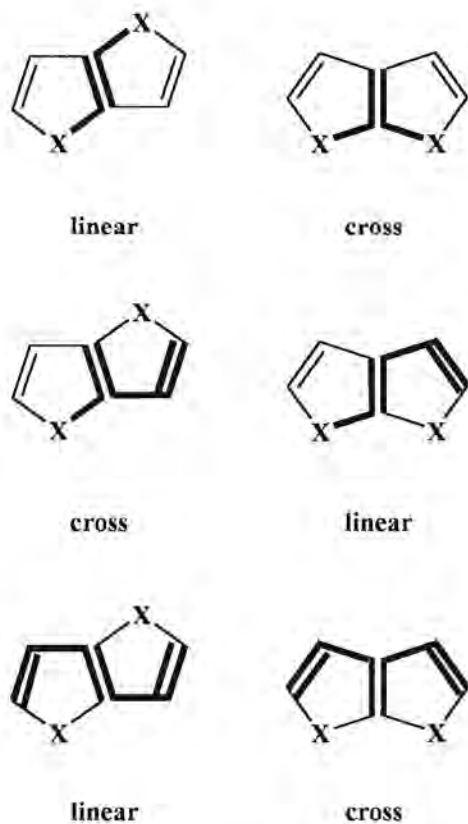
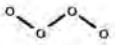
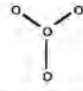
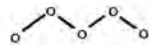
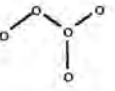
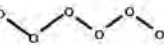
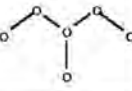


Figure 3: Fused five-membered heteroaromatics and their isomers.

The three-component interactions make the difference, as interactions between neighbouring components do not distinguish between the isomers. In molecules where there are *six* electrons distributed in four [6e/4p], five [6e/5p] and six [6e/6p] *p* orbitals, it has been found that the linear conjugation is more stable than the cross conjugation with *five* (predicted) and *six* orbitals, but the cross conjugation is more stable with *four* orbitals. In table 1 the relative stabilities are shown.

Table 1: Relative stabilities predicted from Orbital Phase Property⁵.

	4p		5p		6p	
						
2e	Unstable	Stable	-	-	-	-
4e	Stable	Unstable	Stable	Unstable	-	-
6e	Unstable	Stable	Stable	Unstable	Stable	Unstable

Inagaki and his coworkers found that the delocalisation between the terminal bonds of the hexatriene [6e/6p] in **1** increased in the order: X = S < O < NH, and the thermodynamic preference increased in the order of X = S < NH. The slight thermodynamic stabilities of **1**, relative to **2**, for X = NH and S suggested a little preference of [6e/6p] over [6e/5p] and [6e/4p]. For X = O the two isomers are equally stable, due to effective delocalisation between the adjacent O and C=C bonds.

Lazzaroni *et al*⁶ did *ab initio* calculations on the electronic structure and theoretically constructed valence XPS of, amongst others, pyrrolo[2,3-*b*]pyrrole and pyrrolo[3,2-*b*]pyrrole. They determined a model structure through MNDO geometry optimisation and mainly attempted to take into account differences in configuration, and relative differences due to the nature of the heteroatoms involved, N and/or S. The [3,2-*b*] derivatives were predicted to be more stable than the [2,3-*b*] ones, mainly because of smaller nuclear repulsions due to larger internuclear distances between heteroatoms in the former series. The energy differences increases with the nitrogen content in the molecule. Gross atomic charges were little affected by the molecular configuration, except those for the α -carbons, which strongly depend on the neighbouring heteroatoms. Overlap populations indicated that double and single bond alternation is less pronounced in the [3,2-*b*] than in the [2,3-*b*] derivatives and in the nitrogen rather than the sulfur molecules.

⁵ S. Inagaki, Y. Hirabayashi; *Chem. Lett.*, **1982**, 709. S. Inagaki, H. Kawata, Y. Hirabayashi; *Bull. Chem. Soc. Jpn.*, **1982**, 55, 3724. S. Inagaki, K. Iwase, H. Kawata; *ibid.*, **1985**, 58, 610. S. Inagaki, K. Iwase, N. Goto, *J. Org. Chem.*, **1986**, 51, 362.

⁶ R. Lazzaroni, J.P. Boutique, J. Riga, J.J. Verbist; *J. Chem. Soc. Perkin. Trans. II*, **1985**, 97-102.

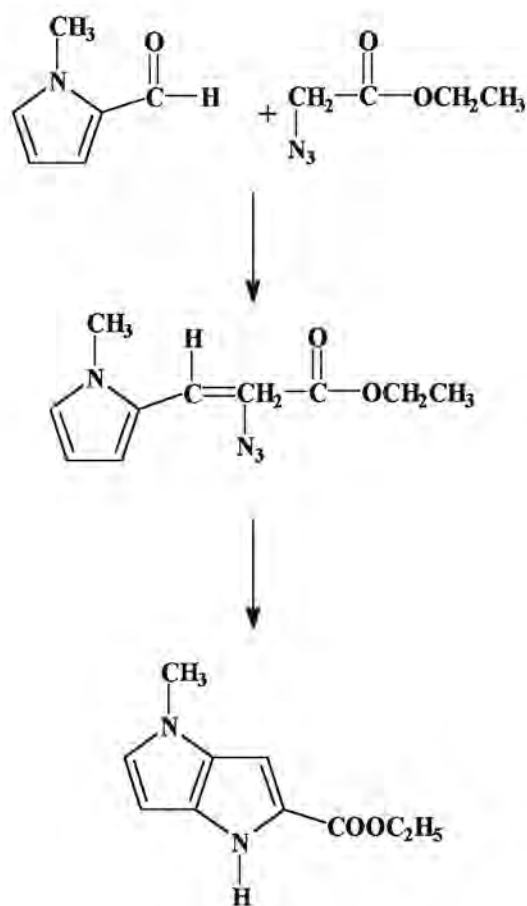
Aromaticity results from cyclic conjugation. High stability, low reactivity and sustained induced ring current imply high aromaticity. Quantitative descriptions of aromaticity usually start from considering the thermodynamic stability of aromatic compounds. Resonance energy is defined as the difference between total π -electron energy of a given conjugated molecule and the total π -electron energy of a corresponding hypothetical reference structure. To characterize the ring current aspect of aromaticity, the minimum bond order in the conjugated molecule of interest has been used. Absolute hardness, which is approximately half the HOMO-LUMO gap, correlates with REPE (resonance energy per π electron), in general. Zhou and Parr⁷ also defined relative hardness for a conjugated molecule. For relative hardness the dividing line between aromatic and anti-aromatic is the zero-value. The advantage of absolute hardness is that it does not depend on the subtleties of a reference structure. However, it does not provide by itself the prediction that all acyclic polyenes are non-aromatic, or the prediction that some cyclic molecules are anti-aromatic, for which purposes relative hardness appears to be useful. Hardnesses, in principle, incorporate information about σ and π electrons. The predictions by their η_r (relative hardness) index, that thieno[3,2-*b*]thiophene is aromatic and that pyrrolo[3,2-*b*]pyrrole is anti-aromatic, agree with experimental data and REPE predictions.

The mono- and biscarbene complexes of *N, N'*-dimethylpyrrolo[3,2-*b*]pyrrole was prepared.

⁷ Z. Zhou, R.G. Parr, *J. Am. Chem. Soc.*, **1989**, *111*, 7371-7379.

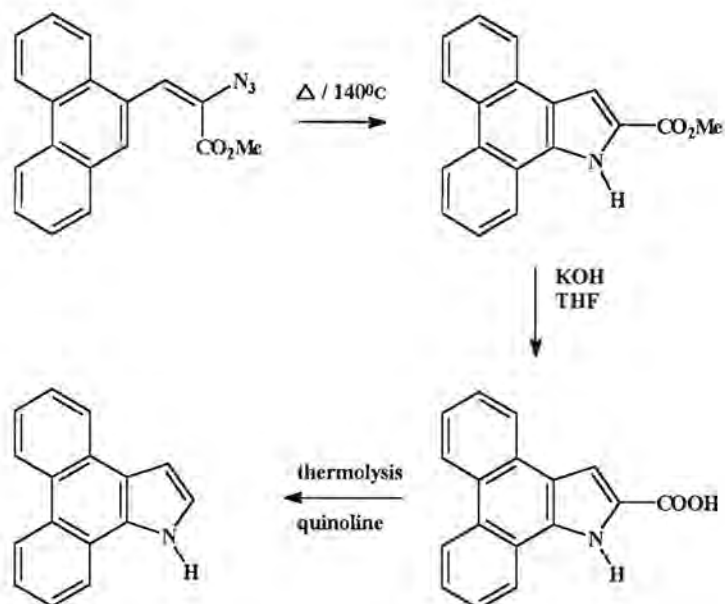
2 Synthesis.

The synthesis of N,N'-dimethylpyrrolo[3,2-*b*]pyrrole was adapted from literature⁸ and modified in our laboratories. Hemetsberger and Knittel prepared vinyl azides by condensation of various aromatic and heterocyclic aldehydes with ethyl azidoacetate or ω-azidoacetophenones:

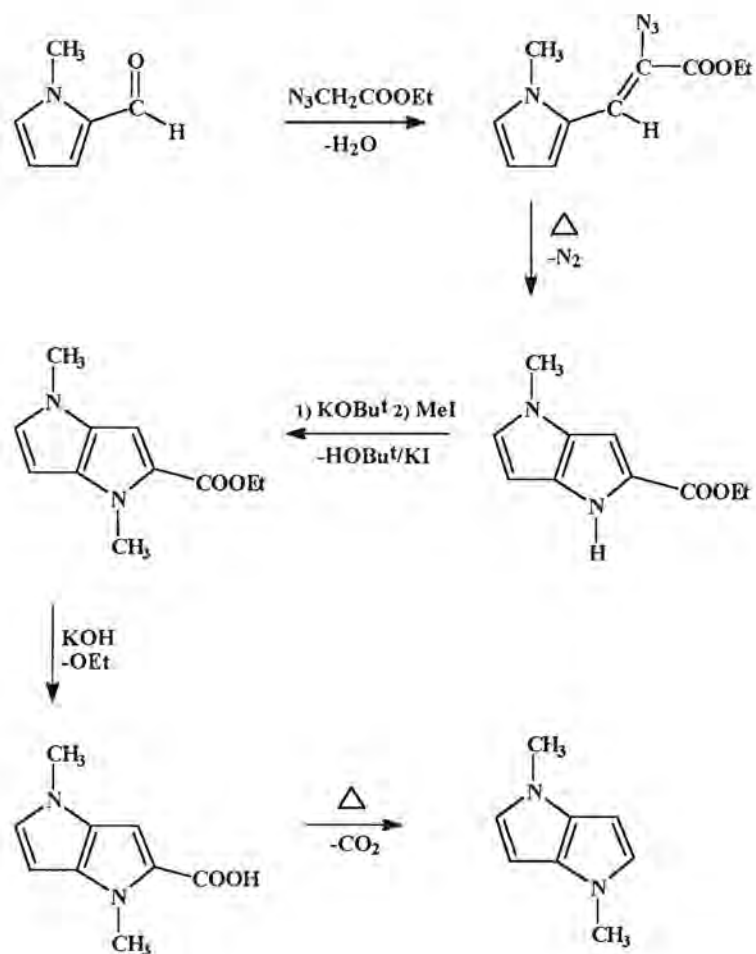


Jones and Matthews synthesized the pyrrolo[9,10]phenanthrene nucleus. The last four steps of their synthesis are of interest and is given in Scheme 1.

⁸ (a) Methoden der Organischen Chemie (Houben Weyl), 1958, Band XI/2, 353; (b) Methoden der Organischen Chemie (Houben Weyl), 1965, Band X/3, 796; (c) H. Hemetsberger, D. Knittel; *Monatshefte fuer Chemie*, 1972, 103, 194-203; (d) T. Aratani, H. Yoshihara, G. Suzukamo; *Tetrahedron Lett.*, 1989, 30, 1655-1656; (e) S. Soth, M. Farnier, C. Paulmier; *Can. J. Chem.*, 1978, 56, 1429; (f) G.B. Jones, J.E. Matthews; *Tetrahedron*, 1997, 53, 14599-14614.



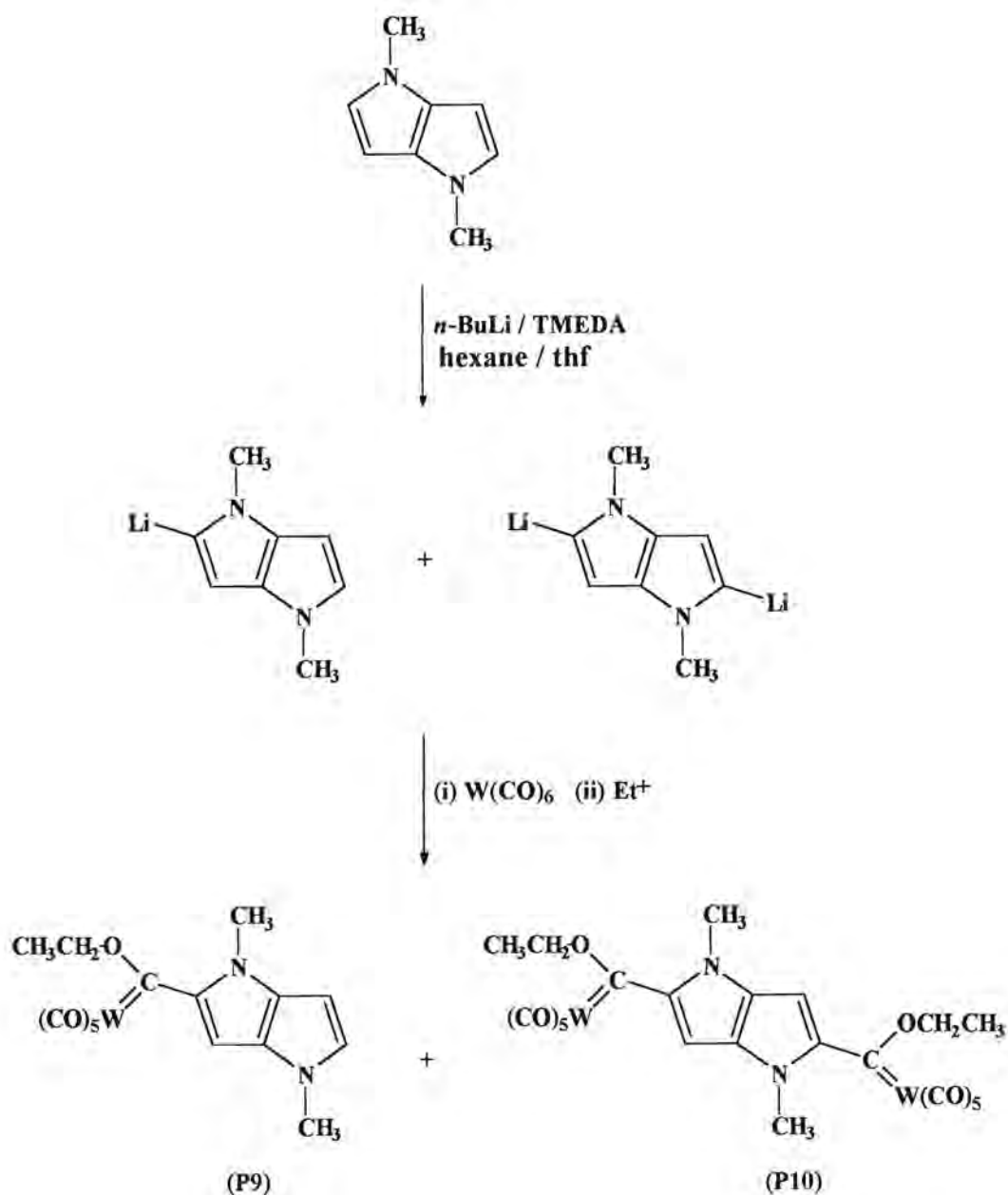
Scheme 1: Synthesis of the pyrrolo[9,10]phenanthrene nucleus.



Scheme 2: Synthesis of N,N'-dimethylpyrrolo[3,2-b]pyrrole.

The aldol is reacted with azide, to give the azide product, which undergoes cyclization upon heating, to give the condensed [3,2-*b*] rings. Nitrogen gas is formed. Next the hydrogen of the nitrogen is deprotonated with KO^tBu and methylated with MeI. The ester is converted to a carboxylic acid with KOH and then the product is decarboxylated by heating it.

The mono- and biscarbene carbene complexes were synthesized (Scheme 3). The mono- (yellow-brown) and the biscarbene (purple) complexes were obtained.



Scheme 3: Synthesis of carbene complexes.

3 Characterization of complexes.

3.1 Tungsten Complexes

Mono- and biscarbene complexes with pyrrolopyrrole substituents were obtained and characterized by NMR, IR and UV spectroscopy and MS spectrometry. The data is given below and discussed.

3.1.1 NMR Spectroscopy

PROTON NMR SPECTROSCOPY

The ^1H NMR data for the mono- and biscarbene complexes is given in table 2.

Monocarbene complex.

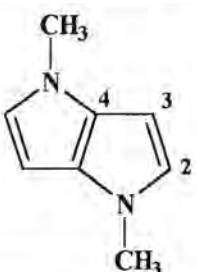
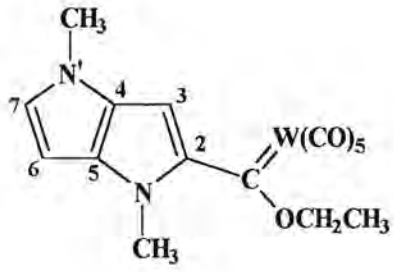
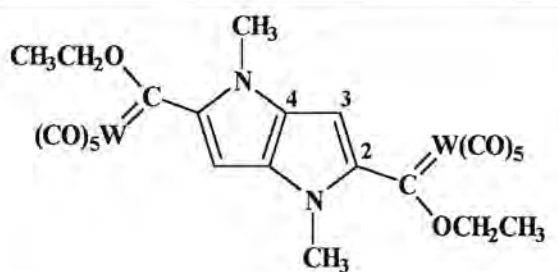
The spectrum of P9 shows that C3-H and C7-H couple with each other, but because four bonds separate them, the coupling is small.

A comparison of the resonances of the ring protons of the monocarbene complex $\text{W}(\text{CO})_5\text{C}(\text{OEt})\text{-PP-H}$ with the resonances of the ring protons of the monocarbene complexes $\text{W}(\text{CO})_5\text{C}(\text{OEt})\text{-P-H}$ and $\text{W}(\text{CO})_5\text{C}(\text{OEt})\text{-P-P-H}$ reveals that C3-H is less deshielded (signal is shifted by 0.70ppm) than C3-H in the other two complexes (1.53ppm).

A comparison of the ring protons that are furthest from the carbene moiety (C5-H in $\text{W}(\text{CO})_5\text{C}(\text{OEt})\text{-P-H}$; C9-H in $\text{W}(\text{CO})_5\text{C}(\text{OEt})\text{-P-P-H}$; C7-H in $\text{W}(\text{CO})_5\text{C}(\text{OEt})\text{-PP-H}$) reveals that the signal of this proton is shifted the most in the complex $\text{W}(\text{CO})_5\text{C}(\text{OEt})\text{-PP-H}$.

A comparison of C4-H in $\text{W}(\text{CO})_5\text{C}(\text{OEt})\text{-P-H}$, C4-H in $\text{W}(\text{CO})_5\text{C}(\text{OEt})\text{-P-P-H}$, and C6-H in $\text{W}(\text{CO})_5\text{C}(\text{OEt})\text{-PP-H}$ reveals the following downfield shifts: 0.13ppm, 0.19ppm and 1.01ppm, respectively.

Table 2: ¹H NMR resonances of the mono- and biscarbene complexes of tungsten.

Compound	Proton	δ (ppm)	J (Hz)
	N-CH ₃	3.68 (<i>s</i>)	-
	C2-H	6.59 (<i>d</i>)	J _{2,3} = 2.59
	C3-H	5.95 (<i>d</i>)	J _{3,2} = 2.58
	N-CH ₃	3.86 (<i>s</i>)	-
	N'-CH ₃	3.83 (<i>s</i>)	-
	OCH ₂ CH ₃	4.95 (<i>q</i>)	7.12
	OCH ₂ CH ₃	1.62 (<i>t</i>)	7.12
	C3-H	7.29 (<i>s</i>)	-
	C6-H	5.96 (<i>d</i>)	J _{7,6} = 3.05
	C7-H	6.96 (<i>dd</i>)	J _{6,7} = 3.06 J _{3,7} = 0.77
	N-CH ₃	3.77 (<i>s</i>)	-
	OCH ₂ CH ₃	4.98 (<i>q</i>)	7.10
	OCH ₂ CH ₃	1.69 (<i>t</i>)	7.12
	C3-H	7.12 (<i>s</i>)	-

Biscarbene complex.

The spectrum for the biscarbene product is quite simple, an indication that the symmetric biscarbene complex formed. Four proton peaks are observed. From the proton NMR data it can be seen that only one isomer existed in solution.

The characteristic carbene quartet is observed at 4.98ppm and the triplet is observed at 1.69ppm. The N-Me signal is shifted downfield compared to N,N'-dimethylpyrrolopyrrole, but not as far downfield as both methyl resonances of the monocarbene complex.

There is a significant deshielding of the C3 proton in the biscarbene product indicating charge transfer from the ring to the electrophilic carbene carbon. The signal of this proton is a singlet. In the ligand it was split into a doublet by the proton on C2.

The C3 proton is less deshielded (1.17ppm) than C3-H of $W(CO)_5C(OEt)-P-P-C(OEt)W(CO)_5$ (1.51ppm), but more than C3-H of $W(CO)_5C(OEt)-P-C(OEt)W(CO)_5$ (1.51ppm).

CARBON NMR SPECTROSCOPY

The ^{13}C NMR spectral data is given in table 3.

Monocarbene complex.

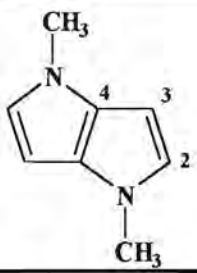
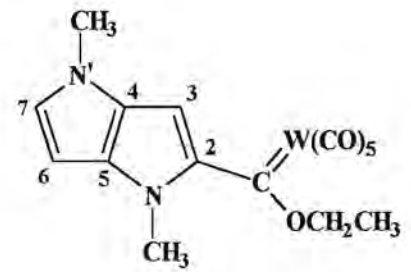
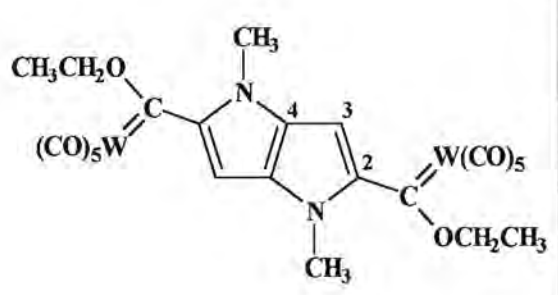
The signals of C4 and C5 could not be assigned with any certainty.

In the pyrrole and bipyrrrole complexes the spectra revealed that the stabilization was mainly a short distance effect, but with this complex indications are that it is an effect over C7, a longer distance. This is implied by the observation that C7 for instance lies much further downfield than C9 of $W(CO)_5C(OEt)-P-P-H$, and is supported by the fact that C7-H is shifted much more downfield as well in the 1H NMR spectrum.

Biscarbene complex.

The signals of the carbene carbons lie very close. This was not seen with the other tungsten complexes. The carbene carbons are deshielded by about the same amount as the carbene carbon of the biscarbene complex $W(CO)_5C(OEt)-P-P-C(OEt)W(CO)_5$ (282.4ppm). Pyrrolo[3,2-*b*]pyrrole is very electron rich.

Table 3: The ^{13}C NMR resonances of the mono- and the biscarbene products of tungsten.

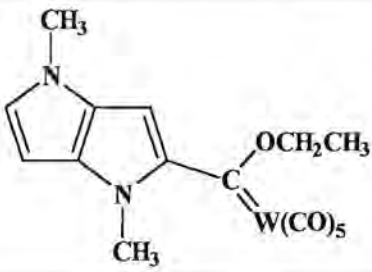
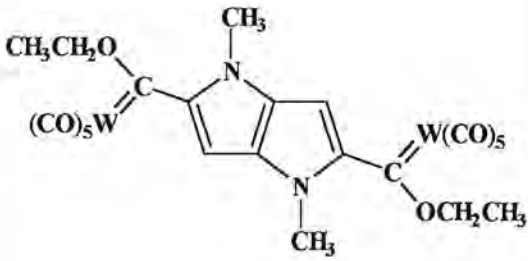
Compound	Carbon	δ (ppm)
	N-CH ₃	34.4
	C2	123.8
	C3	88.9
	C4	129.5
	N-CH ₃	37.4
	N'-CH ₃	34.5
	OCH ₂ CH ₃	78.4
	OCH ₂ CH ₃	15.3
	Carbene-C	284.1
	C2	151.0
	C3	113.2
	C4, C5	126.8, 128.6
	C6	89.6
C7	132.1	
CO	198.0 (<i>cis</i>) 202.0 (<i>trans</i>)	
	N-CH ₃	38.0
	OCH ₂ CH ₃	78.8
	OCH ₂ CH ₃	15.5
	Carbene-C	285.3
	C2	151.0
	C3	110.7
	C4	137.4
CO	198.1 (<i>cis</i>) 202.6 (<i>trans</i>)	

Solvent: CDCl₃

3.1.2 Mass Spectrometry.

Mass spectral data for the complexes are given in table 4.

Table 4: Mass spectrometry data for the tungsten mono- and biscarbene products.

Compound	Fragment Ions (I, %)
	512 (55) M^+ ; 485 (33) $M^+ - CO$; 456 (23) $M^+ - 2CO$; 428 (15) $M^+ - 3CO$; 401 (32) $M^+ - 4CO$; 373 (86) $M^+ - 5CO$; 345 (63) $M^+ - 5CO - Et$; 317 (70) $M^+ - 6CO - Et$; 288 (20) $M^+ - 6CO - Et - 2CH_3$.
	134; 212 $W(CO)^+$; 268 (100) $W(CO)_3^+$; 296 $W(CO)_4^+$; 317; 352 $W(CO)_6^+$; 372; 432; 458; 528; 584; 613; 641; 697; 756; 784 (100) $N^+ = M^+ - 4CO$; 844; 904; 907

Monocarbene Complex.

The molecular mass of the monocarbene complex is 514.15amu. Strong peaks are seen on the spectrum around a value of $m/z = 512$. As tungsten has many isotopes, this is not unexpected. The five carbonyls bonded to tungsten are fragmented first, and then either the ethoxy ethyl group is lost as ethylene or the carbene carbon is eliminated as CO. The peak at $m/z = 317$ is assigned to the ligand ($M_r = 134.18g/mol$) bonded to tungsten. Both the N-methyl groups are fragmented next, after which the ligand breaks up.

Biscarbene Complex.

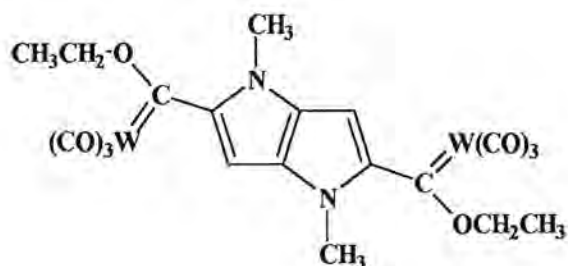
The molecular mass of the product is 870.07amu. The molecular ion peak was not observed, and a mass spectrum showing only fragments of organic products were recorded. Repetition of the determination revealed a different spectrum, and certain peaks differed drastically in intensity, and therefore intensity data was omitted.

The spectrum reveals a large number of unassignable peaks, some with and others without the association of the tungsten isotopes.

Looking at the peak grouping around $m/z = 318$, the strongest peak is $m/z = 317$, and the second strongest $m/z = 315$, where weaker peaks are seen at $m/z = 316$, and $m/z = 319$, with a very weak peak at $m/z = 318$. This close grouping of peaks is due to the presence of tungsten with its many isotopes.

The peaks of the metal carbonyl fragments $W(CO)$ ($M_r = 211.86\text{g/mol}$), $W(CO)_2$, $W(CO)_3$, $W(CO)_4$ and $W(CO)_6$ are seen ($m/z = 212, 240, 268, 296$ and 352). The fragmentation pattern observed indicates that $W(CO)_6$ formed in the mass spectrometer, and then fragmented. The peaks around $m/z = 323$, corresponding to $W(CO)_5$, are very weak, but this is not uncommon for metal carbonyls where the first two carbonyls fragment as a pair.

Smaller peaks from $m/z = 528$ to 844 indicate the fragmentation of carbonyls and ethyl groups. The principle peak is at m/z value 784 (highest m/z value of biscarbene complex) and corresponds to the fragment ion where four carbonyls have been fragmented.



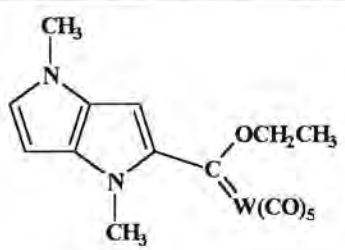
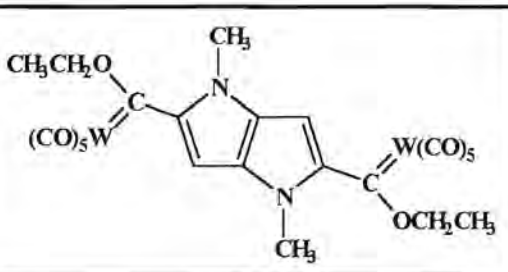
From the ion $m/z = 784$ (assigned as N^+), the following fragments are lost in a stepwise manner: N^+-2CO ; $N^+-2CO-Et$; $N^+-3CO-Et$; $N^+-3CO-Et$; $N^+-5CO-Et$.

The peaks at $m/z = 904$ and 907 are indicative that new products formed in the instrument during the mass spectrum determination.

3.1.3 Infrared Spectroscopy

Infrared data for the mono- and biscarbene complexes are given in table 5.

Table 5: Infrared data of the mono- and biscarbene tungsten complexes.

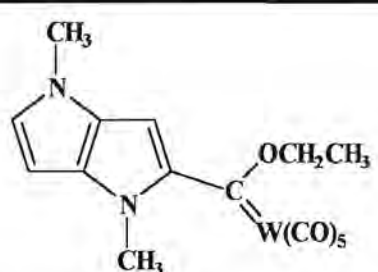
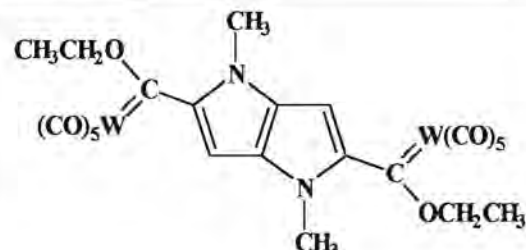
COMPLEX	$A_1^{(1)}$	B_1	$A_1^{(2)}$	E
	2059	-	1944	1937
	2060	1973	1945	1935

The values for the monocarbene and biscarbene complexes are very similar. These values agree with the values for the monocarbene complex $W(CO)_5C(OEt)-P-P-H$.

3.1.4 Ultraviolet Spectroscopy

Ultraviolet spectral data for the mono- and biscarbene complexes are given in table 6.

Table 6: Ultraviolet spectroscopy data of the mono- and biscarbene tungsten complexes.

Compound	Peaks (λ)	Intensity	Transition
	235	3.592	Ligand based
	349	1.944	$\pi \rightarrow \pi^*$
	457	2.658	d \rightarrow d
	235	1.138	Ligand based
	343	0.454	$\pi \rightarrow \pi^*$
	475	0.337	d \rightarrow d
	556	0.254	

The λ_{\max} of N,N'-dimethylpyrrolo[3,2-*b*]pyrrole is at 260nm⁹.

The d-d transition of $W(CO)_5C(OEt)-P-P-H$ is at 457nm. The d-d peak of the biscarbene is at 475nm. The peak is shifted substantially and represents far greater conjugation in the molecule.

⁹ H. Prinzbach, R. Schwesinger, M. Breuninger, B. Gallenkamp, D. Hunkler, *Angew. Chem.*, **1975**, *9*, 349.

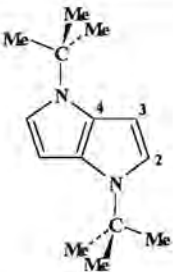
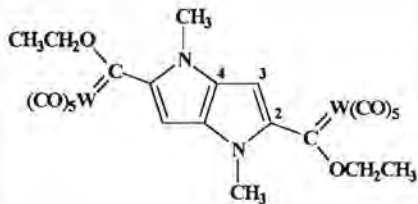
3.1.5 Crystal Structure.

Suitable crystals were obtained from a 1:1 hexane: dichloromethane mixture of the biscarbene tungsten complex. A ball and stick representation of the structure of $W(CO)_5C(OEt)-PP-C(OEt)W(CO)_5$ is given in figure 4. Figure 5 shows another view of the complex. Bond distances and bond angles are included, but the full list with standard deviations is given in Appendix D.

The orientation of the planar condensed pyrrole rings is given such that the N-Me groups are on the same side of the OEt substituents of the carbene ligands. The spacer ligand is completely planar. The dihedral angle W-C-C-N is $+159.5^\circ$.

Tom Dieck *et al*¹⁰ prepared N,N'-dibutylpyrrolo[3,2-*b*]pyrrole and recorded a crystal structure determination. Structural data are compared in table 7.

Table 7: Bond lengths (Å) of N,N'-dibutylpyrrolo[3,2-*b*]pyrrole and the biscarbene tungsten complex.

Bond			Deviation
N-C2	1.376 (3)	1.422 (5)	+0.05
C2-C3	1.359 (3)	1.402 (6)	+0.04
C3-C4	1.409 (3)	1.408 (5)	Same
C4-C4'	1.374 (3)	1.396 (8)	+0.02
N-C4'	1.384 (3)	1.364 (5)	-0.02

The W-C(carbene) bond distance of $W(CO)_5C(OEt)-PP-C(OEt)W(CO)_5$ (2.238Å) is very similar to the W-C(carbene) bond distance of $W(CO)_5C(OEt)-P-P-C(OEt)W(CO)_5$

¹⁰ H. tom Dieck, U Verfürth, K. Diboldt, J. Ehlers, G. Fendesak; *Chem. Ber.*, **1989**, *122*, 129-131.

(2.230Å). The W-C(*trans*-CO) bond is longer (2.034 vs. 2.023Å), although these differences in bond length are small.

The C(carbene)-C(C2) distance is the same in W(CO)₅C(OEt)-PP-C(OEt)W(CO)₅ and W(CO)₅C(OEt)-P-P-C(OEt)W(CO)₅. The hetero-ring substituents do not play a significant role.

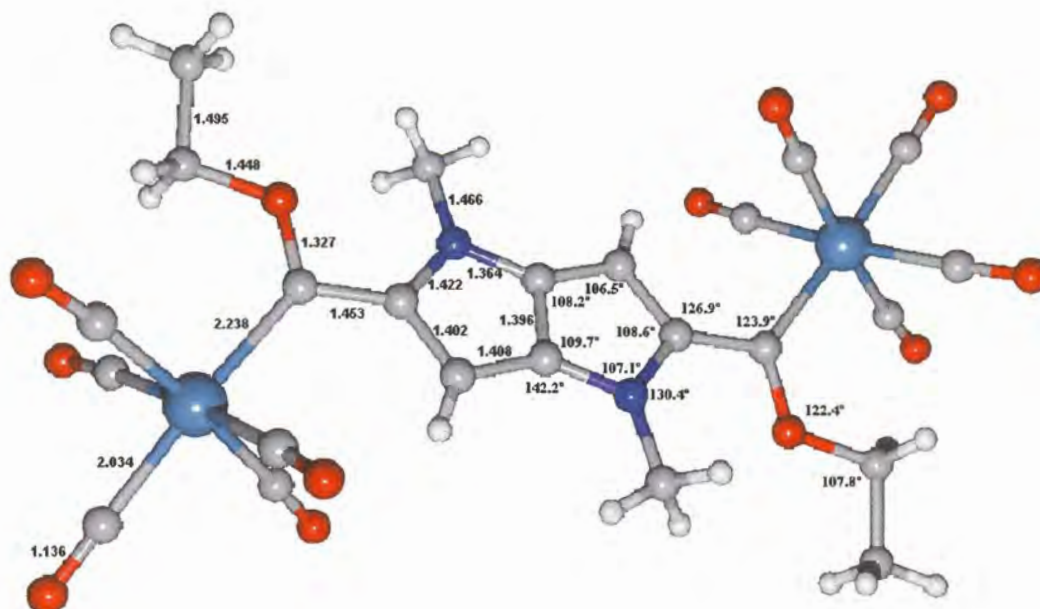


Figure 4: Ball and stick structure of the biscarbene tungsten complex.

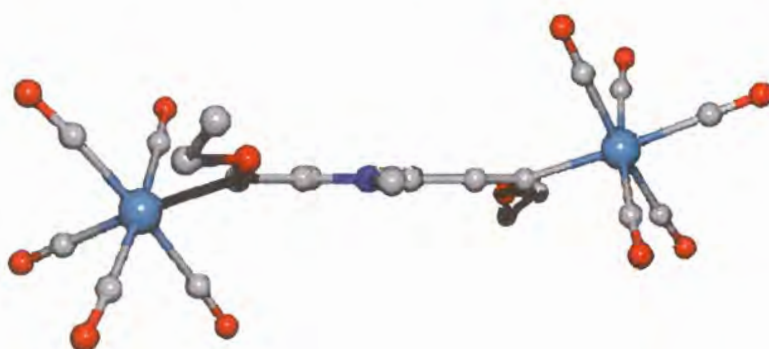


Figure 5: Structure of the biscarbene tungsten complex: Another view.

Chapter 5

Conclusion

The objectives of the study were achieved and a number of new mono- and biscarbene complexes containing pyrrole, bipyrrrole and pyrrolopyrrole were synthesized, characterized and studied in solution as well as in the solid state. Valuable information was obtained from the spectroscopic data.

1 Synthesis

N,N'-dimethylbipyrrrole and N,N'-dimethylpyrrolo[3,2-*b*]pyrrole were prepared. An improved synthesis was developed for pyrrolo[3,2-*b*]pyrrole. The bipyrrrole was prepared by utilizing the Kumada¹ coupling, using NiCl₂ as catalyst. The yields were very low.

Although the metallation and especially the double metallation of the pyrrole substrates are more difficult compared to the corresponding thiophene substrates, these could readily be achieved by using hexane as solvent and TMEDA to activate the butyl lithium base.

Carbene complexes were all prepared in the same way (Fischer synthesis). The pyrrole substrates were lithiated, Cr(CO)₆ or W(CO)₆ was added and then alkylated with an oxonium salt. The metallated pyrroles reacted smoothly with the metal carbonyls and no difficulties were experienced. Both the mono- and the biscarbene complexes were obtained.

¹ K. Tamao, K. Sumitani, M. Kumada; *J. Am. Chem. Soc.*, **1972**, *94*, 4374.

2 Characterization

NMR SPECTROSCOPY

A significant feature noticeable on the ^1H and ^{13}C NMR spectra of the complexes was the downfield shifting of the signals of the ring carbons and the ring protons. The electrophilic carbene carbon withdrew electron density from the pyrrole rings. In some instances isomers could be identified, which resulted from restricted rotations about certain bonds in solution.

When more than one pyrrole ring was involved, as was the case with bipyrrrole, the biscarbene resonances more closely resemble those of the monocarbene bipyrrrole or pyrrole complexes, suggesting that delocalisation was restricted to the ring closest to the carbene carbon. By contrast, in the case with condensed rings, pyrrolopyrrole, delocalisation to the second ring was evident for the monocarbene and biscarbene complexes.

MASS SPECTROMETRY

M^+ peaks could be seen with all of the monocarbene complexes, but with only one of the biscarbene complexes. Mass spectral data, besides for identifying complexes, revealed very little that was new in metal carbonyl fragmentation patterns.

INFRARED SPECTROMETRY

Good spectra could not always be obtained. The better spectra that could be obtained all displayed the peaks that one would expect for a complex that has a metal bonded to five carbonyl ligands and another ligand, a carbene ligand in these complexes. Good agreement was seen between all the tungsten complexes and all the chromium complexes.

ULTRAVIOLET SPECTROSCOPY

Noticable was the bathochromic shift for the biscarbene complexes, as compared to the monocarbene complexes, indicative of the bigger conjugation in the biscarbene complexes.

X-RAY CRYSTALLOGRAPHY

Suitable crystals could be obtained of three of the biscarbene complexes and one monocarbene complex and their crystal structures were determined. Structural features of the complexes gave insights into electronic properties of the carbene ligands. The electron delocalisation could be seen in the shortening and lengthening of bonds in the pyrrole rings. The spacers represented planar bridges and displayed preferred orientations of the N-Me groups with respect to the other carbene substituents.

STABILITIES

Monocarbene complexes were found to be more stable than the biscarbene complexes. The complex $W(CO)_5C(OEt)-PP-C(OEt)W(CO)_5$ was found to be very unstable. The complex $W(CO)_5C(OEt)-P-P-C(OEt)W(CO)_5$, however, was quite stable.

Chapter 6

Experimental Information

1 Products

Table 1: Products. (C-Chapter; T-Table, S-Section)

Compound	Colour	¹ H	¹³ C	MS	IR	UV	Structure
W(CO) ₅ C(OEt)-P-P-H	Orange	C2, T1	C2, T2	C2, T3	C2 S3.1.3	C2, T12	C2 S3.1.5
W(CO) ₅ C(OEt)-P-C(OEt)W(CO) ₅	Red	C2, T1	C2, T2	-	-	-	-
Cr(CO) ₅ C(OEt)-P-H	Orange	C2, T7	C2, T8	C2, T9	C2, T11	C2, T12	-
Cr(CO) ₅ C(OEt)-P-C(OEt)Cr(CO) ₅	Red	C2, T7	C2, T8	C2, T9	C2, T11	C2, T12	C2 S3.2.5
W(CO) ₅ C(OEt)-P-P-H	Orange-Brown	C3, T1	C3, T2	C3, T3	C3 S3.1.3	-	-
W(CO) ₅ C(OEt)-P-P-C(OEt)W(CO) ₅	Orange	C3, T1	C3, T2	-	-	C3, T8	C3 C3.1.5
Cr(CO) ₅ C(OEt)-P-P-H	Orange	C3, T5	C3, T6	C3, T7	C3 S3.3.1	C3, T8	-
Cr(CO) ₅ C(OEt)-P-P-C(OEt)Cr(CO) ₅	Red	C3, T5	C3, T6	-	-	C3, T8	-
W(CO) ₅ C(OEt)-PP-H	Yellow-brown	C4, T2	C4, T3	C4, T4	C4, T5	C4, T6	-
W(CO) ₅ C(OEt)-PP-C(OEt)W(CO) ₅	Purple	C4, T2	C4, T3	C4, T4	C4, T5	C4, T6	C4 S3.1.5

2 Information.

2.1 NMR Spectroscopy

All complexes were dissolved in deuterated chloroform and the NMR spectra were obtained by running the samples on the Bruker AC-300 spectrometer. Nitrogen was bubbled through the chloroform before the compound was dissolved in the solvent. Chemical shifts are relative to the deuterium signals of the deuterated solvents used. ^1H and ^{13}C NMR spectra were measured at 300.133 and 75.469 MHz, respectively.

2.2 MS Spectrometry

Mass spectra were recorded on a Perkin-Elmer RMU-6H instrument operating at 70eV.

2.3 IR Spectroscopy

To obtain Infrared spectra, the products were dissolved in dry hexane. A NaCl cell was used. Spectra were obtained by running the samples on the BOMEM Michelson-100 FT IR spectrometer.

2.4 UV Spectroscopy

Products were dissolved in dry dichloromethane. The solutions were placed in a quartz cell. After a reference was run with dichloromethane alone, the spectrum of the product was measured in the range 200.0 to 700.0nm.

2.5 Reactions

All reactions were carried out under an argon or nitrogen atmosphere, using standard Schlenk techniques¹. Solvents were dried immediately prior to use. N-methylpyrrole and TMEDA were distilled before each reaction.

The Fischer method was followed to make the mono- and biscarbene complexes. An organolithium nucleophile was added to a metal carbonyl to give an acyl metalate, which underwent O-alkylation when trialkyloxonium salt was added, to form alkoxy carbene complexes. In the different reactions that were done, sometimes 2 equivalents and sometimes 1 equivalent of BuLi (1.6-1.5 molar solution in hexane) was added, in order to make the biscarbene and the monocarbene complexes, respectively. Usually both the biscarbene and the monocarbene complexes were obtained when excess BuLi was used and they were then purified by product separation on a column with silicagel (particle size: 0.063-0.200nm). The columns were cooled by circulating cold isopropanol through column jackets.

¹ D.F. Schriver, M.A. Drezdson, 1980, *The manipulation of Air-Sensitive Compounds*, 2nd Ed. Wiley, NY.

3 Preparation of the N-methylpyrrole carbene complexes.

To prepare the 2,5-dilithiopyrrole, the method of Karas *et al*² was used. To a solution of TMEDA (1.75g, 15.9mmol) in hexane was added *n*-butyl lithium, in a 1:1 molar ratio. The mixture was stirred for 15 minutes, after which the 1-methylpyrrole (0.129g, 15mmol) was added. This mixture was refluxed for 9 hours. The mole ratio of the pyrrole to butyl lithium was $< \frac{1}{2}$. The solution was initially yellow, but after 9 hours became brown-yellow.

3.1 Tungsten Complexes.

The Schlenk was placed in an acetone/dry ice bath. $W(CO)_6$ (5.27g, 15.0mmol) was added. The solution became dark. The solvents were removed under vacuum and a little dichloromethane was added. The solution was cooled to $-30^{\circ}C$, and then the oxonium salt, Et_3OBF_4 (2.85g, 15mmol), dissolved in dichloromethane was added. The solution was filtered through silicagel to rid it of salts.

The product was transferred to a column and the mono- and biscarbene tungsten products were obtained after eluting first with hexane and thereafter with hexane-dichloromethane mixtures. Fractions: orange (monocarbene complex); red (biscarbene complex).

Yields:

P1: 2.59g = 35.3%

P2: 3.82g = 28.6%

² J. Karas, G. Huttner, K. Heinze, P. Rutsch, L. Zsolnai; *Eur. J. Inorg. Chem.*, **1999**, 405.

3.2 Chromium Complexes.

The Schlenk was placed in an acetone/dry ice bath. $\text{Cr}(\text{CO})_6$ (2.86g, 13mmol) was added and the same procedure was followed as for the tungsten case.

The product was transferred to a column and the mono- and biscarbene chromium products were obtained. Fractions: yellow; orange (monocarbene complex); red (biscarbene complex)

Yields:

P3: 1.63g = 38.1%

P4: 2.34g = 31.2%

4 Preparation of N,N'-dimethylbipyrrole and the monocarbene and biscarbene tungsten and chromium complexes.

4.1 Preparation of the bipyrrole.

Monolithiation:

N-Methylpyrrole (5.19g, 64mmol) and TMEDA (3.71g, 32mmol) was placed in a dry schlenk tube under nitrogen. At 0⁰C *n*-BuLi (20ml, 32mmol) was added, slowly and carefully. The mixture was slowly warmed to 60⁰C, and after 45 minutes a precipitate had formed. Afterwards the mixture was cooled to room temperature.

Coupling:

A 1:1 thf ether (30ml) mixture was added. The reaction mixture was cooled in a bath with dry ice to -40⁰C. Dry NiCl₂ was added (4.15g, 32mmol). A yellow-brown suspension formed. The cooling bath was removed after ten minutes and the mixture was allowed to warm up slowly. The yellowish colour disappeared and the suspension became deep black. The reaction mixture was stirred for 30 minutes at room temperature. The mixture was quenched with 30ml water. Ether was added (60ml). The water layer was extracted two more times with ether. The organic layers were combined and dried over Na₂SO₄ and the solvents were removed on the rotational evaporator.

Bulb-to-bulb distillation:

At a pressure of 0.1Torr the unreacted N-methylpyrrole and TMEDA disappeared at room temperature. After one hour the reaction mixture was heated slowly to 120⁰C. The bipyrrole was distilled over into the bulbs.

NiCl₂ drying:

NiCl₂·5H₂O (green) was placed in a round-bottomed flask and connected to the vacuum (0.1mmHg) line. The flask was heated in an oil bath to 120-140⁰C and placed on the vacuum for two days.

Yield: L2: 1.18g = 23%

4.2 Tungsten Complexes.

To N,N'-dimethylbipyrrole (0.237g; 1.48mmol) was added TMEDA (0.358g; 3.09mmol) and then, after cooling to 0⁰C, *n*-BuLi (2ml; 3.2mmol) was added. After 10 minutes the ice was removed and the reaction mixture allowed to warm to room temperature. The colour of the solution was yellow. The reaction mixture was heated and the solution became milky and whiter (2,2'-dilithium salt precipitated). The temperature was increased to near the boiling point of hexane, and left for 15 minutes at that temperature, after which the mixture was allowed to cool down to room temperature.

The mixture was cooled to -40⁰C and W(CO)₆ (0.528g; 1.50mmol) was added. The mixture was allowed to warm up to room temperature, until all the W(CO)₆ had dissolved. The solution was observed to become very dark. The solvent was removed. A little dichloromethane was added and then the oxonium salt, Et₃OBF₄ (2.83g, 1.5mmol; dissolved beforehand in dichloromethane) was added. The solvent was removed.

The product was transferred to a column and the mono- and biscarbene chromium products were obtained. Fractions: yellow; yellow; orange (monocarbene complex); red (dark orange)

Yields:

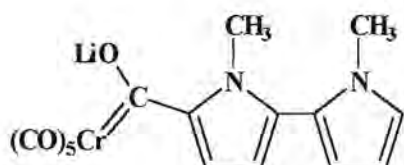
P5: 0.23g = 29.2%

P6: 0.43g = 31.6%

4.3 Chromium Complexes.

TMEDA (0.725ml, 4.81mmol) was put in a Schlenk (A) under argon. The N,N'-dimethyl bipyrrrole (0.73g, 4.56mmol) was added and the two were stirred together for 10 minutes. *n*-BuLi (3.2ml, 4.80mmol) was added and the reaction mixture was stirred until it cooled down. The colour observed was yellow and the solution was slightly milky.

Schlenk A was placed in a dry ice/ acetone bath. Cr(CO)₆ (1.06g, 4.83mmol) was added to Schlenk A. The solution became red-black and was very dark. The bipyrrrole acylate formed:



Half of the solution was taken out and put in a clean, dry Schlenk (B). BuLi (2ml, 3.0mmol) was added to Schlenk B. A dark solid material formed. Cr(CO)₆ (1.06g, 4.83mmol) was added. The solvents were removed from both Schlenks A and B. Dichloromethane was added to each Schlenk. Both Schlenks were placed in a dry ice/ acetone bath. Oxonium salt, Et₃OBF₄ was added to Schlenk A (0.90g, 5.0mmol) and B (1.83g, 10.2mmol). Both reaction solutions were filtered through silica gel to separate it from any oxonium salt that did not react.

The crude reaction mixtures were combined and filtered and the following fractions were isolated: yellow, yellow, orange (monocarbene), red (biscarbene).

Yields:

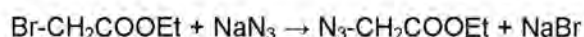
P7: 0.55g = 29.4%

P8: 0.85g = 28.5%

5 Preparation of N,N'-dimethylpyrrolo[3,2-*b*]pyrrole and the monocarbene and biscarbene tungsten complexes.

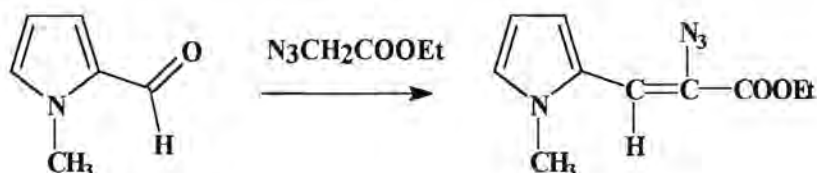
5.1 Preparation of the pyrrolo[3,2-*b*]pyrrole.

Step 1:



Br-CH₂COOEt (83.5g, 0.5mol) in 30ml EtOH and NaN₃ (35.75g, 0.55mol) in 90ml H₂O were added together and heated under reflux for 4 hours. A steam distillation was done (to get rid of salts) and the organic layer was washed twice with water and dried over anhydrous Na₂SO₄. After this a vacuum distillation was done with a water pump vacuum. The fraction between 62^oC and 65^oC was isolated.

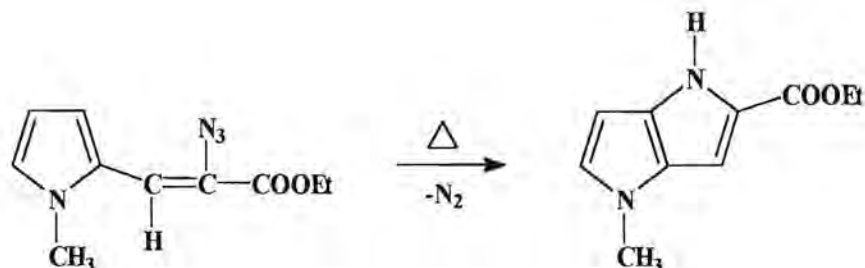
Step 2: Condensation of the aldehyde and the azide.



To a solution of sodium (2.76g, 120mmol) in 55ml ethanol was added, under vigorous stirring at 5-10^oC, a mixture of N₃-CH₂COOEt (15.48g, 120mmol) and aldehyde (4.365g, 40mmol) over a period of 30 minutes. After the development of N₂ had subsided (30- 60 minutes), half of the solution was distilled at a maximum temperature of 30^oC. The brown solution was treated with solid NH₄Cl (6.40g, 120mmol) and 500ml ice water. After this the solution was extracted 3 times with ether, filtered, washed with water until it was neutral, and then dried over Na₂SO₄. The solvent was distilled off and the brown residue dissolved in benzene and filtered through a column with silica gel. Concentrating the solution led to the formation of yellow crystals. The final product was crystallized out of a ether/hexane mixture.

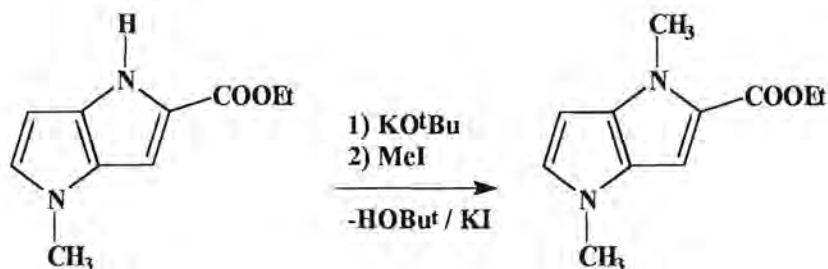
Yield : 4.3g = 49%

Step 3: Cyclization.



The crude product from the previous step was placed in a preheated flask with *p*-xylol (130^oC – 140^oC) in small portions (6g in 250ml solvent). The solution was boiled for an hour. The solvent was removed under vacuum and the dark residue was cleaned by filtration through silica gel (eluent: CH₂Cl₂). The product had a red colour, and was pure according to NMR spectroscopy.

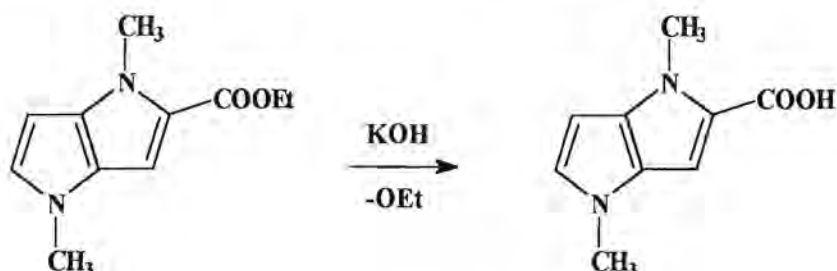
Step 4: Methylation.



In a Schlenk tube with 20ml THF was dissolved the product (5g, 26mmol) from step 3. The solution was cooled (-25^oC to -30^oC) and KO^tBu (4.55g, 40mmol) was added. The solution was stirred for 20 minutes and then the cooling bath was removed and the mixture was allowed to warm up to room temperature. The product was cooled down again (-25^oC) and MeI (7.1g, 50mmol) was added. After 30 minutes the cooling bath was removed and the mixture allowed to warm to room temperature. After a while the magnetic stirrer was able to stir the suspension. After 1 hour the mixture was quenched with water. Ether was added and the organic phase was separated. The aqueous phase was extracted twice with 20ml ether. The organic layers were

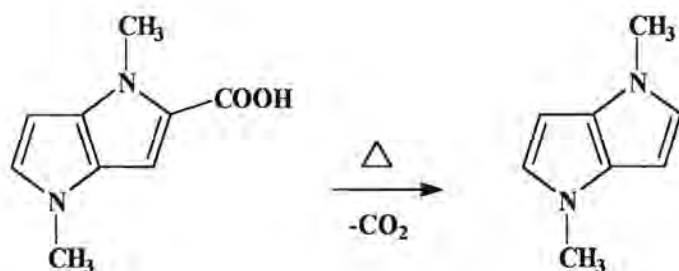
combined and dried with anhydrous Na_2SO_4 . The solvent was removed. The product had a greenish colour, and the yield was quantitative.

Step 5: Hydrolysis of the ester function to give the free acid.



The solvent was removed under vacuum. The product was dissolved in H_2O , acidified with HCl, extracted with ether and dried over Na_2SO_4 . Evaporation under vacuum gave a white crystalline solid. After two days the colour turned black (decomposition).

Step 5: Decarboxylation.



The acid product (1.2g, 6.73mmol) from the previous reaction, quinoline (8ml, 8.74mmol) and Cu powder (0.8g, 12.6mmol) were mixed together in a tube and heated in a preheated bath to ca. 220°C to 230°C . Gas evolved. The mixture was heated for 30minutes, then allowed to cool down to room temperature. The product was purified via column chromatography (silica gel; solvent: ether or ether: hexane 5:2 mixture)

5.2 Tungsten Complexes

To *N,N'*-dimethylpyrrolo[3,2-*b*]pyrrole (0.673g, 5.02mmol) was added TMEDA (1.52ml; 10.12mmol) and then, after cooling to 0⁰C, *n*-BuLi (6.4ml; 10.1mmol) was added. After 10 minutes the ice was removed and the reaction mixture allowed to warm to room temperature. The colour of the solution was yellow. The reaction mixture was heated. The temperature was increased to near the boiling point of hexane, and left for 15 minutes at that temperature, after which the mixture was allowed to cool down to room temperature.

The mixture was cooled to -40⁰C and W(CO)₆ (3.55g, 10.2mmol) was added. The mixture was allowed to warm up to room temperature, until all the W(CO)₆ had dissolved. The solution was observed to become very dark. The solvent was removed. A little dichloromethane was added, the solution cooled (-30⁰C) and then the oxonium salt (Et₃OBF₄, it was dissolved beforehand in dichloromethane) was added. The solvent was removed after the alkylation was complete.

The residue was placed on a column and the mono- and the biscarbene products were obtained after eluting with hexane: dichloromethane mixture.

Yields:

P9: 0.60g = 23.3%

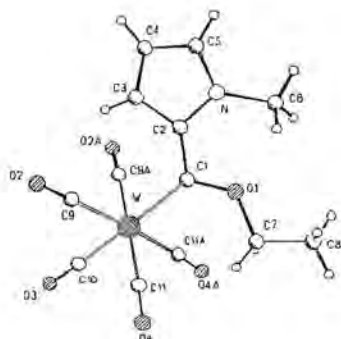
P10: 1.02g = 22.7%

Appendix A: W(CO)₅C(OEt)-P-H

Table 1. Crystal data and structure refinement.

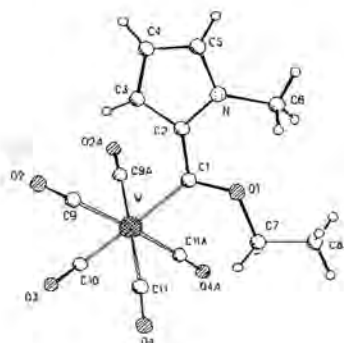
Identification code	FO1206	
Empirical formula	C ₁₃ H ₁₁ N ₁ O ₆ W	
Formula weight	461.08	
Temperature	183(2) K	
Wavelength	0.71073 Å	
Crystal system	Monoclinic	
Space group	P2(1)/m	
Unit cell dimensions	a = 9.604(1) Å	α = 90°
	b = 7.877(1) Å	β = 99.317(8)°
	c = 9.768(1) Å	γ = 90°
Volume	729.2(1) Å ³	
Z	2	
Density (calculated)	2.100 Mg/m ³	
Absorption coefficient	7.946 mm ⁻¹	
F(000)	436	
Crystal size	0.11 x 0.08 x 0.08 mm ³	
Theta range for data collection	3.34 to 27.51°	
Index ranges	-12 ≤ h ≤ 12, -9 ≤ k ≤ 10, -12 ≤ l ≤ 12	
Reflections collected	5347	
Independent reflections	1781 [R(int) = 0.1175]	
Completeness to theta = 27.51°	98.9 %	
Max. and min. transmission	0.5689 and 0.4752	
Refinement method	Full-matrix least-squares on F ²	
Data / restraints / parameters	1781 / 0 / 115	
Goodness-of-fit on F ²	1.085	
Final R indices [I > 2σ(I)]	R ₁ = 0.0565, wR ₂ = 0.1105	
R indices (all data)	R ₁ = 0.0772, wR ₂ = 0.1168	
Largest diff. peak and hole	2.348 and -2.321 e.Å ⁻³	

Table 2: Atomic coordinates ($\times 10^4$) and equivalent isotropic displacement parameters ($\text{\AA}^2 \times 10^3$).



	x	y	z	U(eq)
W	7020(1)	2500	1941(1)	28(1)
O(1)	10169(8)	2500	3731(9)	42(2)
O(2)	5479(7)	-422(9)	3423(7)	51(2)
O(3)	4414(11)	2500	-518(11)	55(3)
O(4)	8364(7)	-333(10)	198(7)	50(2)
C(1)	8786(12)	2500	3744(12)	34(3)
N	9647(10)	2500	6360(10)	31(2)
C(2)	8593(12)	2500	5190(11)	31(2)
C(3)	7310(12)	2500	5737(12)	32(3)
C(4)	7612(14)	2500	7183(13)	40(3)
C(5)	9074(14)	2500	7518(13)	40(3)
C(6)	11259(12)	2500	6399(15)	46(3)
C(7)	10775(13)	2500	2460(13)	45(3)
C(8)	12344(13)	2500	2862(16)	47(3)
C(9)	6041(9)	597(13)	2908(9)	39(2)
C(10)	5388(14)	2500	386(14)	37(3)
C(11)	7920(9)	675(12)	870(9)	36(2)

Table 3: Bond lengths [Å] and angles [°].



W-C(10)	1.998(14)
W-C(11)	2.049(10)
W-C(11)#1	2.049(10)
W-C(9)	2.077(10)
W-C(9)#1	2.077(10)
W-C(1)	2.238(11)
O(1)-C(1)	1.331(14)
O(1)-C(7)	1.455(14)
O(2)-C(9)	1.130(12)
O(3)-C(10)	1.178(15)
O(4)-C(11)	1.155(11)
C(1)-C(2)	1.454(17)
N-C(5)	1.336(16)
N-C(2)	1.399(14)
N-C(6)	1.543(15)
C(2)-C(3)	1.420(16)
C(3)-C(4)	1.395(17)
C(4)-C(5)	1.389(19)
C(7)-C(8)	1.494(17)
C(10)-W-C(11)	87.5(3)
C(10)-W-C(11)#1	87.5(3)
C(11)-W-C(11)#1	89.1(5)
C(10)-W-C(9)	89.3(3)
C(11)-W-C(9)	89.2(4)



C(11)#1-W-C(9)	176.4(3)
C(10)-W-C(9)#1	89.3(3)
C(11)-W-C(9)#1	176.4(3)
C(11)#1-W-C(9)#1	89.2(4)
C(9)-W-C(9)#1	92.4(5)
C(10)-W-C(1)	177.6(5)
C(11)-W-C(1)	94.2(3)
C(11)#1-W-C(1)	94.2(3)
C(9)-W-C(1)	89.0(3)
C(9)#1-W-C(1)	89.0(3)
C(1)-O(1)-C(7)	123.1(9)
O(1)-C(1)-C(2)	107.1(9)
O(1)-C(1)-W	128.5(9)
C(2)-C(1)-W	124.4(8)
C(5)-N-C(2)	110.4(10)
C(5)-N-C(6)	121.9(11)
C(2)-N-C(6)	127.6(10)
N-C(2)-C(3)	104.4(10)
N-C(2)-C(1)	127.2(10)
C(3)-C(2)-C(1)	128.3(10)
C(4)-C(3)-C(2)	109.3(11)
C(5)-C(4)-C(3)	106.0(11)
N-C(5)-C(4)	109.9(11)
O(1)-C(7)-C(8)	107.5(10)
O(2)-C(9)-W	178.4(8)
O(3)-C(10)-W	179.2(11)
O(4)-C(11)-W	175.8(7)

Symmetry transformations used to generate equivalent atoms:

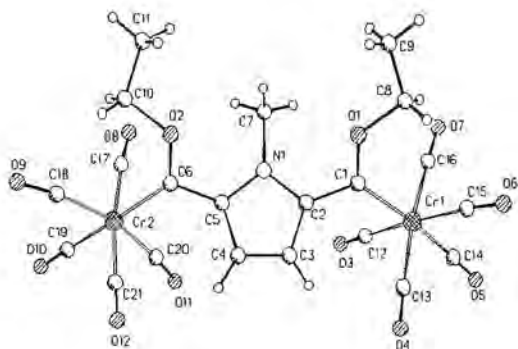
#1 $x, -y+1/2, z$

Appendix B: Cr(CO)₅C(OEt)-P-C(OEt)Cr(CO)₅

Table 1. Crystal data and structure refinement.

Identification code	FO1199	
Empirical formula	C ₂₁ H ₁₅ Cr ₂ N O ₁₂	
Formula weight	577.34	
Temperature	183(2) K	
Wavelength	0.71073 Å	
Crystal system	Monoclinic	
Space group	P2(1)/c	
Unit cell dimensions	a = 14.5658(5) Å	α = 90°
	b = 11.0161(4) Å	β = 114.516(2)°
	c = 16.8936(6) Å	γ = 90°
Volume	2466.3(1) Å ³	
Z	4	
Density (calculated)	1.555 Mg/m ³	
Absorption coefficient	0.944 mm ⁻¹	
F(000)	1168	
Crystal size	0.32 x 0.20 x 0.12 mm ³	
Theta range for data collection	3.57 to 27.52°	
Index ranges	-18 ≤ h ≤ 18, -14 ≤ k ≤ 13, -21 ≤ l ≤ 21	
Reflections collected	9630	
Independent reflections	5630 [R(int) = 0.0526]	
Completeness to theta = 27.52°	99.1 %	
Max. and min. transmission	0.8951 and 0.7521	
Refinement method	Full-matrix least-squares on F ²	
Data / restraints / parameters	5630 / 0 / 385	
Goodness-of-fit on F ²	1.037	
Final R indices [I > 2σ(I)]	R1 = 0.0553, wR2 = 0.0881	
R indices (all data)	R1 = 0.0992, wR2 = 0.0993	
Largest diff. peak and hole	0.312 and -0.372 e.Å ⁻³	

Table 2: Atomic coordinates ($\times 10^4$) and equivalent isotropic displacement parameters ($\text{\AA}^2 \times 10^3$).

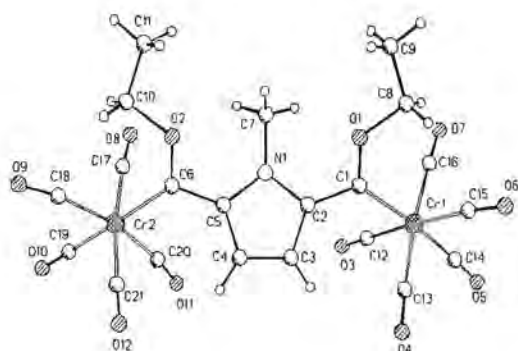


	x	y	z	U(eq)
Cr(1)	9574(1)	2359(1)	5828(1)	27(1)
Cr(2)	3668(1)	522(1)	2666(1)	21(1)
O(1)	7795(1)	2995(2)	6294(1)	30(1)
O(2)	4260(1)	1917(2)	4393(1)	27(1)
O(3)	8581(2)	2434(2)	3841(2)	52(1)
O(4)	9701(2)	-399(2)	5968(2)	52(1)
O(5)	11522(2)	2261(3)	5574(2)	66(1)
O(6)	10778(2)	2239(2)	7800(1)	51(1)
O(7)	9764(2)	5130(2)	5835(2)	51(1)
O(8)	3360(2)	3192(2)	2154(2)	51(1)
O(9)	1684(2)	33(2)	2825(2)	49(1)
O(10)	2411(2)	-296(2)	811(1)	47(1)
O(11)	5298(2)	435(2)	1978(2)	45(1)
O(12)	4347(2)	-2022(2)	3385(2)	54(1)
N(1)	6267(2)	2108(2)	4854(1)	22(1)
C(1)	8143(2)	2399(2)	5795(2)	24(1)
C(2)	7268(2)	1752(2)	5132(2)	24(1)
C(3)	7273(2)	651(3)	4726(2)	32(1)
C(4)	6278(2)	339(3)	4195(2)	31(1)
C(5)	5651(2)	1246(2)	4270(2)	23(1)



C(6)	4539(2)	1259(2)	3871(2)	22(1)
C(7)	5945(2)	3364(3)	4934(2)	28(1)
C(8)	8438(2)	3741(4)	7036(2)	36(1)
C(9)	7749(3)	4494(4)	7290(3)	41(1)
C(10)	3203(2)	2192(3)	4195(2)	30(1)
C(11)	3211(3)	3160(4)	4823(3)	42(1)
C(12)	8928(2)	2386(3)	4582(2)	34(1)
C(13)	9615(2)	638(3)	5893(2)	35(1)
C(14)	10795(2)	2305(3)	5693(2)	41(1)
C(15)	10292(2)	2315(3)	7069(2)	35(1)
C(16)	9666(2)	4103(3)	5832(2)	34(1)
C(17)	3428(2)	2184(3)	2327(2)	30(1)
C(18)	2448(2)	271(3)	2819(2)	31(1)
C(19)	2882(2)	-8(3)	1523(2)	30(1)
C(20)	4732(2)	518(3)	2291(2)	30(1)
C(21)	4074(2)	-1076(3)	3114(2)	31(1)

Table 3: Bond lengths [Å] and angles [°].



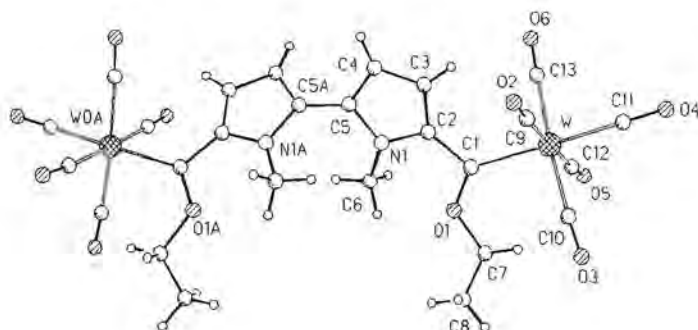
Cr(1)-C(14)	1.886(3)
Cr(1)-C(13)	1.899(3)
Cr(1)-C(15)	1.915(3)
Cr(1)-C(12)	1.918(3)
Cr(1)-C(16)	1.925(3)
Cr(1)-C(1)	2.062(3)
Cr(2)-C(19)	1.883(3)
Cr(2)-C(20)	1.902(3)
Cr(2)-C(17)	1.907(3)
Cr(2)-C(21)	1.910(3)
Cr(2)-C(18)	1.919(3)
Cr(2)-C(6)	2.067(3)
O(1)-C(1)	1.325(3)
O(1)-C(8)	1.467(3)
O(2)-C(6)	1.329(3)
O(2)-C(10)	1.465(3)
O(3)-C(12)	1.139(4)
O(4)-C(13)	1.151(4)
O(5)-C(14)	1.158(4)
O(6)-C(15)	1.144(4)
O(7)-C(16)	1.140(4)
O(8)-C(17)	1.141(3)
O(9)-C(18)	1.148(3)
O(10)-C(19)	1.154(3)
O(11)-C(20)	1.152(4)

Appendix C: W(CO)₅C(OEt)-P-P-C(OEt)W(CO)₅

Table 1: Crystal data and structure refinement.

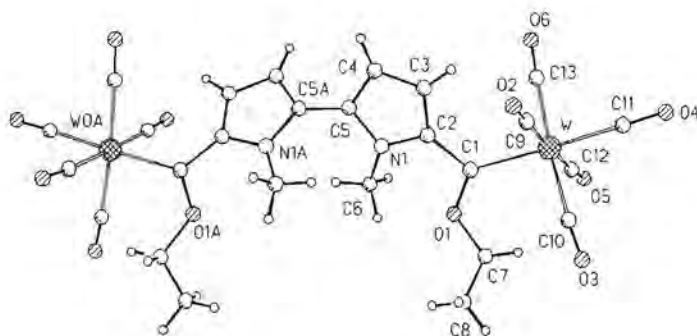
Identification code	FO1045
Empirical formula	C ₂₆ H ₂₀ N ₂ O ₁₂ W ₂
Formula weight	920.14
Temperature	183(2) K
Wavelength	0.71073 Å
Crystal system	Orthorhombic
Space group	Pccn
Unit cell dimensions	a: = 17.7003(6) Å alpha = 90° b: = 12.5957(4) Å beta = 90° c: = 13.4575(3) Å gamma = 90°
Volume, Z	698 3000.32(15) Å ³ , 4
Density (calculated)	2.037 Mg/m ³
Absorption coefficient	7.725 mm ⁻¹
F(000)	1736
Crystal size	1.00 x 0.20 x 0.15 mm ³
Theta range for data collection	3.43 to 27.49°
Limiting indices	-19 ≤ h ≤ 22, -16 ≤ k ≤ 14, -15 ≤ l ≤ 17
Reflections collected	18869
Independent reflections	3431 (R _{int} = 0.0563)
Completeness to theta = 27.49°	99.7 %
Absorption correction	SEMIEMPIRICAL
Max. and min. transmission	0.297 and 0.225
Refinement method	Full-matrix least-squares on F ²
Data / restraints / parameters	3431 / 0 / 190
Goodness-of-fit on F ²	1.054
Final R indices [I > 2σ(I)]	R ₁ = 0.0313, wR ₂ = 0.0663
R indices (all data)	R ₁ = 0.0445, wR ₂ = 0.0709
Largest diff. peak and hole	0.643 and -1.392 e.Å ⁻³

Table 2: Atomic coordinates [$\times 10^4$] and equivalent isotropic displacement parameters [$\text{\AA}^2 \times 10^3$].



	x	y	z	U (eq)
W	4352 (1)	3396 (1)	2082 (1)	27 (1)
O (1)	3213 (2)	4856 (2)	3353 (2)	32 (1)
N (1)	2760 (2)	6298 (3)	2028 (2)	26 (1)
C (1)	3558 (2)	4700 (3)	2499 (3)	25 (1)
C (2)	3326 (2)	5554 (3)	1829 (3)	24 (1)
C (3)	3663 (2)	5853 (3)	936 (3)	29 (1)
C (4)	3319 (2)	6791 (3)	591 (3)	31 (1)
C (5)	2759 (2)	7053 (3)	1279 (3)	27 (1)
C (6)	2160 (3)	6232 (4)	2775 (3)	40 (1)
C (7)	3271 (3)	4153 (4)	4204 (3)	46 (1)
C (8)	3365 (5)	4741 (5)	5096 (4)	97 (3)
O (2)	5559 (2)	5119 (4)	1380 (4)	75 (1)
O (3)	5197 (3)	3300 (4)	4166 (3)	92 (2)
O (4)	5504 (3)	1592 (4)	1440 (3)	92 (2)
O (5)	3156 (3)	1599 (3)	2663 (3)	55 (1)
O (6)	3605 (3)	3272 (3)	-65 (3)	57 (1)
C (9)	5124 (3)	4508 (4)	1634 (4)	43 (1)
C (10)	4875 (3)	3353 (4)	3437 (4)	50 (1)
C (11)	5083 (3)	2244 (4)	1667 (3)	51 (1)
C (12)	3585 (3)	2257 (4)	2488 (3)	35 (1)
C (13)	3872 (3)	3343 (3)	700 (3)	35 (1)

Table 3: Bond lengths [Å] and angles [°].



W-C(11)	2.022 (5)
W-C(13)	2.045 (5)
W-C(12)	2.049 (5)
W-C(10)	2.046 (5)
W-C(9)	2.048 (5)
W-C(1)	2.234 (4)
O(1)-C(1)	1.317 (5)
O(1)-C(7)	1.451 (5)
N(1)-C(5)	1.385 (5)
N(1)-C(2)	1.398 (5)
N(1)-C(6)	1.463 (5)
C(1)-C(2)	1.462 (5)
C(2)-C(3)	1.394 (5)
C(3)-C(4)	1.409 (5)
C(4)-C(5)	1.395 (5)
C(5)-C(5)#1	1.453 (8)
C(7)-C(8)	1.421 (7)
O(2)-C(9)	1.141 (6)
O(3)-C(10)	1.137 (6)
O(4)-C(11)	1.151 (6)
O(5)-C(12)	1.148 (6)
O(6)-C(13)	1.137 (5)
C(11)-W-C(13)	89.50 (18)
C(11)-W-C(12)	89.7 (2)
C(13)-W-C(12)	86.82 (18)
C(11)-W-C(10)	86.4 (2)
C(13)-W-C(10)	175.87 (18)
C(12)-W-C(10)	92.5 (2)
C(11)-W-C(9)	89.0 (2)
C(13)-W-C(9)	91.79 (19)
C(12)-W-C(9)	178.14 (18)
C(10)-W-C(9)	88.8 (2)
C(11)-W-C(1)	178.12 (18)
C(13)-W-C(1)	89.48 (15)
C(12)-W-C(1)	91.79 (16)
C(10)-W-C(1)	94.62 (17)
C(9)-W-C(1)	89.43 (17)
C(1)-O(1)-C(7)	124.4 (3)
C(5)-N(1)-C(2)	108.7 (3)
C(5)-N(1)-C(6)	122.6 (3)

C(2)-N(1)-C(6)	127.8(3)
O(1)-C(1)-C(2)	107.3(3)
O(1)-C(1)-W	128.4(3)
C(2)-C(1)-W	124.3(3)
N(1)-C(2)-C(3)	106.9(3)
N(1)-C(2)-C(1)	125.3(3)
C(3)-C(2)-C(1)	127.5(4)
C(2)-C(3)-C(4)	109.0(3)
C(5)-C(4)-C(3)	106.7(3)
N(1)-C(5)-C(4)	108.7(3)
N(1)-C(5)-C(5)#1	122.2(3)
C(4)-C(5)-C(5)#1	129.1(3)
C(8)-C(7)-O(1)	110.9(4)
O(2)-C(9)-W	179.2(5)
O(3)-C(10)-W	176.4(5)
O(4)-C(11)-W	179.2(5)
O(5)-C(12)-W	176.3(4)
O(6)-C(13)-W	177.3(4)

Symmetry transformations used to generate equivalent atoms:

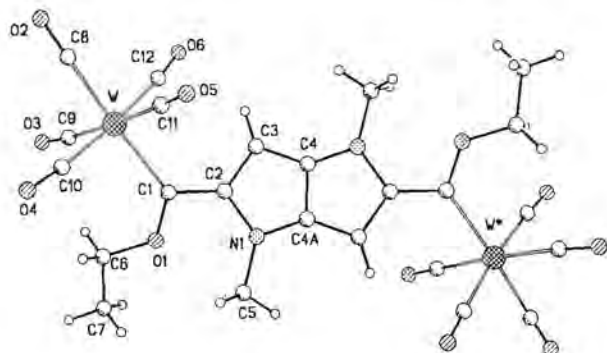
#1 $-x+1/2, -y+3/2, z$

Appendix D: W(CO)₅C(OEt)-PP-C(OEt)W(CO)₅

Table 1: Crystal data and structure refinement.

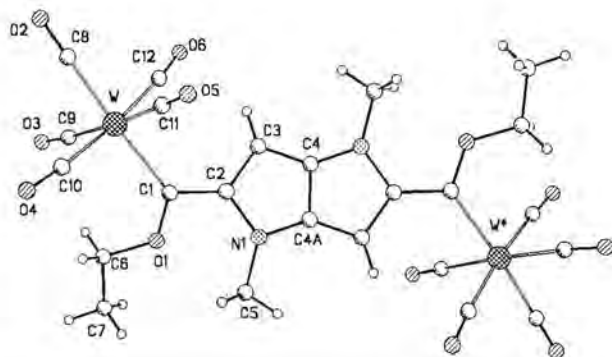
Identification code	FO956
Empirical formula	C ₂₄ H ₁₈ N ₂ O ₁₂ W ₂
Formula weight	894.10
Temperature	183(2) K
Wavelength	0.71073 Å
Crystal system	Triclinic
Space group	P ⁻ 0B1
Unit cell dimensions	a = 6.5306(2)Å α = 72.286(1)° b = 8.9872(2)Å β = 81.923(2)° c = 12.6945(4)Å γ = 83.705(2)°
Volume	700.93(3)Å ³
Density (calculated)	2.118 Mg/m ³
Absorption coefficient	8.263 mm ⁻¹
F(000)	420
Crystal size	0.20 × 0.18 × 0.10 mm ³
Theta range for data collection	3.53 to 26.35°
Limiting indices	-8 ≤ h ≤ 8, -11 ≤ k ≤ 11, -15 ≤ l ≤ 14
Reflections collected	6177
Independent reflections	2833 (R(int)=0.0379)
Completeness to theta = 26.35°	99.1%
Absorption correction	Psi-scan
Max. and min. transmission	0.9436 and 0.4471
Refinement method	Full-matrix least-squares on F ²
Data / restraints / parameters	2833/0/182
Goodness-of-fit on F ²	1.051
Final R indices [I > 2σ(I)]	R ₁ =0.0269, wR ₂ =0.0674
R indices (all data)	R ₁ =0.0278, wR ₂ =0.0682
Extinction coefficient	0.0212(12)
Largest diff. peak and hole	1.547 and -1.609 e.Å ⁻³

Table 2: Atomic coordinates ($\times 10^4$) and equivalent isotropic displacement parameters ($\text{\AA}^2 \times 10^3$).



	x	y	z	U (eq)
W	-3993 (1)	-2445 (1)	-2260 (1)	19 (1)
O (1)	-2699 (5)	1122 (3)	-2961 (3)	27 (1)
O (2)	-5471 (6)	-5694 (4)	-2251 (3)	42 (1)
O (3)	-8155 (6)	-928 (5)	-3323 (3)	39 (1)
O (4)	-1752 (7)	-2271 (5)	-4692 (4)	48 (1)
O (5)	131 (6)	-4316 (5)	-1277 (4)	40 (1)
O (6)	-6658 (6)	-2997 (5)	127 (3)	42 (1)
N (1)	-301 (5)	1002 (4)	-1372 (3)	22 (1)
C (1)	-2735 (7)	-262 (5)	-2191 (4)	20 (1)
C (2)	-1650 (6)	-179 (4)	-1289 (3)	21 (1)
C (3)	-1722 (6)	-1224 (4)	-211 (3)	24 (1)
C (4)	-424 (6)	-673 (4)	364 (3)	21 (1)
C (5)	338 (8)	2339 (5)	-2318 (4)	34 (1)
C (6)	-3470 (10)	1401 (6)	-4025 (4)	46 (1)
C (7)	-3433 (8)	3115 (5)	-4616 (4)	37 (1)
C (8)	-4942 (8)	-4531 (6)	-2251 (4)	27 (1)
C (9)	-6645 (7)	-1406 (6)	-2935 (4)	25 (1)
C (10)	-2516 (8)	-2281 (6)	-3811 (4)	28 (1)
C (11)	-1336 (7)	-3635 (6)	-1607 (4)	26 (1)
C (12)	-5679 (7)	-2760 (5)	-713 (4)	26 (1)

Table 3: Bond lengths [Å] and angles [°]



W-C(8)	2.034(5)
W-C(10)	2.038(5)
W-C(9)	2.045(5)
W-C(12)	2.067(5)
W-C(11)	2.074(5)
W-C(1)	2.238(4)
O(1)-C(1)	1.327(5)
O(1)-C(6)	1.448(5)
O(2)-C(8)	1.136(6)
O(3)-C(9)	1.146(6)
O(4)-C(10)	1.157(7)
O(5)-C(11)	1.139(6)
O(6)-C(12)	1.136(6)
N(1)-C(4)#1	1.364(5)
N(1)-C(2)	1.422(5)
N(1)-C(5)	1.466(5)
C(1)-C(2)	1.453(6)
C(2)-C(3)	1.402(6)
C(3)-C(4)	1.408(5)
C(4)-N(1)#1	1.364(5)
C(4)-C(4)#1	1.396(7)
C(6)-C(7)	1.495(6)
C(8)-W-C(10)	87.3(2)
C(8)-W-C(9)	87.65(18)
C(10)-W-C(9)	90.11(19)
C(8)-W-C(12)	87.48(19)
C(10)-W-C(12)	174.36(15)
C(9)-W-C(12)	87.50(18)
C(8)-W-C(11)	88.54(19)
C(10)-W-C(11)	88.52(19)
C(9)-W-C(11)	176.01(14)
C(12)-W-C(11)	93.53(18)
C(8)-W-C(1)	175.26(15)
C(10)-W-C(1)	93.21(18)
C(9)-W-C(1)	97.05(17)
C(12)-W-C(1)	92.15(17)
C(11)-W-C(1)	86.77(17)
C(1)-O(1)-C(6)	122.4(3)
C(4)#1-N(1)-C(2)	107.1(3)
C(4)#1-N(1)-C(5)	122.5(3)



C(2)-N(1)-C(5)	130.5(3)
O(1)-C(1)-C(2)	108.0(3)
O(1)-C(1)-W	128.0(3)
C(2)-C(1)-W	123.9(3)
C(3)-C(2)-N(1)	108.6(3)
C(3)-C(2)-C(1)	126.9(3)
N(1)-C(2)-C(1)	124.5(4)
C(2)-C(3)-C(4)	106.5(3)
N(1)#1-C(4)-C(4)#1	109.6(4)
N(1)#1-C(4)-C(3)	142.2(4)
C(4)#1-C(4)-C(3)	108.2(4)
O(1)-C(6)-C(7)	107.8(4)
O(2)-C(8)-W	179.7(5)
O(3)-C(9)-W	175.0(4)
O(4)-C(10)-W	175.4(4)
O(5)-C(11)-W	177.5(4)
O(6)-C(12)-W	176.2(4)

Symmetry transformations used to generate equivalent atoms:

#1 -x,-y,-z

Synthesis of carbene complexes of tungsten with pyrrolyl substituents.

Andrew Oliver,^[a] Hubert Nienaber,^[a]

Helmar Görls,^[b] and Simon Lotz*^[a]

^[a] Department of Chemistry, University of Pretoria,
Pretoria, South Africa, 0002

Fax: +27 12 3625297

E-mail: slotz@postino.up.ac.za

^[b] Friedrich-Schiller-Universität
Institut für Anorganische und Analytische Chemie,

Lessingstrasse 8, D-07743, Jena

Fax: +949 3641 948121

E-mail: goerls@xa.nwl.uni-jena.de

Dinuclear biscarbene complexes, $[W(CO)_5C(OEt)spacerC(OEt)W(CO)_5]$, were synthesized employing the classical Fischer method. The connecting spacer units used were obtained from the reaction of the doubly deprotonated N-methylpyrrole (P'), N,N'-dimethyl-2,2'-bispyrrole (P'-P') and N,N'-dimethylpyrrolo[3,2-b]pyrrole (P'P') precursors. In each of the cases the particular monocarbene pyrrolyl complexes (HP') **1**, (HP'-P') **2** and (HP'P') **3** was yielded as a byproduct of the reaction which afforded the biscarbene pyrrolylene complexes **4** (P'), **5** (P'-P') and **6** (P'P') in high yields.

Polypyrrole films are formed through electrochemical oxidation and polymerization of the monomers¹, whereas polypyrrole becomes conducting when properly doped². In 1976 Fischer *et al*³ prepared a series of products by reacting pentacarbonyl(arylmethoxycarbene) complexes of chromium and tungsten with aryllithium compounds at low temperatures. These include examples of pyrrole and thiophene. The importance of the electronic effects of the heteroatom in the rings were investigated and results showed that pyrrole was different from furan, thiophene and selenophene⁴. Binuclear biscarbene complexes with pyrrole substituents has not yet been investigated before and forms the basis of this study. Applications of carbene complexes in organic synthesis have been widely employed and recognized for their usefulness in carbon-carbon bond formation reactions⁵. The importance of carbene complexes as intermediates in olefin metathesis was exploited by Grubbs⁶, who synthesized ruthenium(II) carbene complexes to catalyze the polymerization of highly strained cyclic olefins. Fischer⁷ and Casey⁸ reported the thermal dimerization of several carbene complexes. Fischer concluded that the thermal dimerization of the carbene ligand

occurred only in carbene complexes where no α -hydrogens were present⁹. In complexes where the stabilizing heteroatom in the carbene ligand is absent, the metal-carbene bond is cleaved at temperatures as low as room temperature¹⁰ to yield the dimer. Casey and Anderson kinetically investigated the mechanism of the thermal decomposition of (2-oxacyclopentylidene)-pentacarbonylchromium(0) to confirm the presence of free carbenes as intermediates in this thermal reaction. The synthesis of bimetallic complexes with σ,σ -coordinated transition metal fragments bridged by a π -conjugated bridge has been the focus of current research in our laboratories. Although several Fischer carbene complexes with thiophene as ligand have already been synthesized¹¹, the pyrrole analogues was prepared for comparison with the oligothiophene and condensed thiophene complexes. It was therefore anticipated that, in the light of the interesting decomposition reactions encountered for the dinuclear biscarbene complexes of thiophene $[M(CO)_5C(OEt)-T-C(OEt)M(CO)_5]$ ($M = Cr, W$)¹², the bipyrrrole derivatives could represent more stable complexes. According to Fischer¹³ the stability of carbene complexes increases in the order $LMo(CO)_5 < LCr(CO)_5 < LW(CO)_5$. The trend established in this study for oligopyrrole spacer units is pyrrole $<$ pyrrolopyrrole $<$ bipyrrrole.

Results and discussion

Synthesis

The N,N' -dimethyl-2,2'-bipyrrrole was synthesized according to the method of Kauffman and Lexy¹⁴. N -methylpyrrole was lithiated, after which a second equivalent of N -methylpyrrole was added. For the coupling reaction $NiCl_2$ was used as catalyst. The synthesis of N,N' -dimethylpyrrolo[3,2-*b*]pyrrole was adapted from literature¹⁵ and modified in our laboratories. Hemetsberger and Knittel¹⁶ prepared vinyl azides by condensation of various aromatic and heterocyclic aldehydes with ethyl azidoacetate or ω -azidoacetophenones (Figure 1).

Figure 1

The novel pyrrole carbene complexes were synthesized using the classical Fischer method. Pyrrole is readily monolithiated under mild conditions as well as dilithiated under refluxing conditions with n -butyllithium¹⁷. The dimetallation of the pyrrole precursors was done in hexane rather than in THF or ether solvents, since it was found that the ether solvent is attacked under forcing conditions. Using hexane as solvent, the n -butyllithium-TMEDA complex is capable of abstracting both protons of the pyrrole derivative upon adding two equivalents of the base to one equivalent of pyrrole derivative. The first deprotonation occurs at room temperature while the removal of the second proton is afforded at elevated

temperatures under refluxing conditions. A suspension forms which was subsequently dissolved by adding freshly distilled THF. The tungsten hexacarbonyl was added at low (-40°C) temperature and the resulting dilithium salt was alkylated with triethyloxonium tetrafluoroborate yielded the desired carbene complexes. The reactions afforded both the mono- and dinuclear biscarbene complexes.

Figure 2

The tungsten monocarbene complexes of N-methylpyrrole (HP') **1**, N,N'-dimethyl-2,2'-bispyrrole (HP'-P') **2** and N,N' dimethylpyrrolo[3,2-*b*]pyrrole (HP'P') **3** and dinuclear tungsten biscarbene pyrrolylene complexes **4** (P'), **5** (P'-P') and **6** (P'P') were isolated in high yields (Figure 2). Complexes were recrystallized from dichloromethane-hexane mixtures.

Spectroscopic properties

The spectroscopic data support the proposed molecular structures of the complexes and the atom numbering of the pyrrole units is shown in Figure 3. The protons of the complexes are shifted further downfield than for the uncoordinated pyrrole compounds¹⁸. Upon coordination to the metal, the carbene moiety causes draining of electron density from the double bonds of the pyrrole rings to the carbene carbon atom.

Table 1

From the ^1H NMR data of **1**, **3** and **5** it is clear that the chemical shift of H3 is downfield compared to its position on the spectra of the corresponding biscarbene complexes **2**, **4** and **6**, while the chemical shift of H4 is upfield. This can be explained when considering the π -resonance structures of the complex. It is concluded that H3 will shift more downfield than H13 since it is closer to the carbene moiety. H4, however, is not affected by the resonance effect and its chemical shift is therefore comparable with the chemical shift of the uncoordinated pyrrole moiety. In the case of the biscarbene complexes, **2**, **4** and **6**, the ring protons are affected by two metal nuclei and the combined withdrawing effect of the two carbene substituents results in an unfavorable electronic effect. The methylene protons of the ethoxy substituents are observed at chemical shift values corresponding to an ordering of $\text{Cr} > \text{Mo} > \text{W}$, which is representative of their group positions in the periodic table. For a methylene group of a carbene moiety, the proton chemical shift value ranges between 5.05 and 4.95 ppm for the monocarbene complexes and 5.16 and 4.96 ppm for the biscarbene complexes. The same sequences were observed in the ^{13}C NMR

spectra for the complexes with respect to the resonances of the carbonyl and carbene carbons. The range of resonances for the carbene carbons are greater with W is around 285 ppm. The IR frequencies and patterns observed in the carbonyl region confirm the presence of a $W(CO)_5$ fragment on the spectra of all the complexes.

Crystal structure

A single crystal X-ray diffraction study confirmed the molecular structures of **1**, **4**, **5** and **6**. Selected bond distances and angles are given in table 2. Figures 4-7 represents a ball-and-stick plot of the structures.

Figure 4-7

The $W(CO)_5$ fragments are *trans* to the sulfur atoms of the terthienyl spacer which places them on the same side of the molecule. The $W(CO)_5$ fragment is slightly distorted (124.3°) and bend away from the terthienyl substituent. From the reasonably small dihedral angle of 166.2° (W-C-C-S) it is deduced that the thiophene units are rigid and orientated planar and parallel to the carbene moieties.

Experimental

All reactions were performed under an inert atmosphere using standard Schlenk-tube techniques¹⁹. Solvents were dried by the usual procedures and distilled under nitrogen prior to use. The starting materials 2-acetylthiophene, $[M(CO)_6]$ and n-BuLi were used as obtained from Aldrich. N,N'-dimethyl-2,2'-bispyrrole (HP'-P'H)¹⁴ and N,N'-dimethylpyrrolo[3,2-*b*]pyrrole (HP'P'H)¹⁵ and triethyloxonium tetrafluoroborate²⁰ were prepared according to literature methods. Column chromatography was performed on silica gel (0.063-0.200 mm) on columns that were cooled by circulating cold isopropyl alcohol through column jackets. NMR spectra were recorded in $CDCl_3$ as solvent on a Bruker AC-300 spectrometer with reference to the deuterium signal $CDCl_3$. 1H and ^{13}C spectra were measured at 300.133 and 75.469 MHz respectively. Infrared spectra were recorded as liquid CH_2Cl_2 solutions on a BOMEM Michelson-100 FT spectrophotometer. Mass spectra were recorded on a Perkin-Elmer RMU-6H instrument operating at 70 eV. Melting points were recorded in capillaries on a Gallenkamp hot-stage apparatus and are uncorrected.

Syntheses

[(CO)₅WC(OEt)P'H] 1 and [(CO)₅WC(OEt)P'C(OEt)W(CO)₅] 4: 10.0 ml (16. mmole) of n-butyl lithium (15% solution in hexane) was added to 1.75 g (16 mmole) of TMEDA and stirred for 15 minutes. 0.129 g (15 mmole) of N-Methylpyrrole and 50 ml of hexane was added at room temperature. The mixture was refluxed for 6 hours during which time the lithiated salt precipitated as a white-yellowish solid. This suspension was cooled to 0°C and 30 ml of THF was added. The mixture was then further cooled to -20°C and 5.99 g (22.7 mmole) of W(CO)₆ was added gradually. The reaction was kept at this temperature for 15 minutes, stirring vigorously, and then allowed to rise to room temperature. Stirring was continued for another hour, during which time the colour of the reaction mixture changed to a dark red-brown. After completion of the reaction, the solvent was removed *in vacuo*. 4.55 g (24.7 mmole) of triethyl oxonium tetrafluoroborate was dissolved in 20 ml of dichloromethane. This was added to the residue of the reaction mixture at -20°C and the solution, red-brown-coloured, was stirred for an hour while the temperature was allowed to rise to room temperature. The mixture was filtered through silica gel with dichloromethane and the solvent removed under reduced pressure. Column chromatography was used to purify the mixture of carbene complexes. Hexane was employed as starting eluent and the polarity was gradually increased by adding dichloromethane to separate the different compounds. Two compounds were isolated. The first orange product was identified as the monocarbene complex **1**, while the second red product was characterized as the dinuclear biscarbene complex **4**.

1: Yield: 1.50 g (32%), mp.: 155°C. – C₁₃H₁₁O₆NW (461.1): calcd. C 33.87, H 2.40; found C 33.98, H 2.61 - MS (EI); *m/z* (based on ¹⁸³W): 459 (M⁺).

4: Yield: 1.41 g (17%), C₂₁H₁₅O₁₂NW₂ (841.0): calcd. C 29.99, H 1.80; found C 30.14, H 1.97

[(CO)₅WC(OEt)P'-P'H] 2 and [(CO)₅WC(OEt)P'-P'C(OEt)W(CO)₅]: N,N'-bisdimethylpyrrole (0.237 g, 1.48 mmol) was added to 0.358 g (3.1 mmol) of TMEDA and 2.0 ml (3.2 mmol) of n-butyl lithium were added dropwise to the stirred solution at 0°C. The mixture was stirred for 15 minutes after the additions and then allowed to warm to room temperature. It was stirred for another 15 minutes at this temperature during which time the solution turned yellow. Refluxing for 30 minutes afforded a milky white suspension. The solution was cooled to -40°C and W(CO)₆ (1.06 g, 3.0 mmol) in 50 ml THF was added and the mixture turned dark red. After stirring for 1 hour, the reaction mixture was allowed to warm to room temperature and was stirred for another hour. The THF/hexane was removed under reduced pressure. 50 ml of dichloromethane was added and the solution was cooled to -20°C. 0.58 g (3 mmol) of triethyl oxonium tetrafluoroborate in 50 ml of dichloromethane was added and the mixture stirred for 1 hour while allowing to reach room temperature. The deeply coloured brown mixture was filtered through

silica gel and dried *in vacuo*. Column chromatography of the residue, using hexane/dichloromethane mixtures, yielded two products. The first product was the monocarbene complex **2**, followed by the red dinuclear biscarbene complex **5**.

2: Yield: 0.80 g (35%), – C₁₈H₁₆O₆N₂W (540.2): calcd. C 40.02, H 2.99; found C 40.26, H 3.18. – MS (EI); *m/z* (based on ¹⁸³W): 540 [M⁺], 512 [M⁺ - CO], 484 [M⁺ - 2CO], 456 [M⁺ - 3CO], 428 [M⁺ - 4CO], 400 [M⁺ - 5CO]

5: Yield: 1.35 g (36%), C₂₆H₂₀O₁₂N₂W₂ (920.1): calcd. C 33.94, H 2.19; found C 34.11, H 2.32.

[(CO)₅WC(OEt)P'P'H] **3** and [(CO)₅WC(OEt)P'P'C(OEt)Mo(CO)₅] **6**: 0.673 g (5.0 mmole) of N,N'-dimethylpyrrolo[3,2-*b*]pyrrole was dissolved in 50 ml of hexane. 1.52 ml (10.1 mmole) of TMEDA and 6.4 ml (10.1 mmole) of *n*-butyl lithium were added at 0°C. The mixture was refluxed for 15 minutes and then cooled to 0°C. THF (50 ml) was added and the dilithio species was treated with W(CO)₆ (3.55 g, 10.2 mmole) at -40°C. The reaction mixture was stirred for 2 hours, while the temperature gradually rose to room temperature. The solvent was removed under reduced pressure. 2.0 g (10.0 mmole) of triethyl oxonium tetrafluoroborate in 50 ml of dichloromethane was added to the reaction residue and an immediate colour change to dark brown was observed. Column chromatography yielded two products. The first orange product was identified as the monocarbene complex (**3**), yield: 0.34 g (37%) while the second red complex was the biscarbene complex (**6**), yield: 0.32 g (21%). Several other complexes, formed in very low yields, were products of this reaction but it was impossible to isolate in significant quantities.

3: Yield: 0.34 g (37%). – C₁₆H₁₄O₆N₂W (514.1): calcd. C 37.38, H 2.74; found C 37.51, H 2.87. – MS (EI); *m/z* (based on ¹⁸³W): 512 [M⁺], 484 [M⁺ - CO], 456 [M⁺ - 2CO], 428 [M⁺ - 3CO], 400 [M⁺ - 4CO], 472 [M⁺ - 5CO]

6: Yield: 0.32 g (21%). – C₂₄H₁₈O₁₂N₂W₂ (894.1): calcd. C 32.24, H 2.03; found C 32.52, H 2.22.

Crystal structure determination

The intensity data for the compounds were collected at -90°C on a Nonius KappaCCD diffractometer, using graphite-monochromated Mo-K_α radiation. Data were corrected for Lorentz and polarization effects, but not for absorption²¹. The structures were solved by direct methods (SHELXS)²² and refined by full-matrix least squares techniques against Fo² (SHELXL-97)²³. The hydrogen atoms of the structures were included at calculated positions with fixed thermal parameters. All non-hydrogen atoms were refined anisotropically. XP (SIEMENS Analytical X-ray Instruments, Inc.) was used for structure representations. Other experimental details are given in table 3. Crystallographic data (excluding structure factors) for the structures reported in

this paper have been deposited with the Cambridge Crystallographic Data Centre as supplementary material. Copies of the data can be obtained free of charge on application to CCDC, 12 Union Road, Cambridge CB21EZ, UK [Fax: + 44) 1223-336-033; E-mail: deposit@ccdc.cam.ac.uk].

Acknowledgments

We wish to thank Mr E. Palmer for the NMR measurements and the University of Pretoria and the Foundation for Research and Development, Pretoria, for financial assistance.

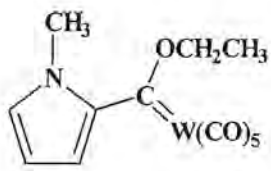
References

1. R. J. Waltman, J. Bargon, A. F. Diaz, *J. Phys. Chem.*, **1983**, *87*, 1459.
2. R. Colle, A. Currioni, *J. Am. Chem. Soc.*, **1998**, *120*, 4832.
3. E.O. Fischer, W. Held, F. R. Kreissl, A. Frank, G. Huttner, *Chem. Ber.*, **1977**, *110*, 656.
4. R. Gleiter, M. Kobayashi, J. Spanget-Larsen, S. Gronowitz, A. Konar, M. Farnier, *J. Org. Chem.*, **1977**, *42*, 2230.
5. K.H. Dötz, *Angew. Chem. Int. Ed. Engl.*, **1984**, *23*, 587.
6. S.T. Nguyen, L.K. Johnson, R.H. Grubbs, *J. Am. Chem. Soc.*, **1992**, *114*, 3974.
7. E.O. Fischer, B. Heckl, K.H. Dötz, J. Müller, H. Werner, *J. Organomet. Chem.*, **1969**, *16*, P29. (b)
8. C.P. Casey, R.L. Anderson, *J. Chem. Soc., Chem. Commun.*, **1975**, 895.
9. E.O. Fischer, A. Maasböl, *J. Organomet. Chem.*, **1968**, *12*, P15.
10. M. Brookhart, G.O. Nelson, *J. Am. Chem. Soc.*, **1977**, *99*, 6099.
11. J.A. Connor, E.M. Jones, E.W. Randall, E. Rosenberg, *J. Chem. Soc., Dalton Trans.*, **1972**, 2419.
12. Y.M. Terblans, H.M. Roos, S. Lotz, *J. Organomet. Chem.*, **1998**, *566*, 133.
13. K.H. Dötz, H. Fischer, P. Hofmann, F.R. Kreissl, U. Schubert, K. Weiss, *Transition Metal Carbene Complexes*, VCH Verlag Chemie, Weinheim, **1983**.
14. T. Kauffman, H. Lexy, *Chem. Ber.*, **1981**, *114*, 3674.
15. N. Gjos, S. Gronowitz, *Acta Chem. Scan.*, **1971**, *25*, 2596.
16. H. Hemetsberger, D. Knittel, *Monats. Chem.*, **1972**, *103*, 194.
17. J. Karas, G. Huttner, K. Heinze, P. Rutsch, L. Zsolnai, *Eur. J. Inorg. Chem.*, **1999**, 405
18. R. J. Cushley, R. J. Sykes, C-K. Shaw, H. H. Wasserman, *Can. J. Chem.*, **1975**, *53*, 148.

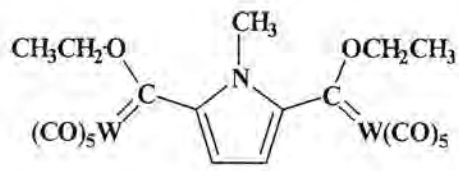
19. D. F. Shriver, M.A. Drezdson, *The Manipulation of Air-sensitive Compounds*, 2nd edn. Wiley, New York, 1980.
20. H. Meerwein, *Org. Synth.*, 1966, 46, 113.
21. COLLECT, Data Collection Software; Nonius B.V., Delft, Netherlands, 1998. Z. Otwinowski and W. Minor, "Processing of X-Ray Diffraction Data Collected in Oscillation Mode" in *Methods in Enzymology*, Vol.276, Macromolecular Crystallography, Part A, edited by C.W. Carter and R.M. Sweet, pp. 307-326, Academic Press, 1997.
22. G.M. Sheldrick, *Acta Crystallogr.*, 1990, A46, 467-473.
23. G..M. Sheldrick, SHELXL-97 (Release 97-2), University of Göttingen, Germany, 1997.

Table 1 Spectroscopic data for 1-6

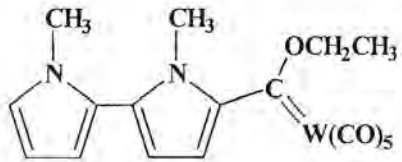
Complex	IR ^a (ν/cm ⁻¹ in hexane)	¹ H NMR (δ/ppm in CDCl ₃ , J/Hz)	¹³ C NMR (δ/ppm in CDCl ₃)
1	2062 (m), 1950 (vw), 1942 (s), 1934 (vs)	7.66 (d, 1H, H3, ³ J _{HH} = 4.4), 6.90 (dt, 1H, H5, ³ J _{HH} = 2.3, ⁴ J _{HH} = 1.8), 6.26 (dd, 1H, H4, ³ J _{HH} = 4.4, ³ J _{HH} = 2.33), 4.92 (q, 2H, CH ₂ , ³ J _{HH} = 7.0), 3.78 (s, 3H, N-CH ₃), 1.62 (t, 3H, CH ₃ , ³ J _{HH} = 7.1)	278.7 (carbene), 202.5, 198.4 (M(CO) ₅), 146.1 (C2), 136.2 (C3), 135.0 (C5), 111.2 (C4), 78.1 (CH ₂), 40.7 (N-CH ₃), 15.3 (CH ₃)
2	2062 (m), 1971 (vw), 1944 (s), 1934 (vs)	7.71 (d, 1H, H3, ³ J _{HH} = 4.4), 6.79 (dd, 1H, H9, ³ J _{HH} = 2.7, ⁴ J _{HH} = 1.8), 6.33 (d, 1H, H4, ³ J _{HH} = 4.7), 6.26 (dd, 1H, H8, ³ J _{HH} = 3.8, ³ J _{HH} = 2.7), 6.23 (dd, 1H, C7, ³ J _{HH} = 3.6, ³ J _{HH} = 1.8), 4.92 (q, 2H, CH ₂ , ³ J _{HH} = 7.1), 3.65 (s, 3H, N-CH ₃), 3.57 (s, 3H, N'-CH ₃), 1.62 (t, 3H, CH ₃ , ³ J _{HH} = 7.1)	288.2 (carbene), 202.3, 198.2 (M(CO) ₅), 137.1 (C2), 135.5 (C3), 134.3 (C5), 125.1 (C9), 114.9 (C4), 114.0 (C6), 112.9 (C7), 108.5 (C8), 75.4 (CH ₂), 37.8 (N-CH ₃), 15.5 (CH ₃)
3	2059 (m), 1944 (s), 1937 (vs)	7.29 (s, 1H, H3), 6.96 (dd, 1H, H7, ³ J _{HH} = 3.1, ⁴ J _{HH} = 0.8), 5.96 (d, 1H, H6, ³ J _{HH} = 3.1), 4.95 (q, 2H, CH ₂ , ³ J _{HH} = 7.1), 3.86 (s, 3H, N-CH ₃), 3.83 (s, 3H, N'-CH ₃), 1.62 (t, 3H, CH ₃ , ³ J _{HH} = 7.1)	284.1 (carbene), 202.0, 198.0 (M(CO) ₅), 151.0 (C2), 132.1 (C7), 128.6, 126.8 (C4,C5), 113.2 (C3), 89.6 (C6), 78.4 (CH ₂), 37.4 (N-CH ₃), 34.5 (N'-CH ₃), 15.3 (CH ₃)
4		7.17 (s, 1H, H3), 4.96 (q, 2H, CH ₂ , ³ J _{HH} = 7.1), 3.58 (s, 3H, N-CH ₃), 1.67 (t, 3H, CH ₃ , ³ J _{HH} = 7.2)	296.1 (carbene), 203.0, 197.2 (M(CO) ₅), 151.7 (C2), 125.8 (C3), 79.1 (CH ₂), 38.5 (N-CH ₃), 15.0 (CH ₃)
5		7.69 (d, 1H, H3, ³ J _{HH} = 4.4), 6.39 (d, 1H, H4, ³ J _{HH} = 4.4), 4.98 (q, 2H, CH ₂ , ³ J _{HH} = 7.1), 3.62 (s, 3H, N-CH ₃), 1.65 (t, 3H, CH ₃ , ³ J _{HH} = 7.2)	282.4 (carbene), 202.3, 198.2 (M(CO) ₅), 148.7 (C2), 134.6 (C5), 134.2 (C3), 114.9 (C4), 78.6 (CH ₂), 37.8 (N-CH ₃), 15.3 (CH ₃)
6	2060 (m), 1973 (vw), 1945 (s), 1935 (vs)	7.12 (s, 1H, H3), 4.98 (q, 2H, CH ₂ , ³ J _{HH} = 7.1), 3.77 (s, 3H, N-CH ₃), 1.69 (t, 3H, CH ₃ , ³ J _{HH} = 7.1)	285.3 (carbene), 202.6, 198.1 (M(CO) ₅), 151.0 (C2), 137.4 (C4), 110.7 (C3), 78.8 (CH ₂), 38.0 (N-CH ₃), 15.5 (CH ₃)



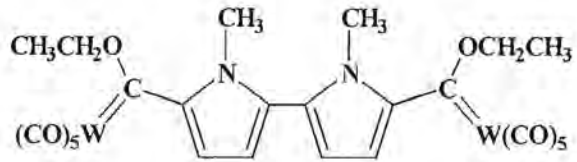
1



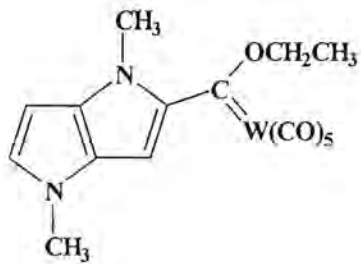
4



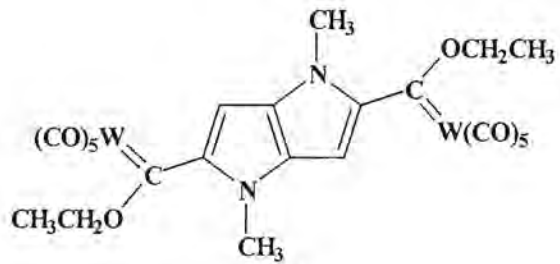
2



5



3



6

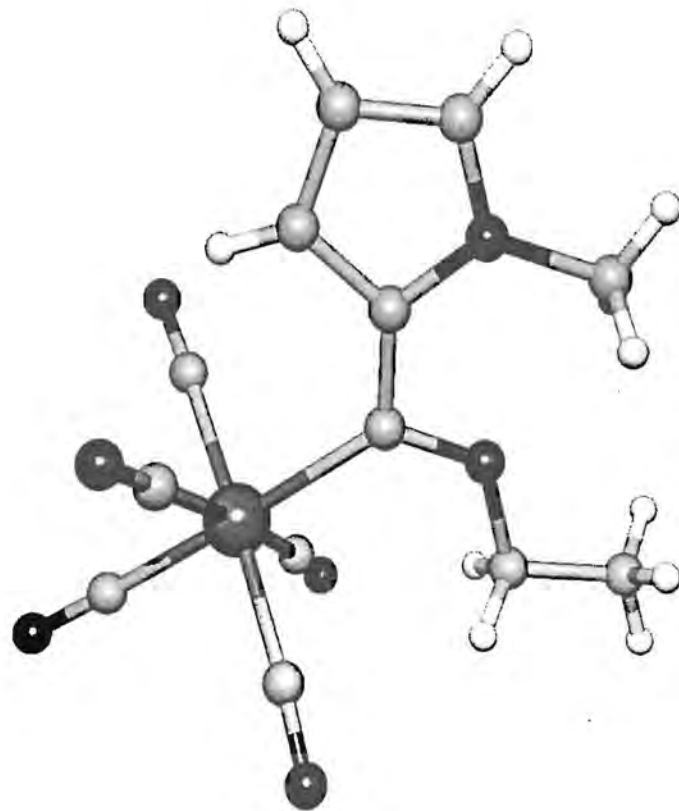


Figure 4. Molecular structure of 1

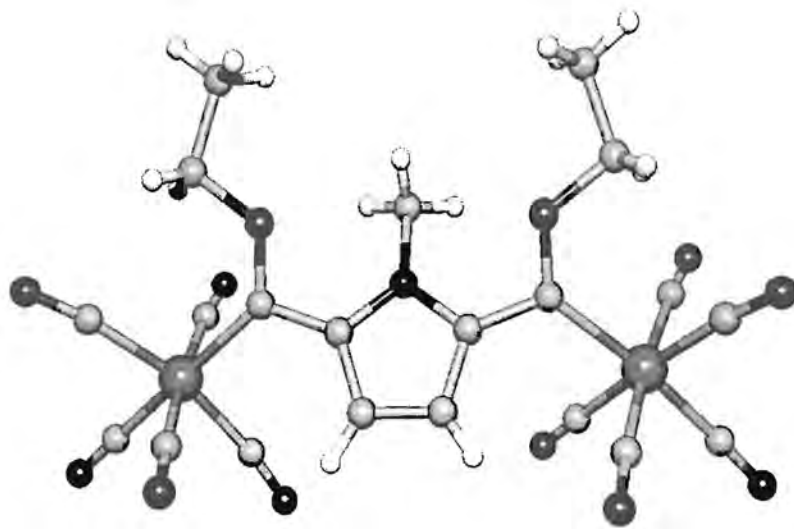


Figure 5. Molecular structure of 4

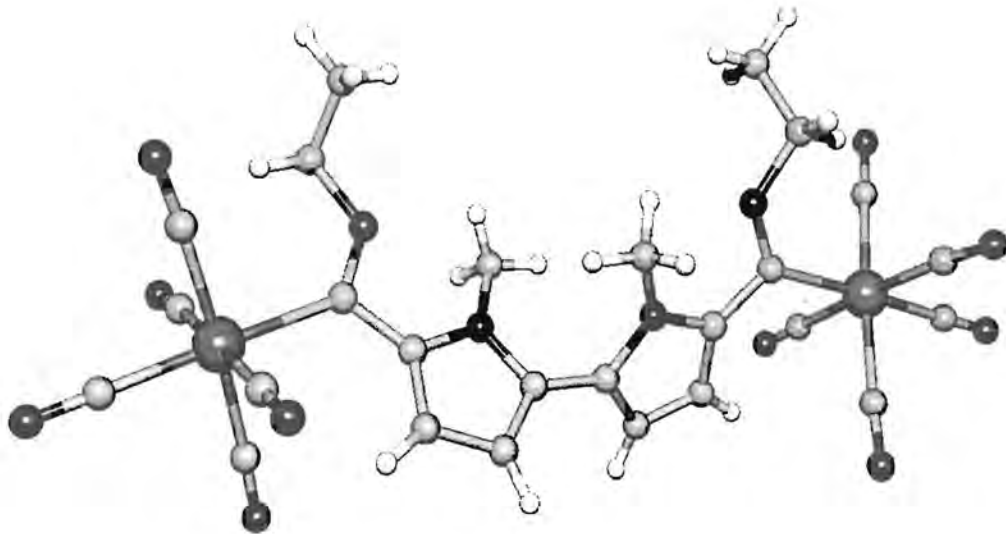


Figure 6. Molecular structure of **5**

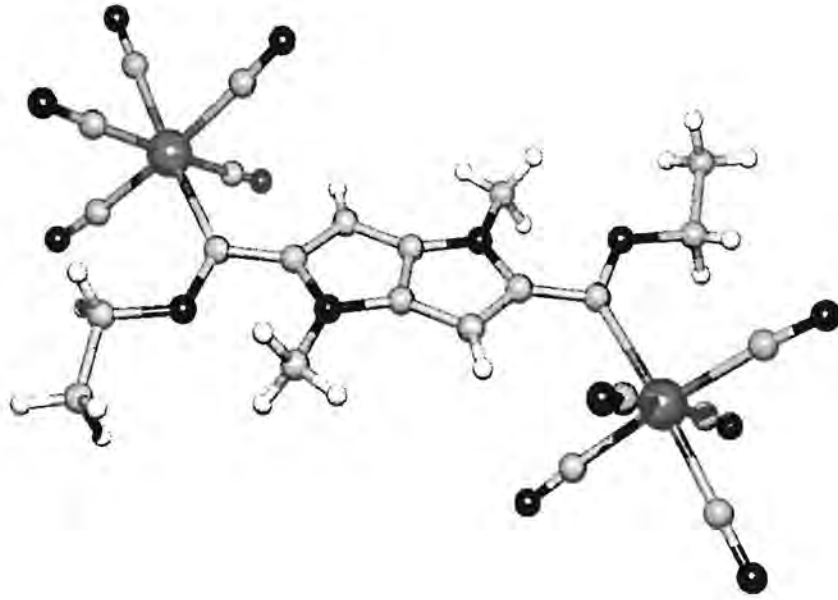


Figure 7. Molecular structure of **6**